MSW effect, solar neutrinos and searches for new physics

A. Yu. Smirnov

Max-Planck Institute fuer Kernphysik, Heidelberg, Germany

5th Int. Solar neutrino conference
Dresden, June 13, 2018

Content

The MSW effect and the LMA solution

Oscillations in the Earth

Searches for new physics

A. Y. Smirnov, Solar neutrinos and matter effects. p. 149 - 209. In "The state of the Art of Neutrino physics". World Scientific, 2018

The MSW effect
the LMA solution

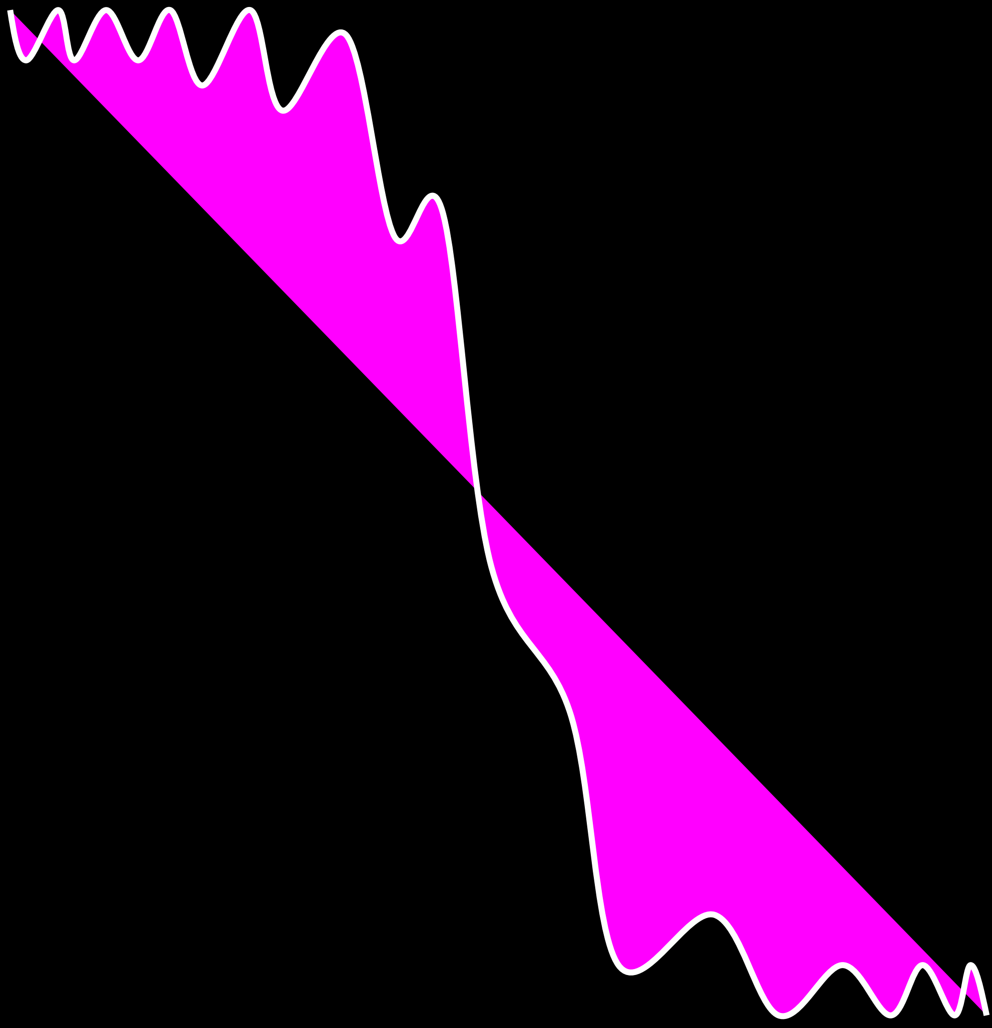

The MSW effects

- the flavor transformations driven by the energy and density dependence of the mixing in matter

$$\nu_f = U^m(E, n)\, \nu_H$$

Flavor states

Mixing matrix in matter

Eigenstates of Hamiltonian in mater - Eigenstates of propagation

Mixing angles $\theta^m(E, n)$ become dynamical variables

in contrast, to mixing in vacuum

Dependence of $\sin^2 2\theta^m$ on E and n has resonance character

Mixing in matter

in vacuum:

H_0

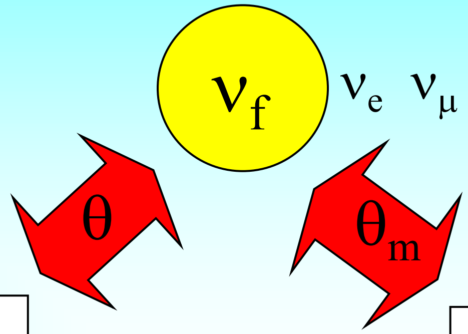

ν_e ν_μ

in matter:

$H(n_e, E) = H_0 + V$

ν_1 ν_2 ν_{mass}

ν_H ν_{1m} ν_{2m}

Eigenstates of H_0 in vacuum

Eigenstates of H in medium

θ_m depends on n_e, E

Mixing angle determines flavor content of eigenstates of propagation

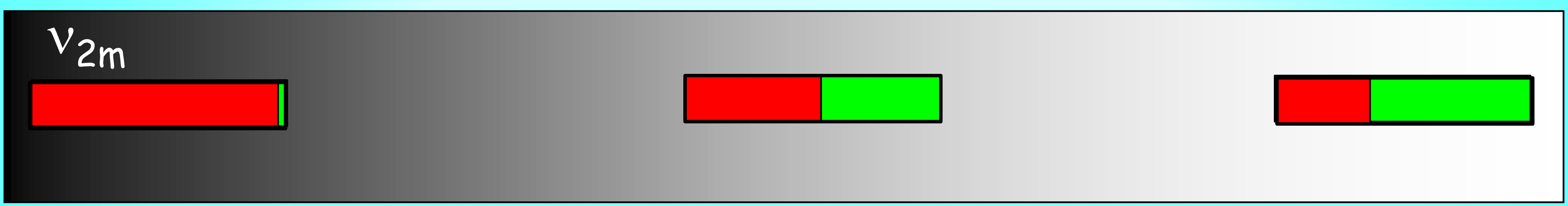

High density
mixing suppressed

Resonance: $l_\nu = l_0 \cos 2\theta$
- maximal mixing

Low density
Vacuum mixing

Two realizations

Constant density

ν

Slowly changing density

Different E

Resonance enhancement of oscillations

Fixed E

Adiabatic flavor conversion

$\frac{F(E)}{F_0(E)}$

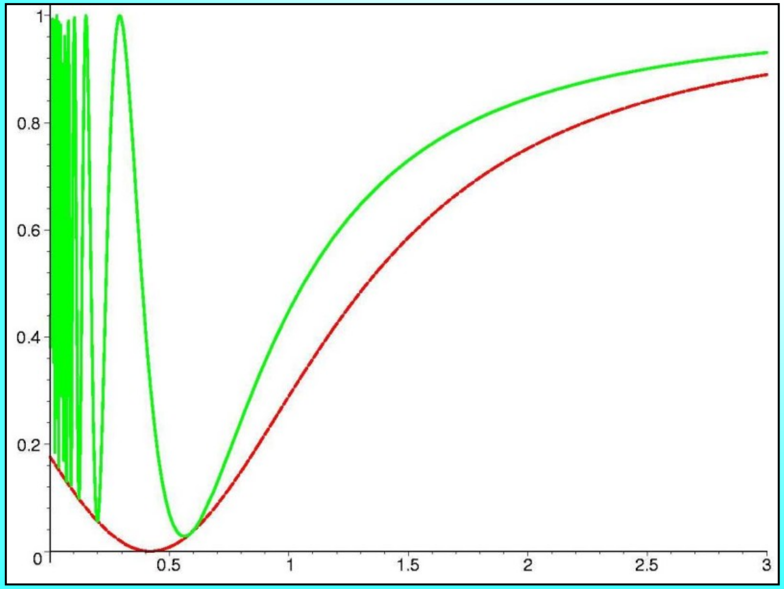

E/E_R

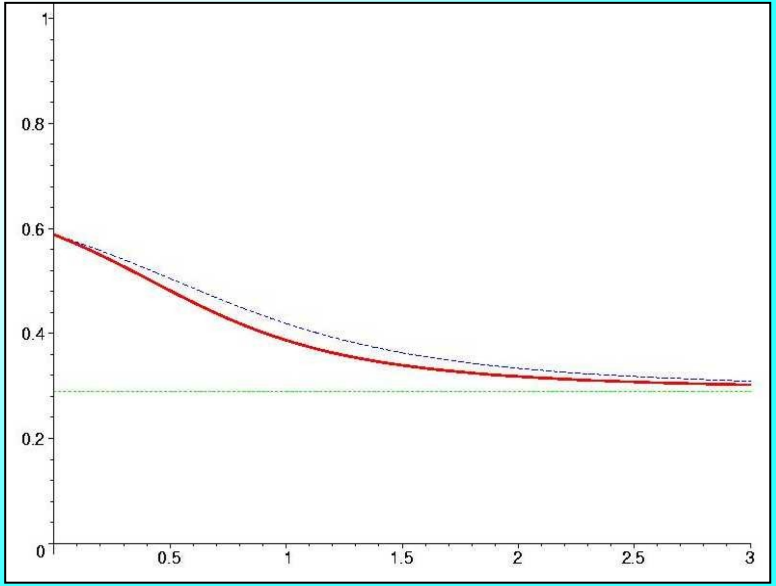

E/E_R

Spatial picture

Oscillations

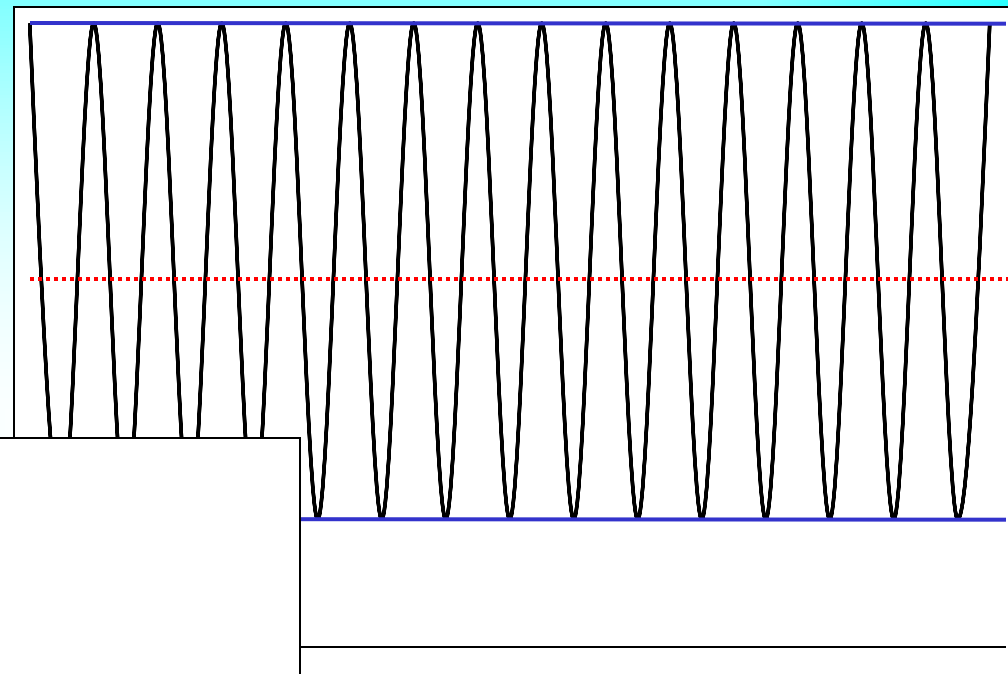

distance

Adiabatic conversion

survival probability

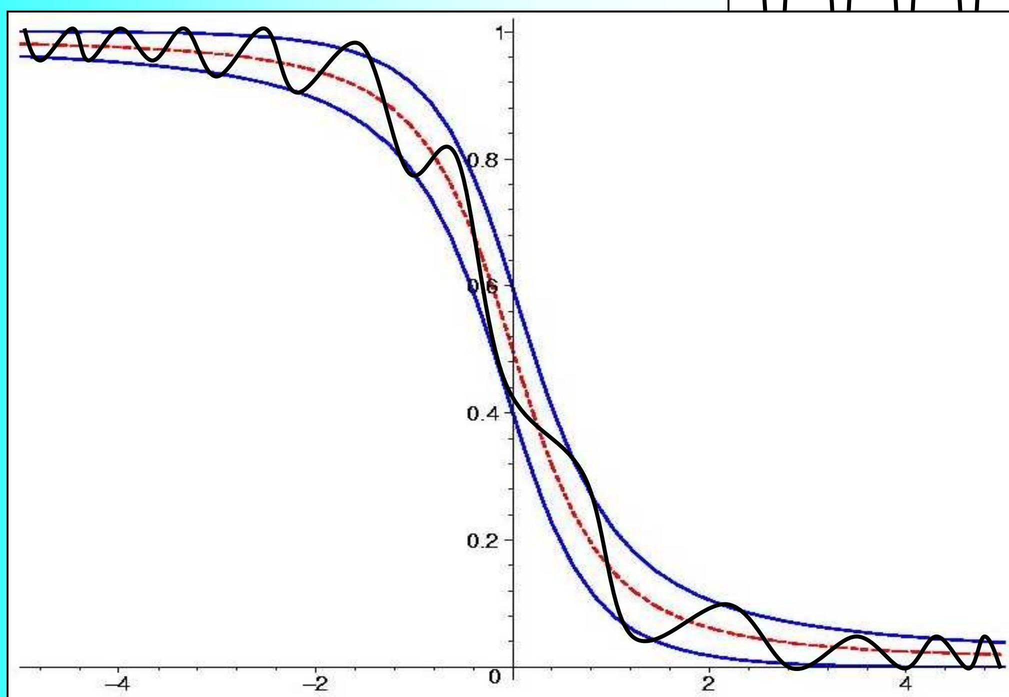

distance

Adiabaticity

For varying density –another degree of freedom: eigenstates composition of a given propagating state

It can change which is related to transitions

$\nu_{1m} \Leftrightarrow \nu_{2m}$

Efficiency of the transitions is determined by the degree of adiabaticity.

If density changes slowly enough, so that

$$\left|\frac{d\theta_m}{dt}\right| \ll H_{2m} - H_{1m}$$

"adiabaticity condition"

Difference of ehgenvalues

The transitions between eigenstates can be neglected

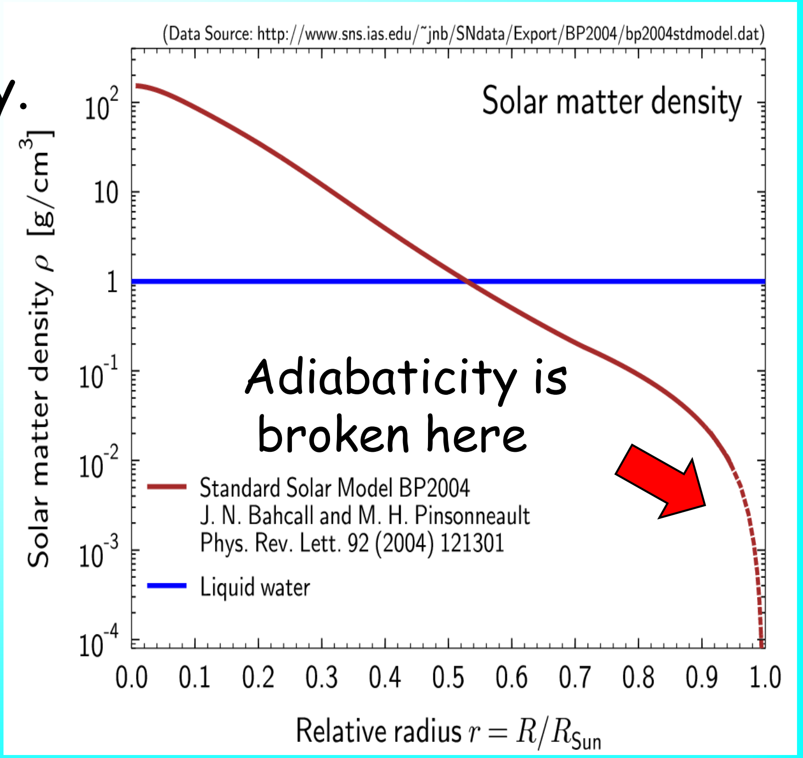

Adiabatic conversion

in general if density changes slowly (adiabatically)

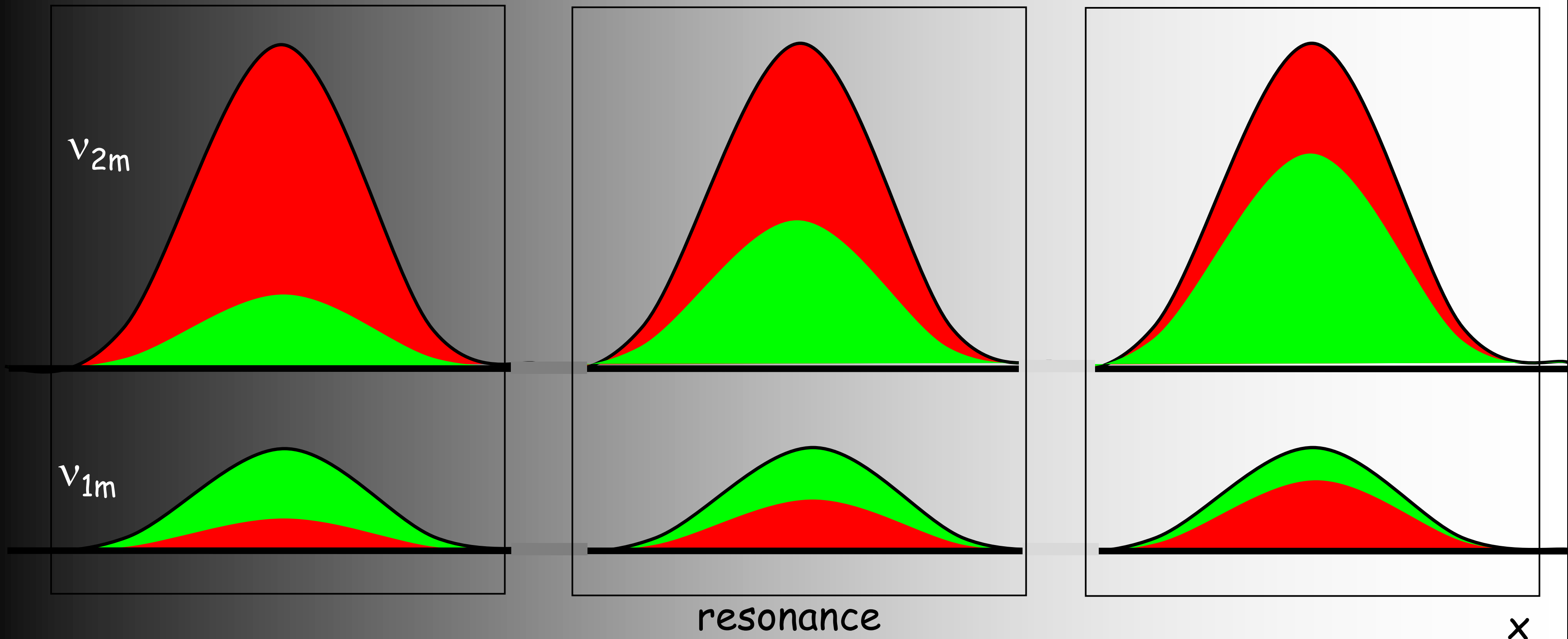

if initial density is not very big: mixing is not suppressed → both eigenstates are produced → interference → oscillations

- the amplitudes of the wave packets do not change
- flavors of the eigenstates being determined by mixing angle follow the density change

Coherence in propagation

In the configuration space: separation of the wave packets due to difference of group velocities

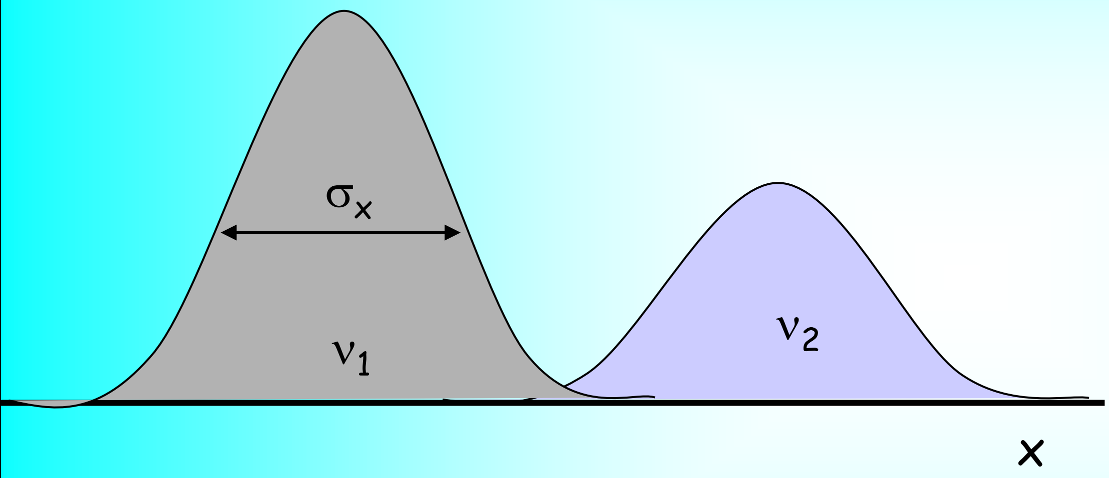

$\Delta v_{gr} = \Delta m^2 / 2E^2$

separation: $\Delta v_{gr} L = \Delta m^2 L / 2E^2$

no overlap: $\Delta v_{gr} L > \sigma_x$

coherence length:

$L_{coh} = \sigma_x E^2 / \Delta m^2$

In the energy space: averaging over oscillations

Oscillatory period in the energy space $E^T = 4\pi E^2 / (\Delta m^2 L)$

Averaging (loss of coherence) if energy resolution σ_E is $E^T < \sigma_E$

→ leads to the same coherence length

LMA-MSW physics

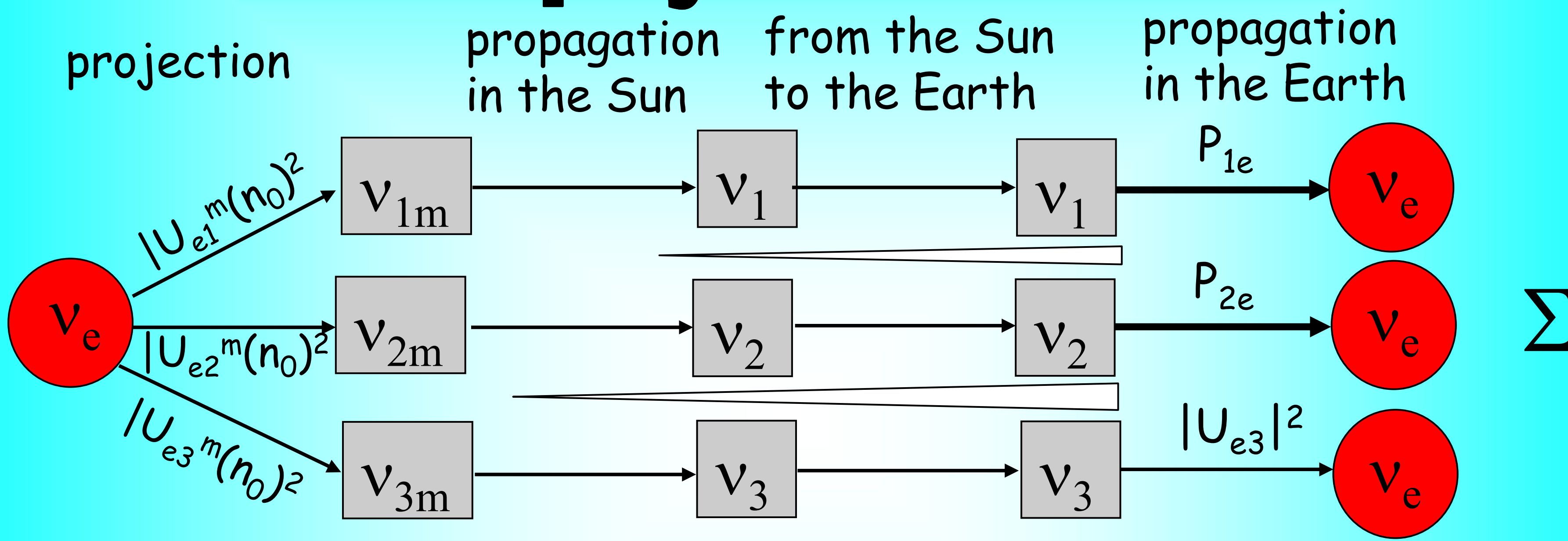

mixing at production

adiabatic conversion

loss of coherence

oscillations in multi-layer medium

$$P_{ee} = \Sigma_i |U_{ei}^m(n_0)|^2 \, P_{ie}$$

during a day

$$P_{ie} = |U_{ei}|^2$$

In the Sun: scale invariance: no dependence of P_{ee} on distance and phase - oscillations irrelevant

Oscillations in the Earth

Distance and phase matter

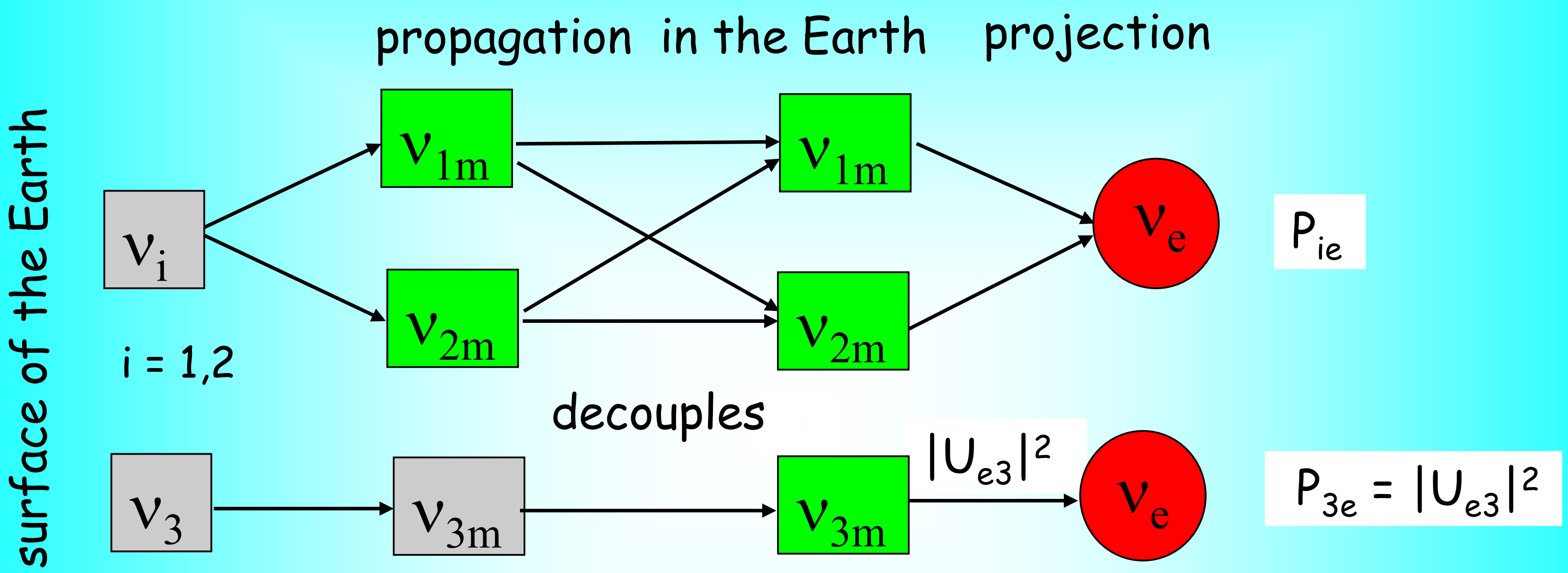

mixing of mass states in matter

oscillations in multi-layer medium

flavor mixing in matter

Σ

Adiabaticity violation at the border between layers

$P_i = |U_{ei}^m(n_0)|^2$

mixing at production in the Sun

Properties of LMA: scaling

$P_{ee} = P_{ee}(\theta_m^0)$ (day) $\theta_m^0 = \theta_m^0\left(\theta, \frac{2VE}{\Delta m_{21}^2}\right)$

Invariance: $\Delta m_{21}^2 \to a\, \Delta m_{21}^2, \quad V \to a\, V$

P_{ee} is scale invariant - no dependence on distance, scales of density profile

a = -1 flip of the mass hierarchy implies the change of sign of V

(NSI)

Oscillations in the Earth break scaling: phase

$$\phi_E = \frac{\Delta m_{21}^2 L}{2E} f\left(\frac{2VE}{\Delta m_{21}^2}\right)$$

L – the length of the trajectory in the Earth

If oscillations in the Earth are averaged (valid for the present accuracy) - the scaling is restored

Also invariance $\Delta m_{ij}^2 \to b\, \Delta m_{ij}^2, \quad E \to b\, E$

Status of LMA-MSW

Good agreement between

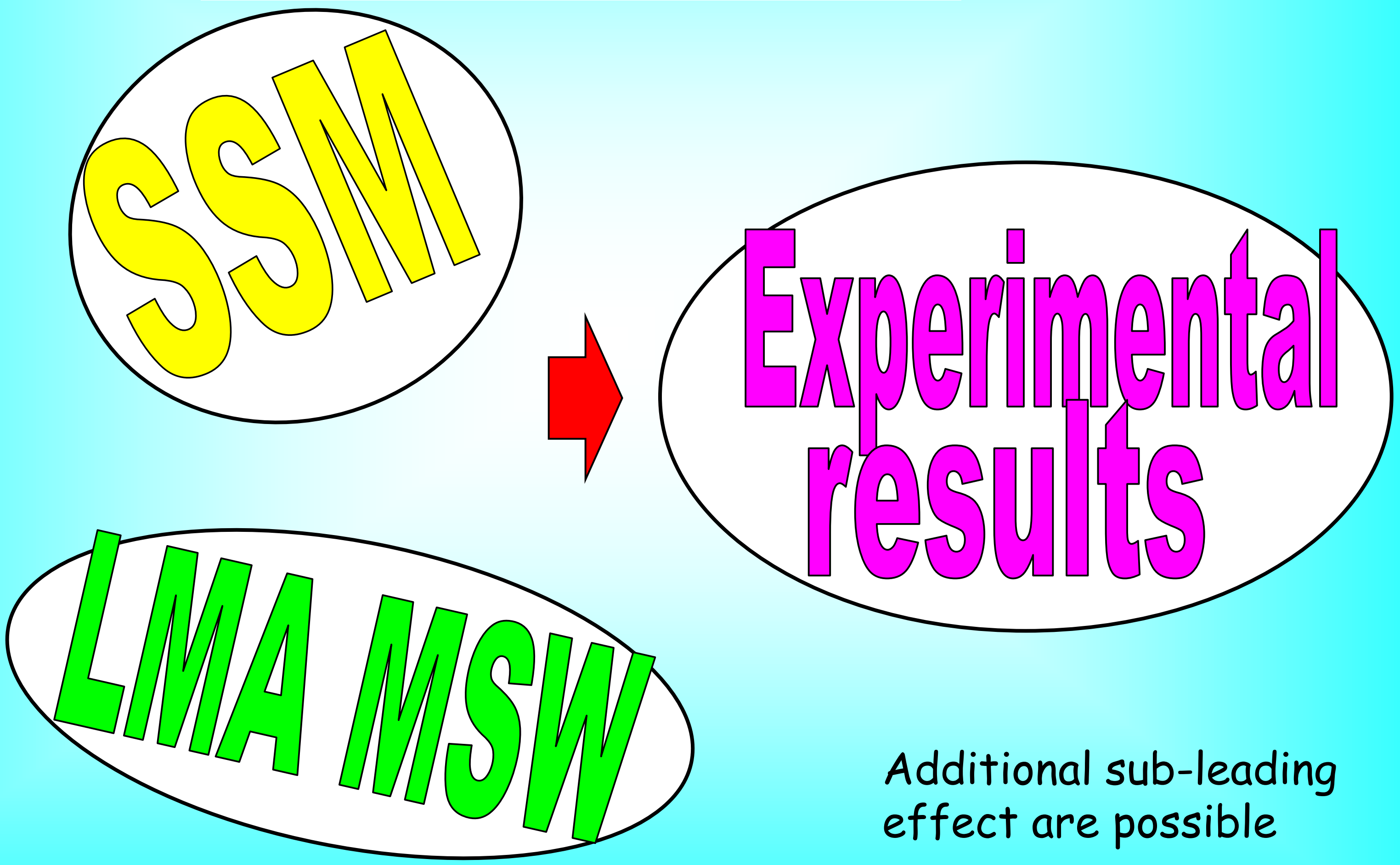

Additional sub-leading effect are possible

Neutrino parameters

M. Maltoni, A.Y.S.
1507.05287 [hep-ph]

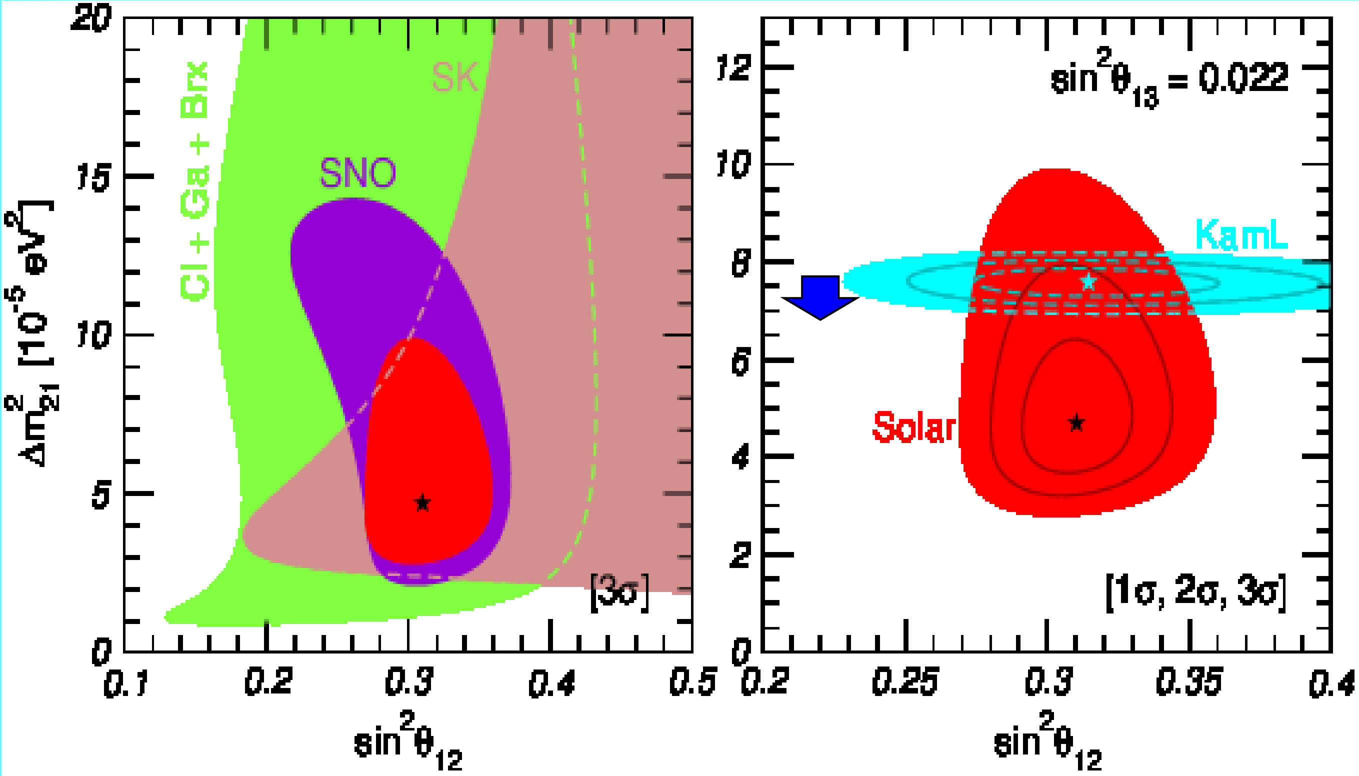

Red: all solar neutrino data

Δm^2_{21} (KL) > Δm^2_{21} (solar)   2 σ

KamLAND data reanalized in view of reactor anomaly (no front detector) bump at 4 -6 MeV

Δm^2_{21} decreases by 0.15 10^{-5} eV^2

Spectroscopy

M. Maltoni, A.Y.S. 1507.05287 [hep-ph]

Borexino Collaboration (Agostini, M. et al.) arXiv:1707.09279 [hep-ex]

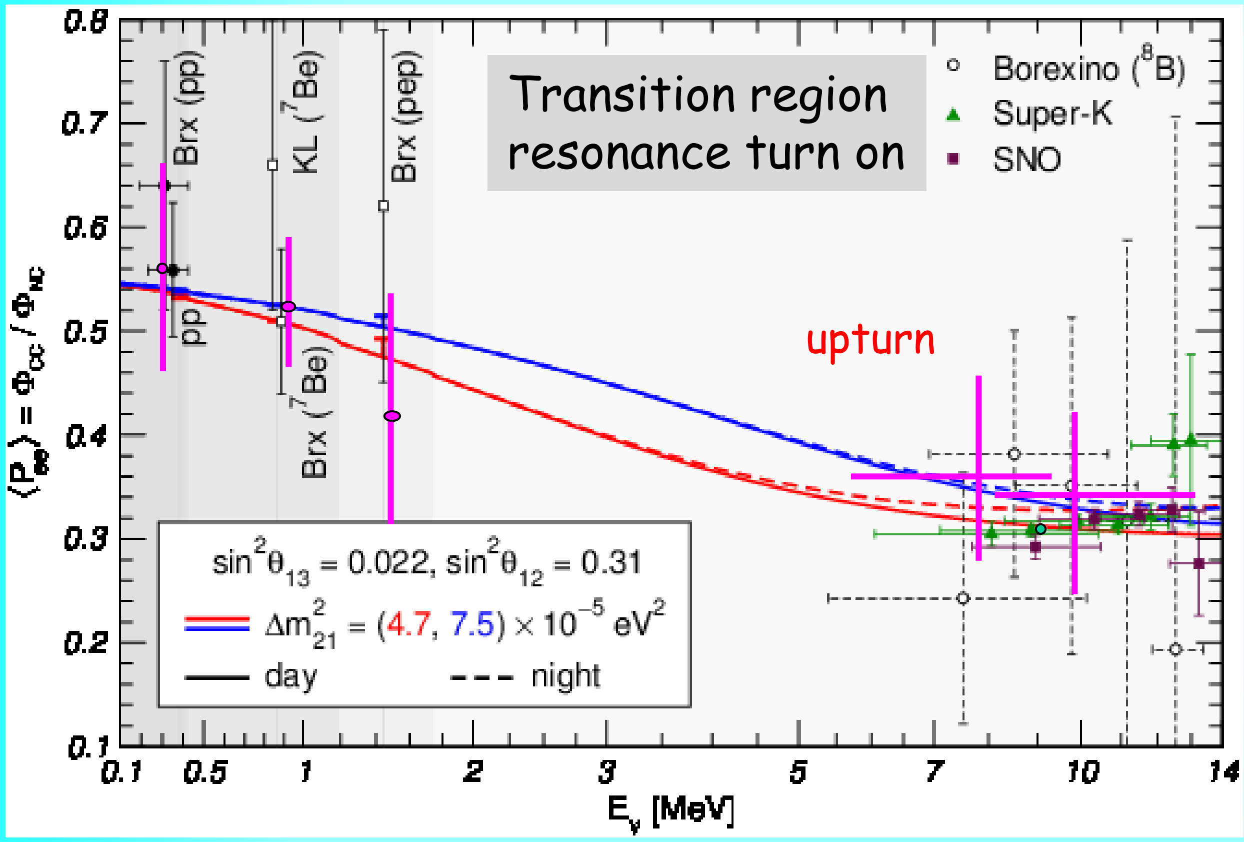

LMA MSW predicion for two different values of Δm_{21}^2

best fit value from solar data

best global fit

Reconstructed exp. points for SK, SNO and BOREXINO at high energies

BOREXINO

pep: (phase I + phase II – ideal agreement)

B: 2 times smaller errors, upturn...

Precision measurements in 5 – 10 MeV

Tensions

Absence of spectral upturn

SK, SNO, BOREXINO?

Large Day-night asymmetry

SK

Different Δm_{21}^2 from solar and KamLAND

Low rate in Homestake

> 2σ

1.6 Larger V

$P = P(\Delta m_{21}^2 / V)$

scaling

Spectrum of all SK data

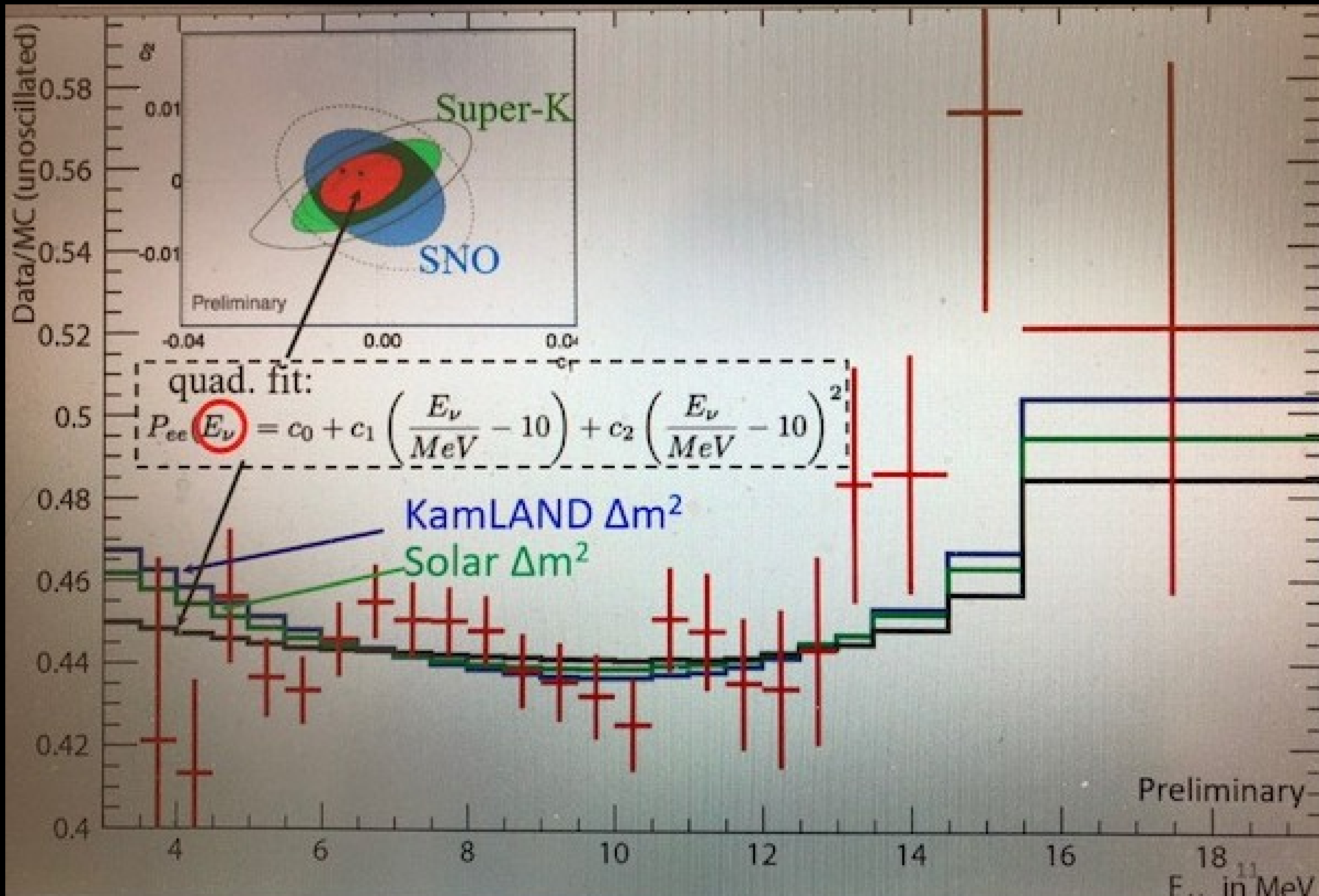

SK: Earth matter effect

SK Collaboration (Abe, K. et al.) arXiv:1606.07538 [hep-ex]

SK-IV solar zenith angle dependence

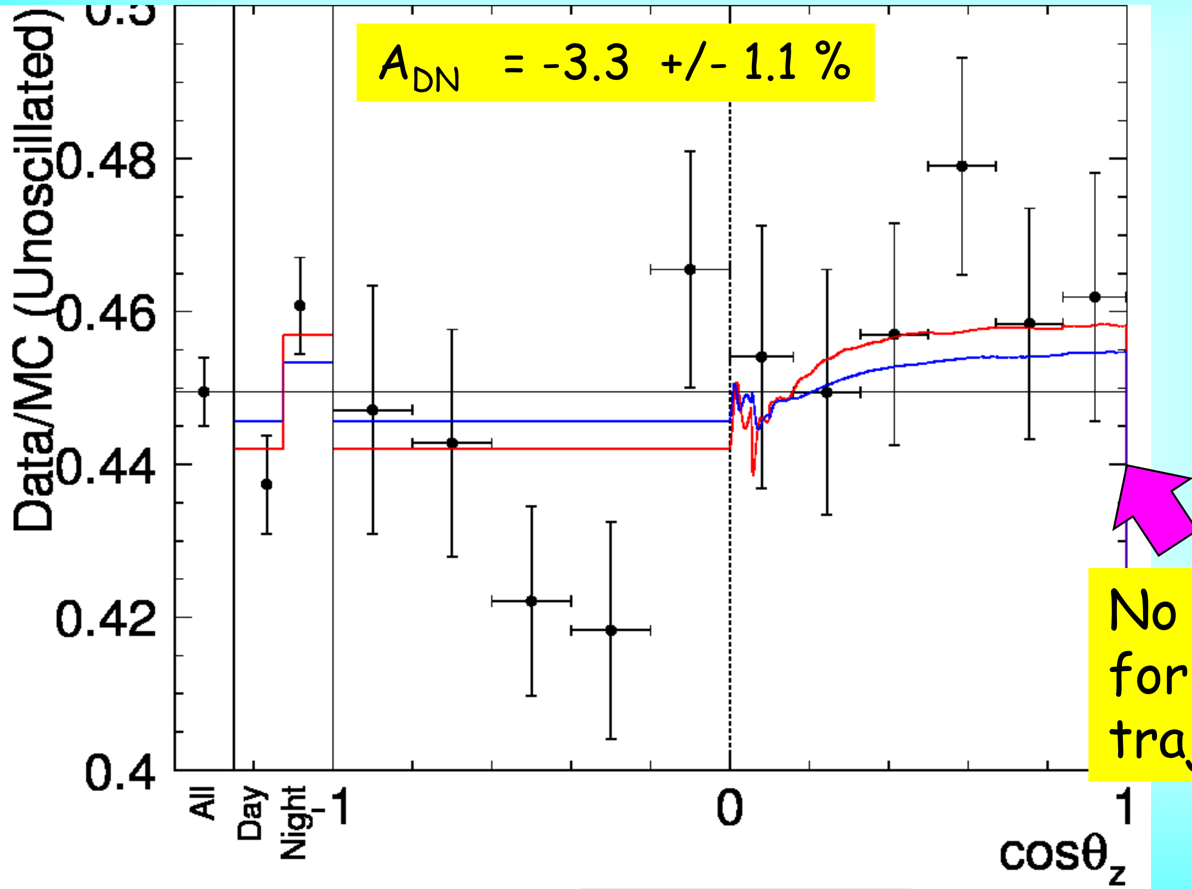

Strong fluctuations

No enhancement for core crossing trajectories

Generic features:

Oscillatory pattern

dip

Explained by the Attenuation effect

SK analysis

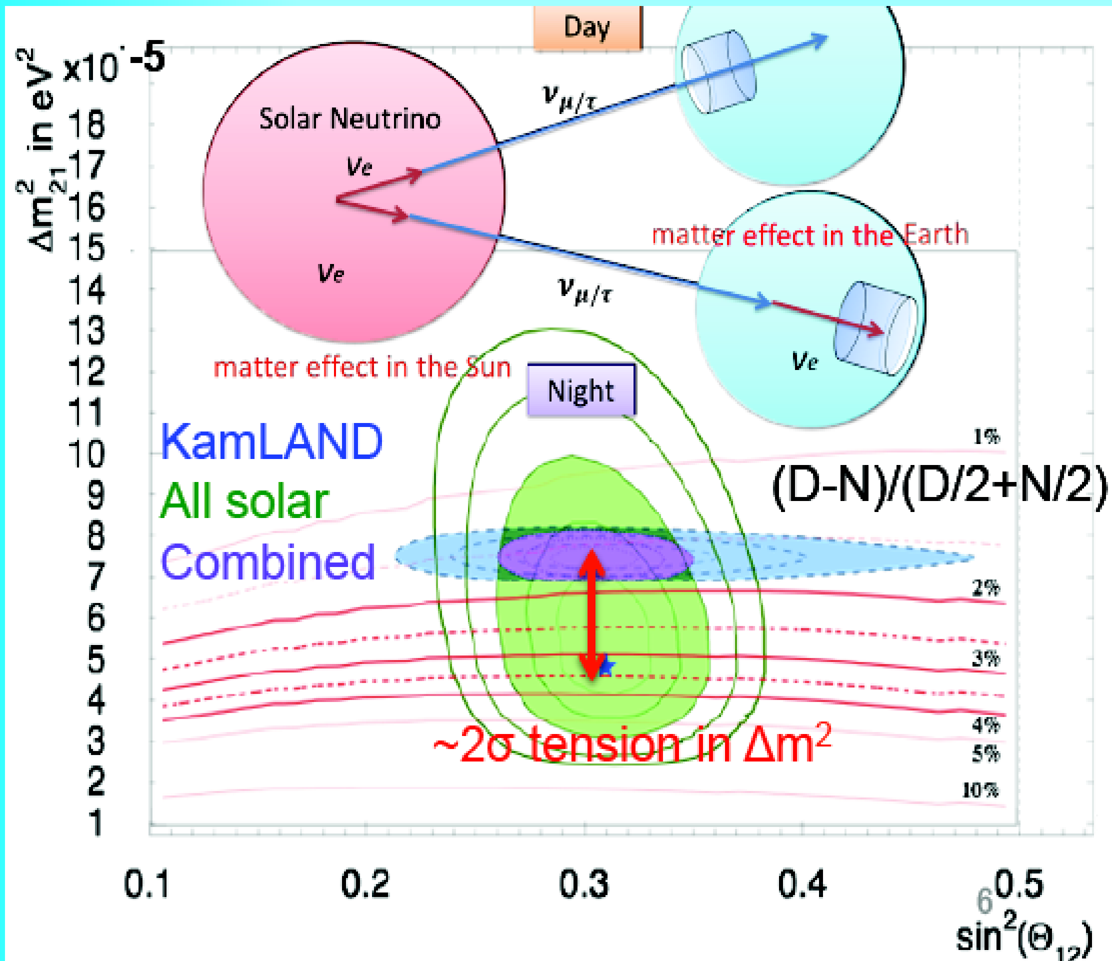

T. Yano. ICRC 2017

A_{DN} = -3.3 +/- 1.1 %

Expected for global mass difference

A_{DN} = -1.8

M. Smy: improve Sensitivity to D-N
Lower bkgr- increase F.V for high energy
Solar meutrinos

How things may develop

Solar value $\Delta m_{21}^2 = 7x10^{-5}$ eV^2 (before 2010) was reduced after SK data on D-N asymmetry and measurements of spectrum

- JUNO: precise measurements of Δm_{21}^2 with (0.7 -1)% accuracy

$\sigma(\Delta m_{21}^2) = (0.05 - 0.07) \times 10^{-5}$ eV^2

Difference of solar and KamLAND

$\Delta(\Delta m_{21}^2) = 2.5 \times 10^{-5}$ eV^2

If $\Delta m_{21}^2(\text{JUNO}) = \begin{cases} \Delta m_{21}^2(\text{solar}) & \text{problem solved} \\ \Delta m_{21}^2(\text{KL}) & \text{problem sharpens} \end{cases}$

- Stronger bounds on NSI from COHERENT and other experiments
- SNO+ spectrum measurements above 3 MeV (testing upturn)
- Hyper-Kamiokande — Day-night asymmetry, spectrum
- DUNE

Oscillations
In the Earth

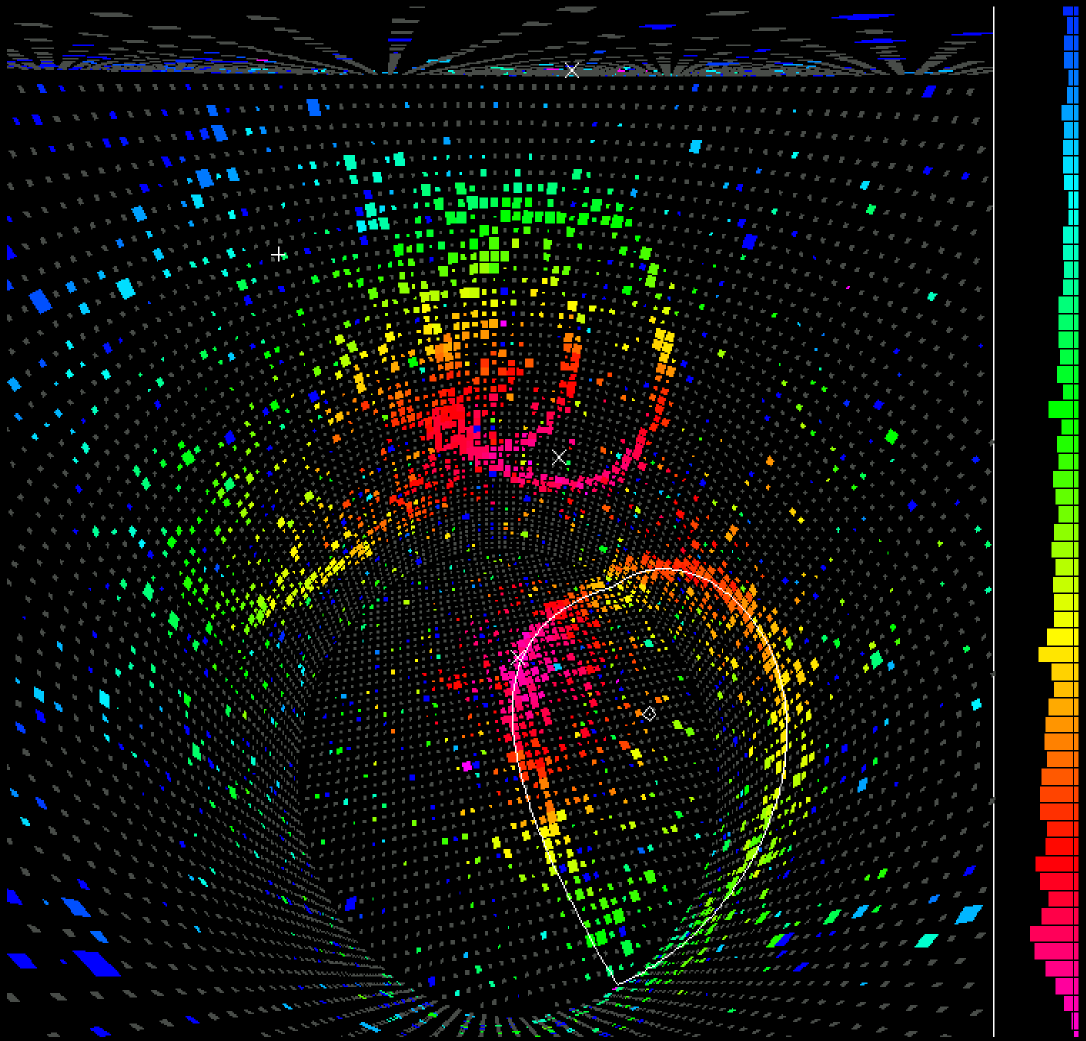

Oscillations in the Earth

Distance and phase matter

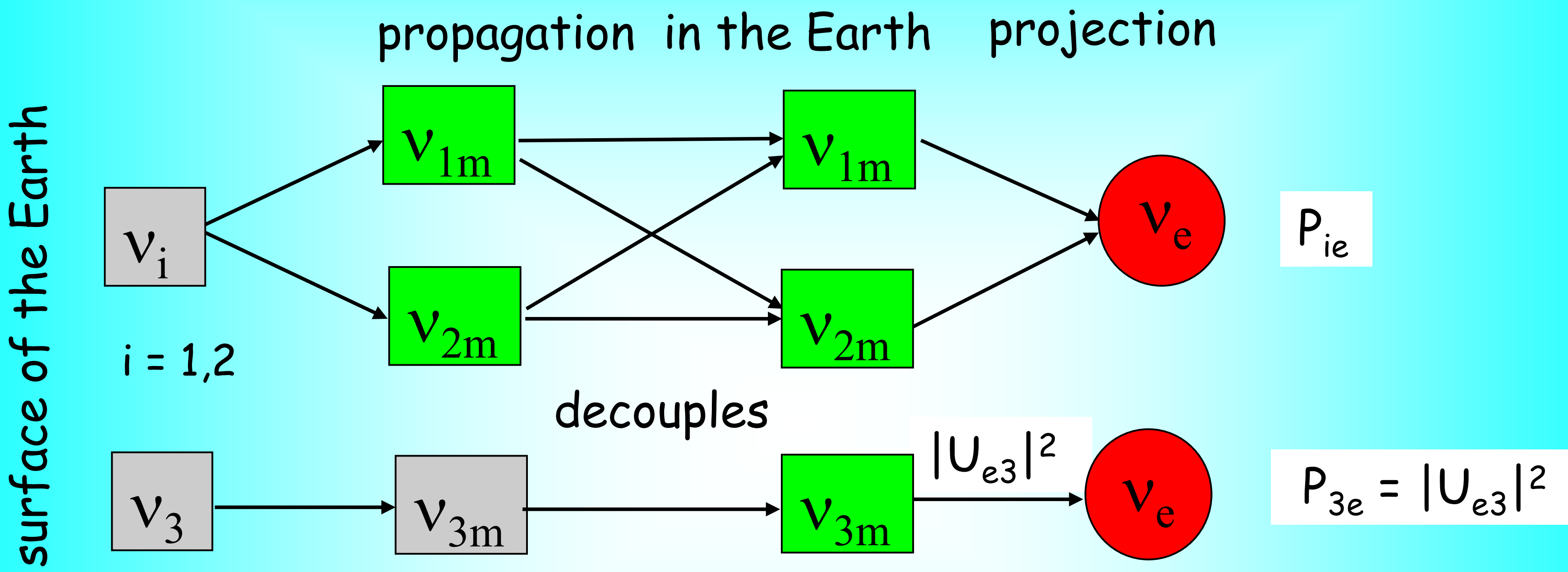

mixing of mass states in matter

oscillations in multi-layer medium

flavor mixing in matter

Σ

Adiabaticity violation at the border between layers

$P_i = |U_{ei}^m(n_0)|^2$

mixing at production in the Sun

The earth density profile

PREM model

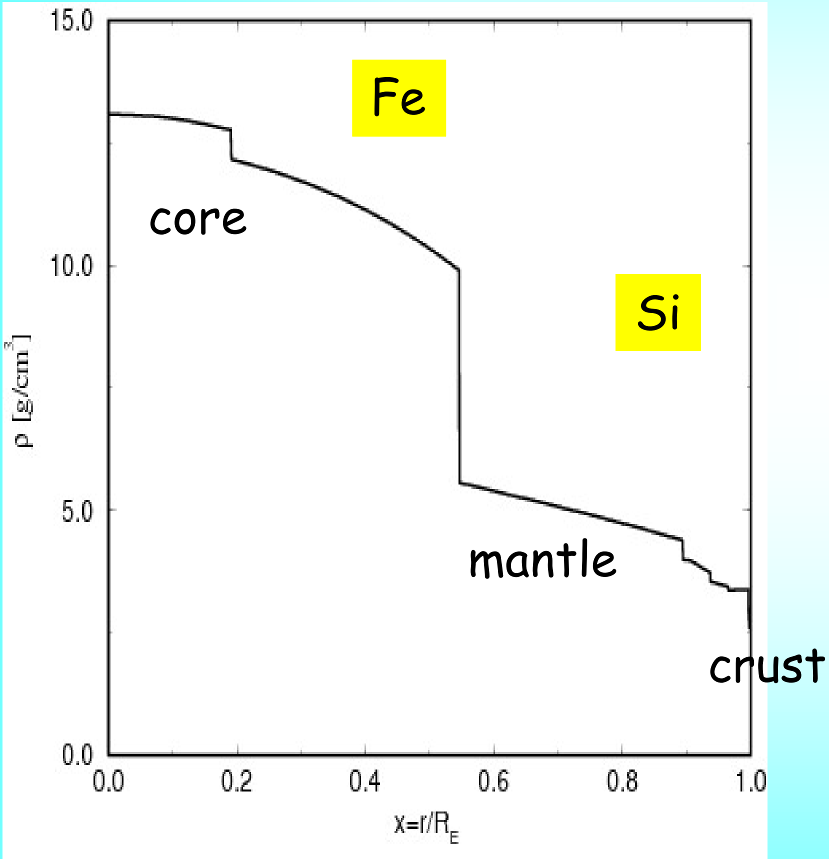

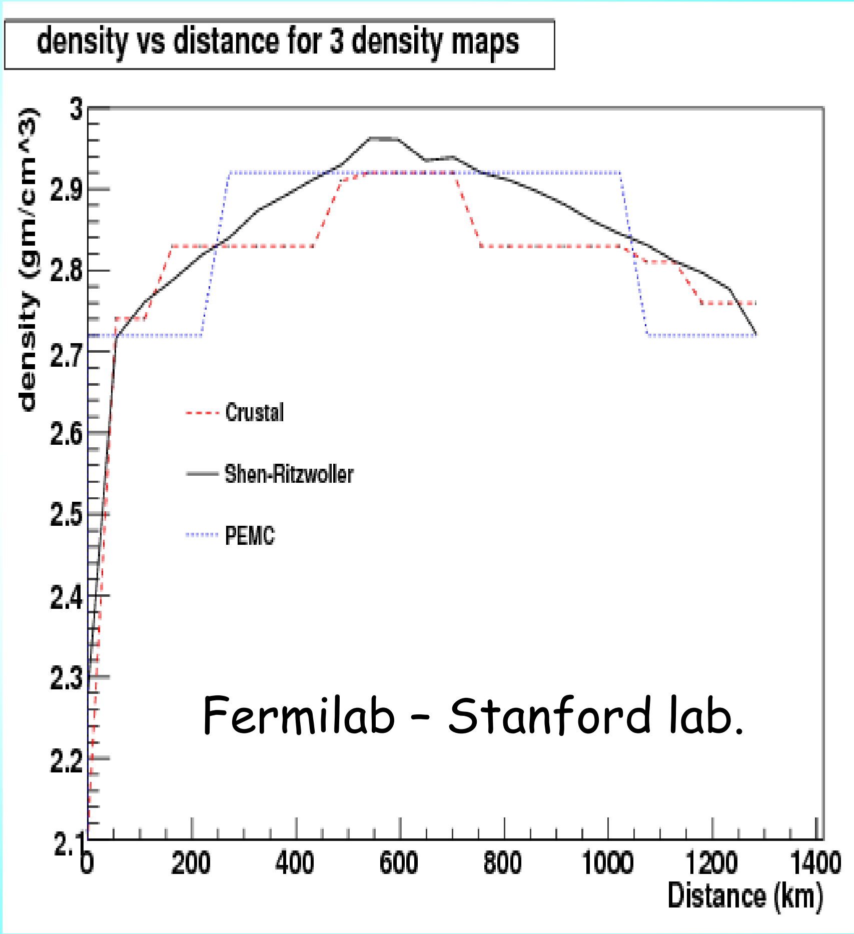

A.M. Dziewonski
D.L Anderson 1981

R_e = 6371 km

Byron Roe, Phys.Rev. D95 (2017) no.11, 113004
arXiv:1707.02322 [hep-ex]

Oscillations in the Earth

Incoherent fluxes of mass state arrive at the Earth.
They split into eigenstates in matter and oscillate.

Mixing of the mass states in matter

$$U^{mass} = U_{PMNS}^{+} U^{m}$$

For 2ν case

$$\sin 2\theta' = \frac{c_{13}^2 \varepsilon \sin 2\theta_{12}}{\sqrt{(\cos 2\theta_{12} - c_{13}^2 \varepsilon)^2 + \sin^2 2\theta_{12}}} = c_{13}^2 \varepsilon \sin 2\theta_{12}^m$$

$$\varepsilon = \frac{2V E}{\Delta m_{21}^2} = 0.03 E_{10} \rho_{2.6}$$

determines smallness of effects
Low density regime

MeV g/cm^3

Regeneration

A. Ioannisian, A. Smirnov, D. Wyler,
Phys.Rev. D96 (2017) no.3, 036005
arXiv:1702.06097 [hep-ph]

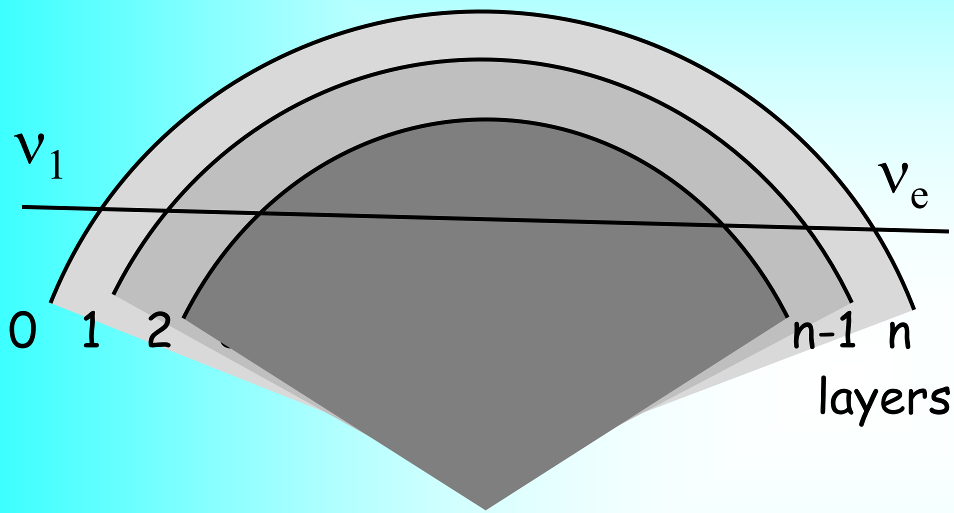

Layers with slowly changing density and density jump

Evolution matrix (matrix of transition amplitudes)

$$S = U^m{}_n \, \Pi_k \, D_k U_{k,k-1}$$

flavor mixing matrix, at the detector

D_k - describe the adiabatic evolution within layers

$$D_k = \mathrm{diag}\,(e^{-0.5i\phi_\kappa},\ e^{0.5i\phi_\kappa})$$

$$\phi_\kappa = \int dx (H_{2m} - H_{1m})$$

adiabatic phase acquired in k layer

$U_{k,k-1}$ - describes change of basis of eigenstates between k and k-1 layers

$$U_{k,k-1} = U(-\Delta\theta_{k-1})$$

$\Delta\theta_{k-1}$ -change of the mixing angle in matter after k-1 layer

Oscillation waves

The lowest order plus waves emitted from different jumps

$$P_{1e} \sim c_{13}^2 \cos^2\theta_n^f + c_{13}^2 \sin 2\theta_n^f \, \Sigma_{j=0\ldots n-1} \sin\Delta\theta_j \cos\phi_j^{after}$$

initial wave without density jumps

sum over density jumps

total phase acquired after jump j

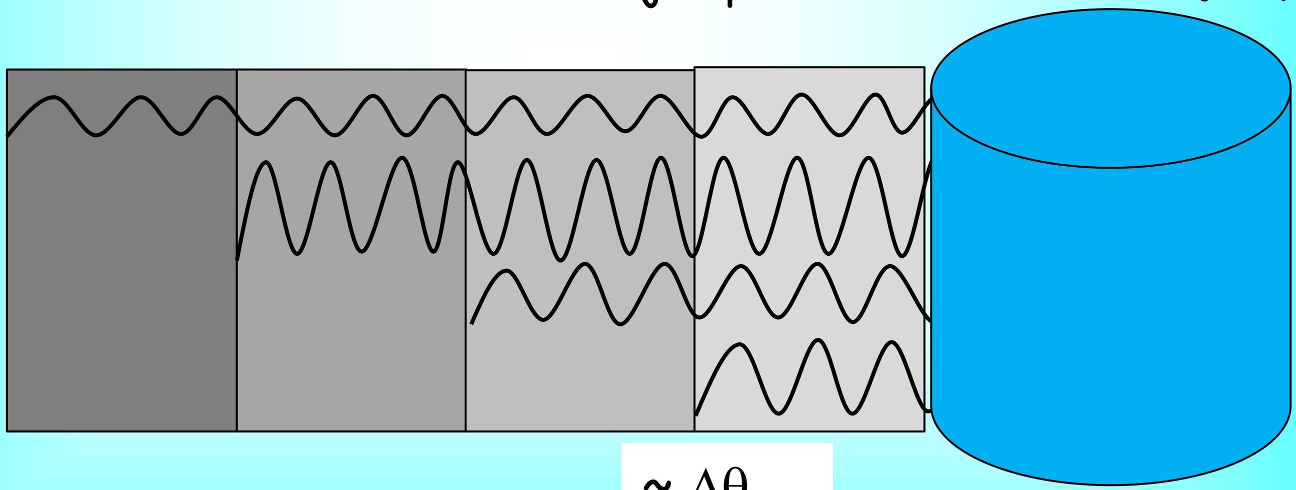

$\sim \Delta\theta_j$

the amplitude of wave: $c_{13}^2 \sin 2\theta_n^f \sin\Delta\theta_j$

superposition of waves

$$\sin \Delta\theta_j - c_{13}^2 \sin 2\theta_{12} \, \Delta V_j \, \frac{E}{\Delta m_{21}^2}$$

Attenuation effect

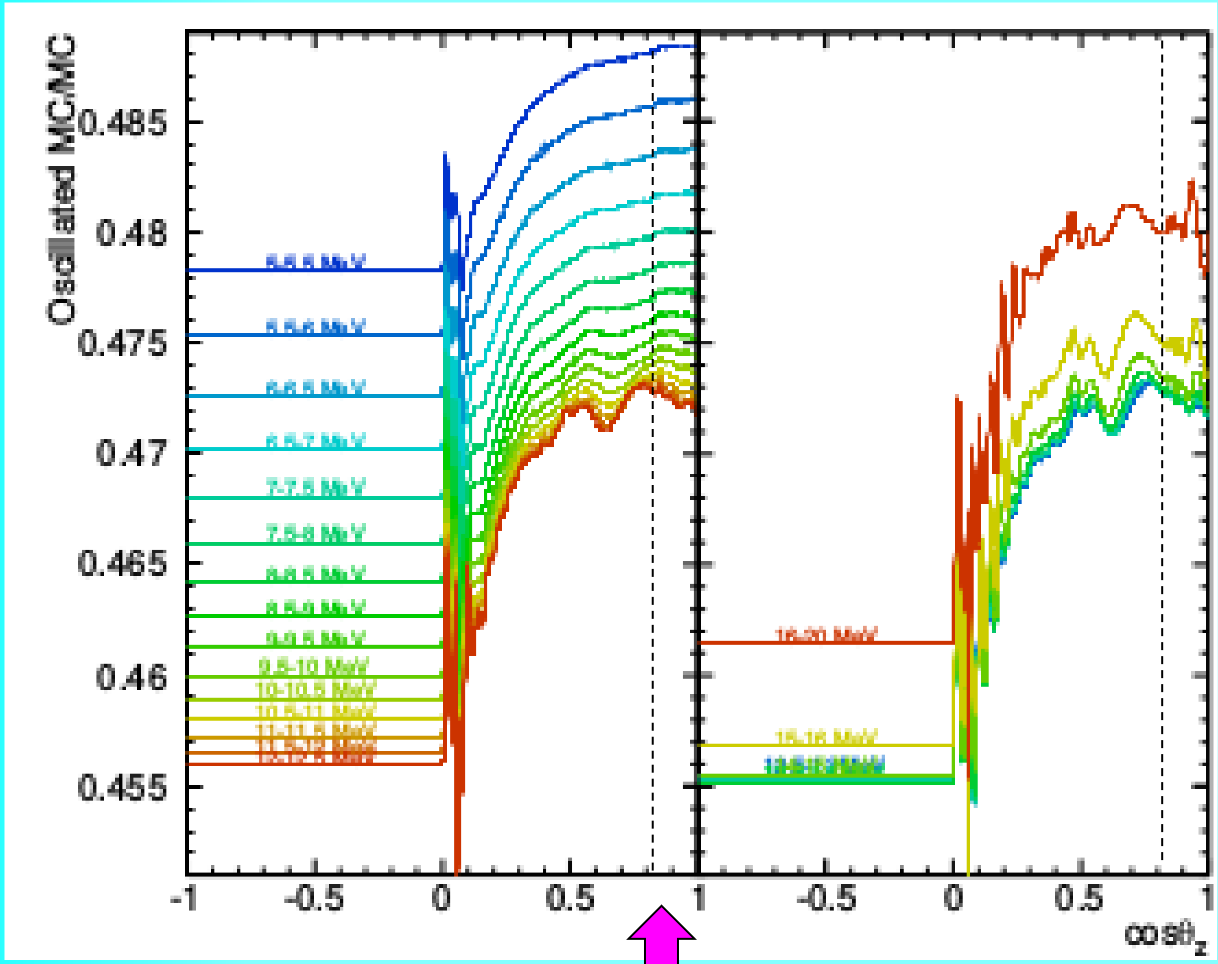

M. Smy

Predicted solar zenith angle variations of SK the signal
$\Delta m^2 = 6.3 \times 10^{-5}$ eV ^{2},
$\tan 2\theta = 0.52$

Core crossing trajectories

No enhancement of the effect for core-crossing trajectories

Attenuation effect

A. Ioannisian, A. Y. Smirnov,
Phys.Rev.Lett., 93, 241801 (2004), 0404060 [hep-ph]

Integration with the energy resolution function R(E, E'):

$$\langle f_{reg} \rangle = \int dE' \, R(E, E') \, f_{reg}(E')$$

$$\langle f_{reg} \rangle = 0.5 \sin^2 2\theta \int_{x_0}^{x_f} dx \, F(x_f - x) \, V(x) \sin\Phi^m(x \rightarrow x_f)$$

F(d)

Attenuation factor

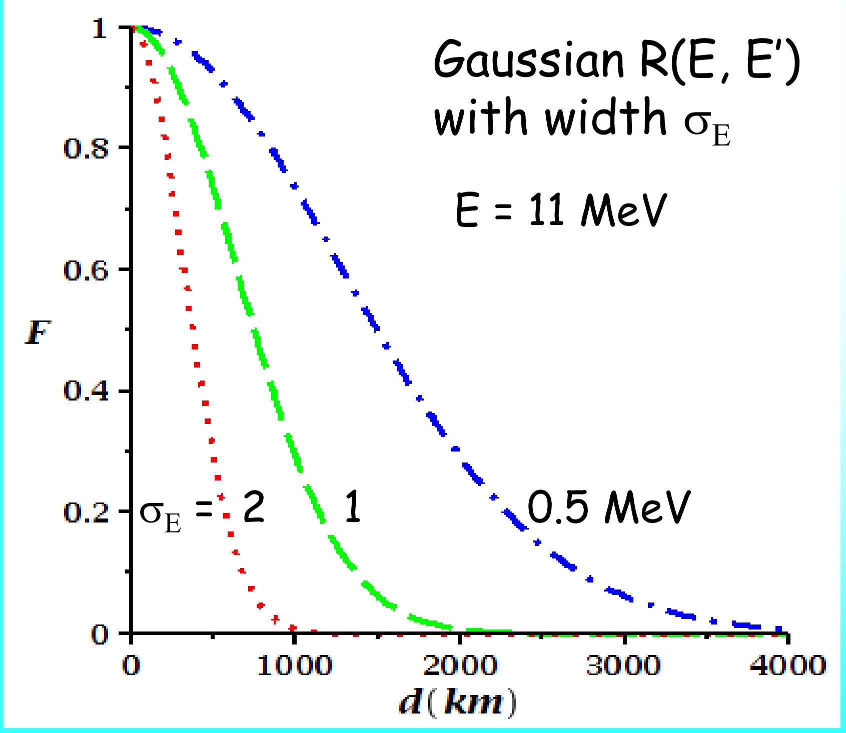

The sensitivity to remote structures $d > \lambda_{att}$ is suppressed

Attenuation length

$$\lambda_{att} = l_\nu \frac{E}{\pi \sigma_E}$$

l_ν is the oscillation length

The better the energy resolution, the deeper structures can be seen

Attenuation and decoherence

The oscillation phase acquired along the attenuation length:

$\phi = 2$ … E

Diff…

For $\Delta E = \pi\sigma_E$

integration over the … resolution interval leads to … averaging of oscillations

λ_{att} is the distance over which oscillations observed with the energy resolution σ_E are averaged

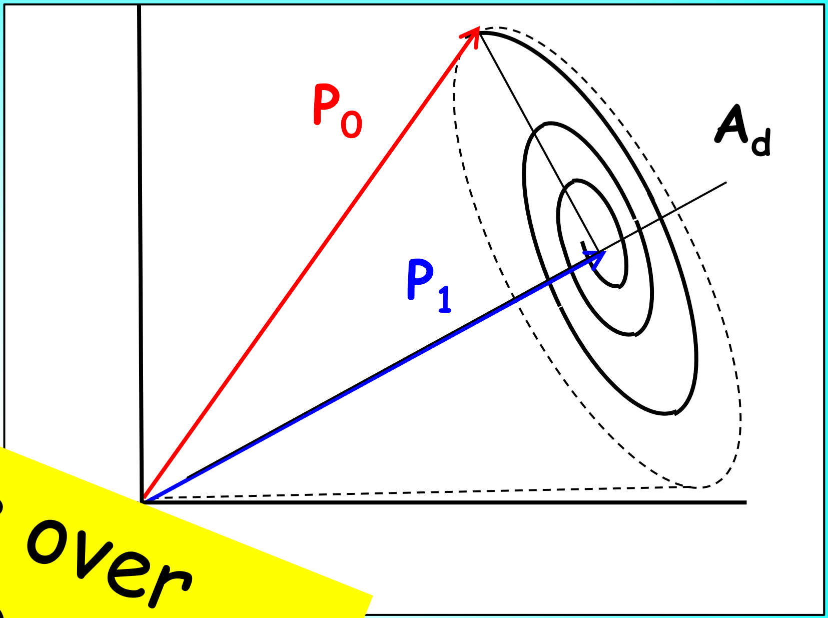

… – loss of coherence

$P_0 \rightarrow P_1$

…rges to its projection … axis of eigenstates A_d

A.N. Ioannisian, A. Yu. S. Phys.Rev. D96 (2017) no.8, 083009, 1705.04252 [hep-ph]

Paradoxes of attenuation

A.N. Ioannisian, A. Yu. Smirnov
Phys.Rev. D96 (2017) no.8, 083009
arXiv:1705.04252 [hep-ph]

Not only decoherence: effect does not disappear completely.
Even for very large distances: it survives in the ε^2 level

Info. about structure is still stored in spite of averaging

$\nu_1 \rightarrow \nu_e$ - channel

Remote structures are attenuated to the ε^2 level;
near structures are seen at ε

$\nu_e \rightarrow \nu_1$ - channel

Near structures are attenuated the ε^2 level;
remote structures are seen at ε

T-symmetry

$\nu_e \rightarrow \nu_e$ - channel

Three layer case: first layer prepare incoherent states:
applications for flavor – flavor transitions

Scanning the Earth

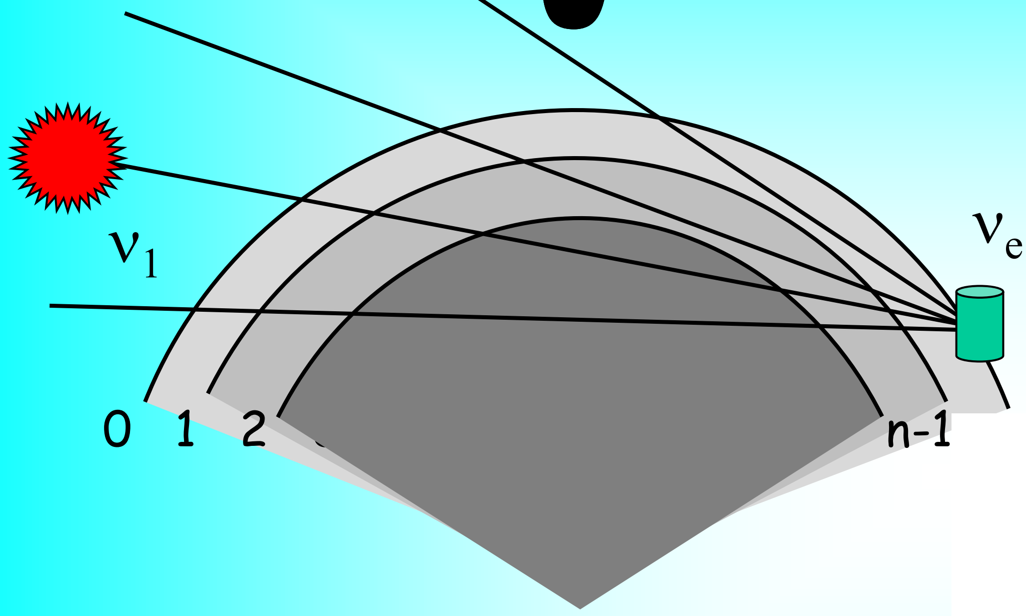

A. Ioannisian, A. Smirnov, D. Wyler, Phys.Rev. D96 (2017) no.3, 036005 arXiv:1702.06097 [hep-ph]

Integration above 11 MeV

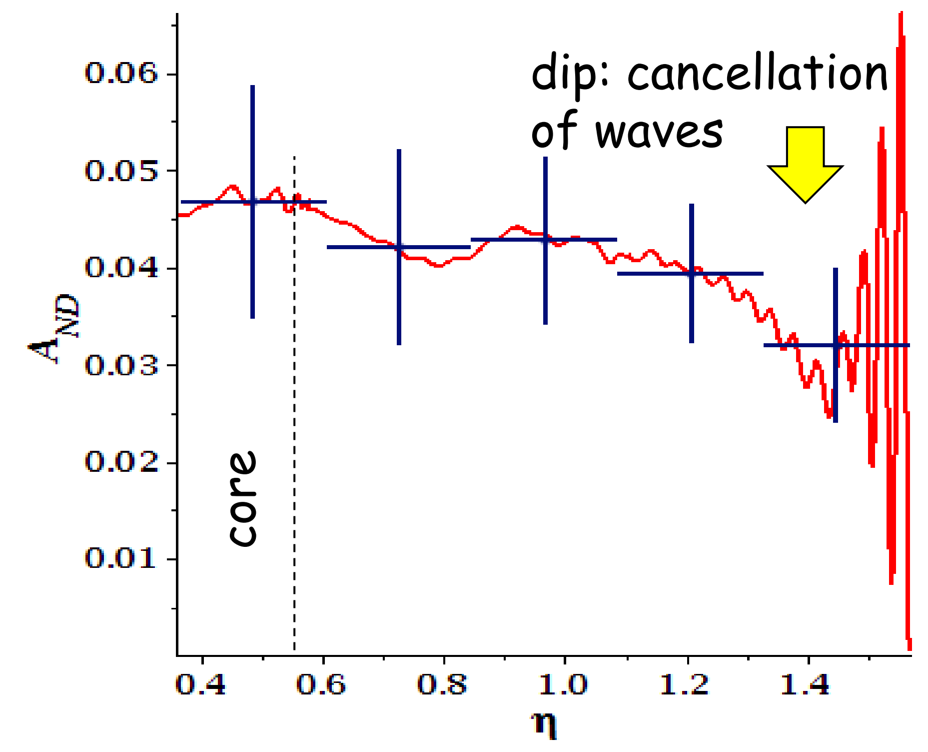

Day –Night asymmetry

$$A_{DN} = \frac{N(\eta)}{D} - 1$$

nadir angle →

Searches for New physics

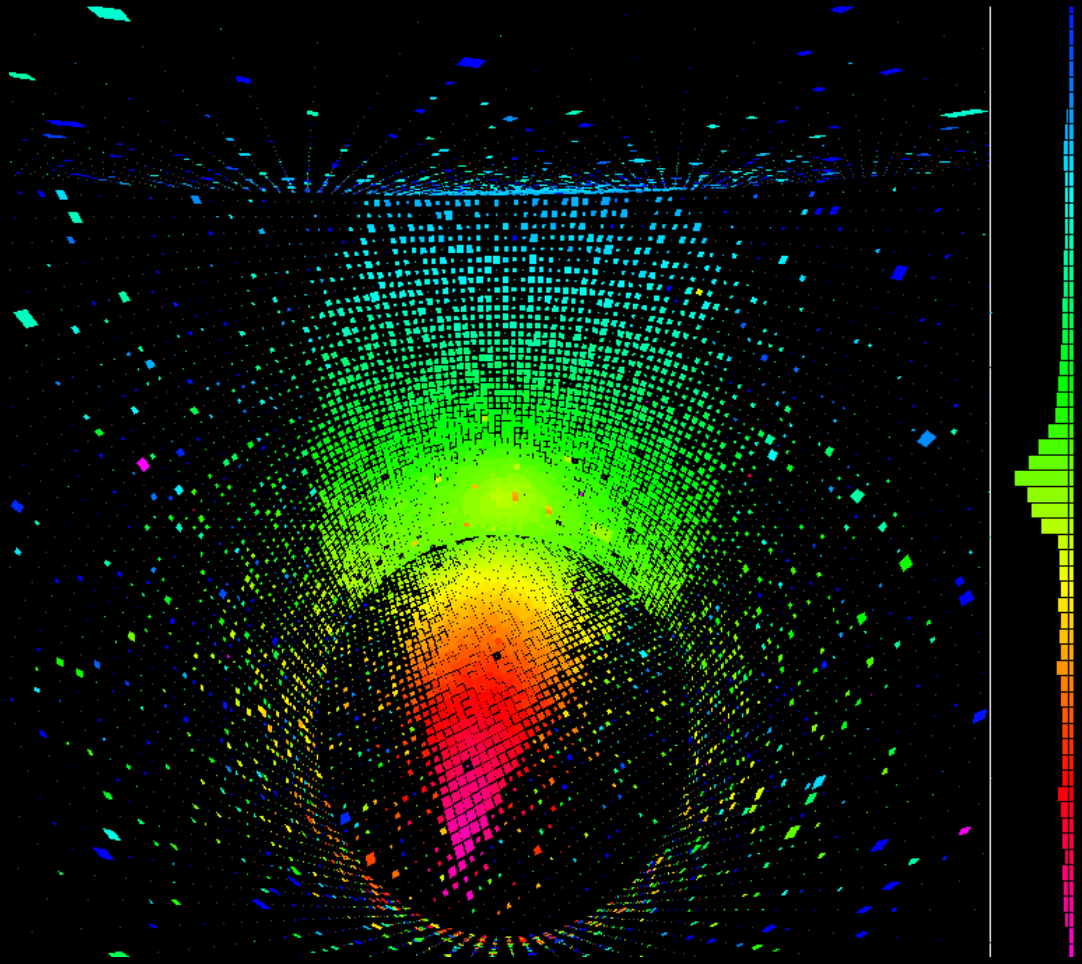

"Standard set" of non-standard physics

ν_{sun}

Steriles *

NSI *

Interactions with DM

Decays

Magnetic moments W

Decoherence

Long range forces

Violation of fundamental symmetries W

~ E^n

Lorentz CPT

* - motivated by the present tensions

New physics

$H = H_{st} + H_{np}$ in most of the cases

Decoherence - density matrix

Classification:

More neutrino States: steriles, anti-nu

Modification of the potential

Decoherence
Inelastic collisions
absorption

Signatures:

Spectra distortions
Time dependence
Appearance of antineutrins

Previous bound, essentially: $H_{NP} < H_{st}$

Now $H_{NP} \ll H_{st}$

New physics effects

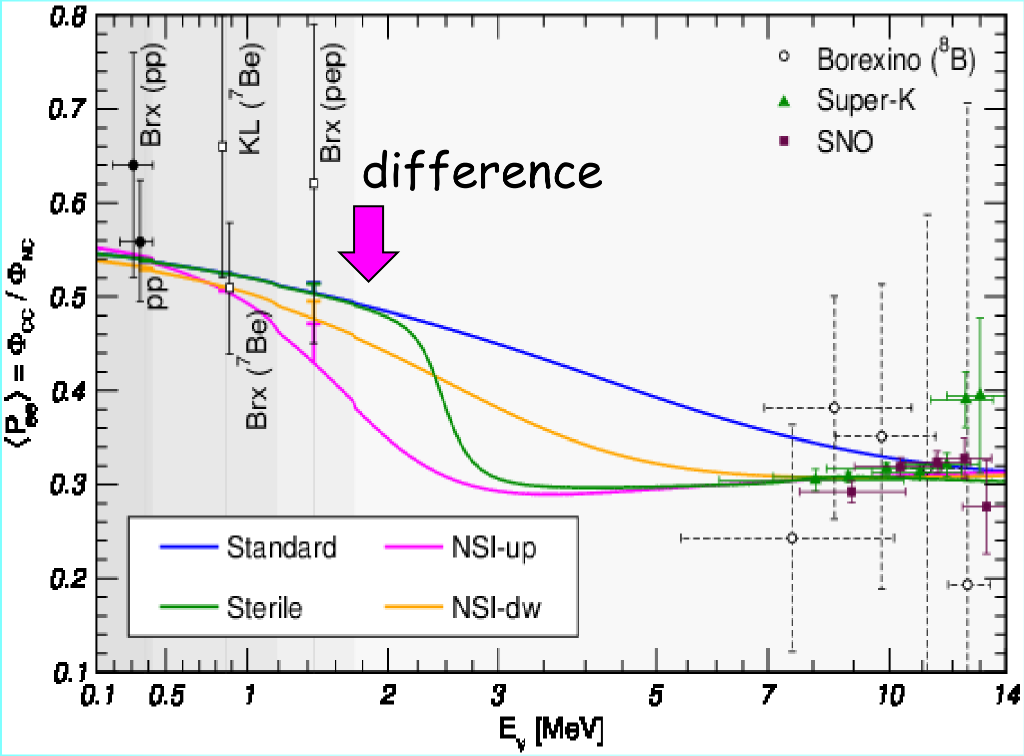

M. Maltoni, A.Y.S.
1507.05287 [hep-ph]

Extra sterile neutrino with
$\Delta m^2_{01} = 1.2 \times 10^{-5}$ eV^2, and
$\sin^2 2\alpha = 0.005$

Non-standard interactions with
$\varepsilon^u_D = -0.22$, $\varepsilon^u_N = -0.30$
$\varepsilon^d_D = -0.12$, $\varepsilon^d_N = -0.16$

Also enhances the
D-N asymmetry

meV sterile neutrino

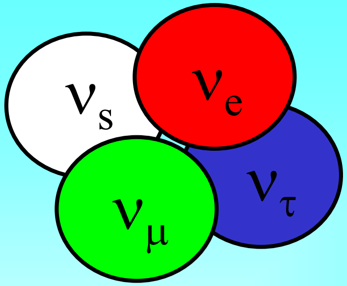

sterile neutrino m_0 ~ 0.003 eV

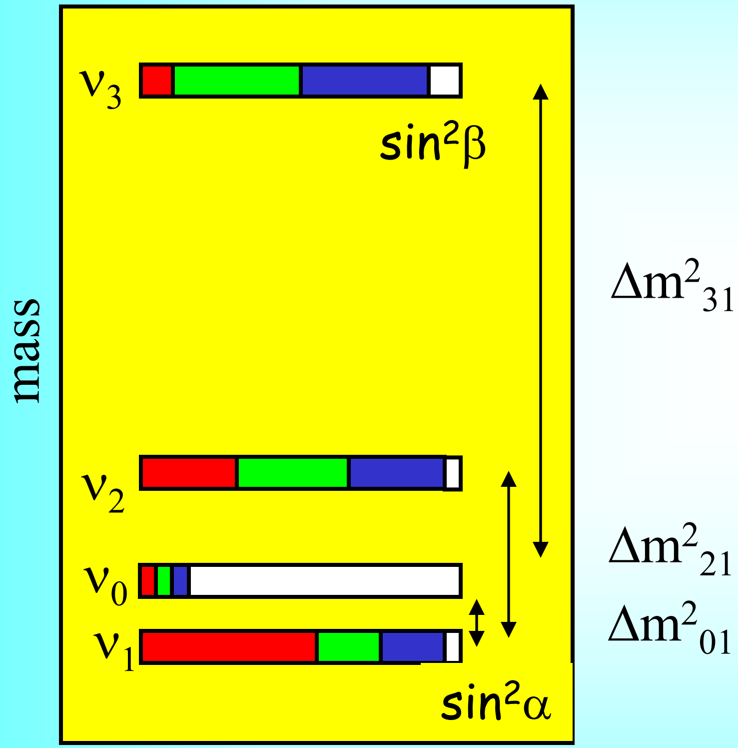

For solar nu: $\sin^2 2\alpha \sim 10^{-3}$

Conversion for small mixing angle - Adiabaticity violation

Allows to explain absence of upturn and reconcile solar and KAMLAND mass splitting but not large D-N asymmetry

Additional radiation in the Universe

$\Delta N_{eff} \sim 0.1$

Searches for this sterile in atmospheric neutrinos if mixes with ν_3

Non-standard interactions

Additional contribution to the matrix of potentials in the Hamiltonian

M C. Gonzalez-Garcia , M. Maltoni arXiv 1307.3092

$$V_{NSI} = \sqrt{2}\, G_F\, n_f \begin{pmatrix} \varepsilon^f{}_D & \varepsilon^f{}_N \\ \varepsilon^f{}_N & \varepsilon^f{}_D \end{pmatrix} \qquad f = e, u, d$$

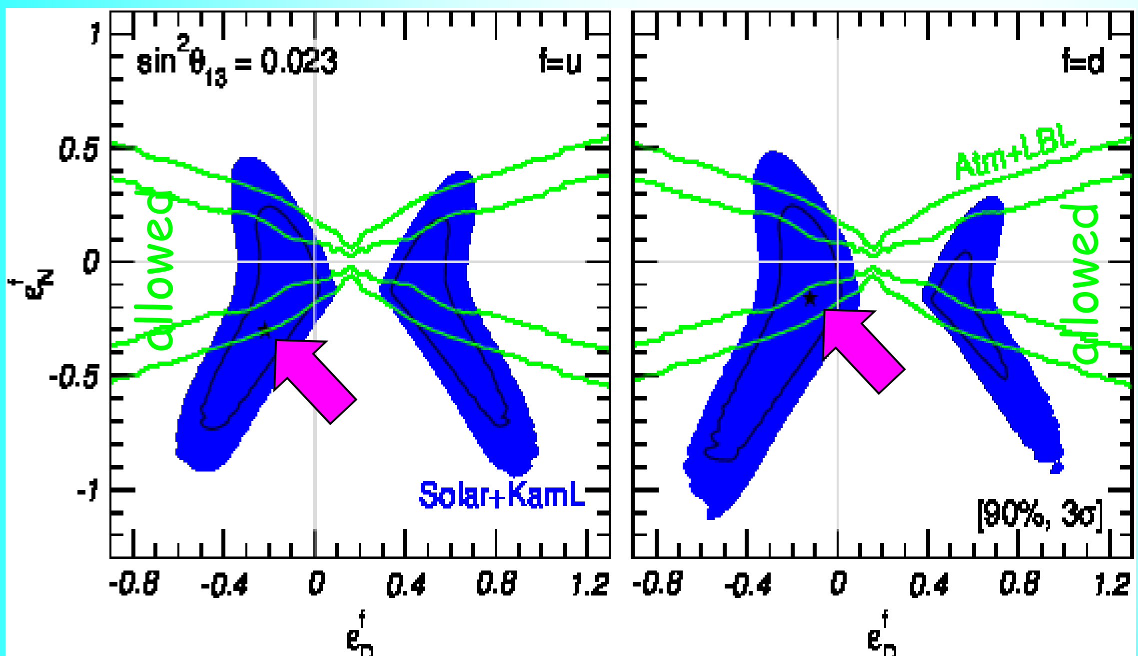

Allowed regions of parameters of NSI

Removing tension:

$V_{NSI} = 0.6\, V_e$

⇒ $\varepsilon \sim 0.2$

In the best fit points the D-N asymmetry is 4 - 5%

NSI

Update including COHERENT

I. Esteban, et al. arXiv:1805.04530

The 1σ, 90%, 2σ, 99% and 3σ CL (2 dof.) allowed regions for the NSI parameters from solar and KamLAND data for different values of the quark composition parameter η

$$\varepsilon_{\alpha\beta}{}^{f} = \varepsilon_{\alpha\beta}{}^{\eta}\ \xi^{f}$$

$\tan\eta = \frac{1}{2} \rightarrow \quad \xi^{u} = 1$

$\tan\eta = 2 \rightarrow \quad \xi^{d} = 1$

Shaded green areas - 90% and 3σ CL allowed regions from the atmospheric and LBL data.

$\sin^2 2\theta_{13} = 0.022$

zoomed

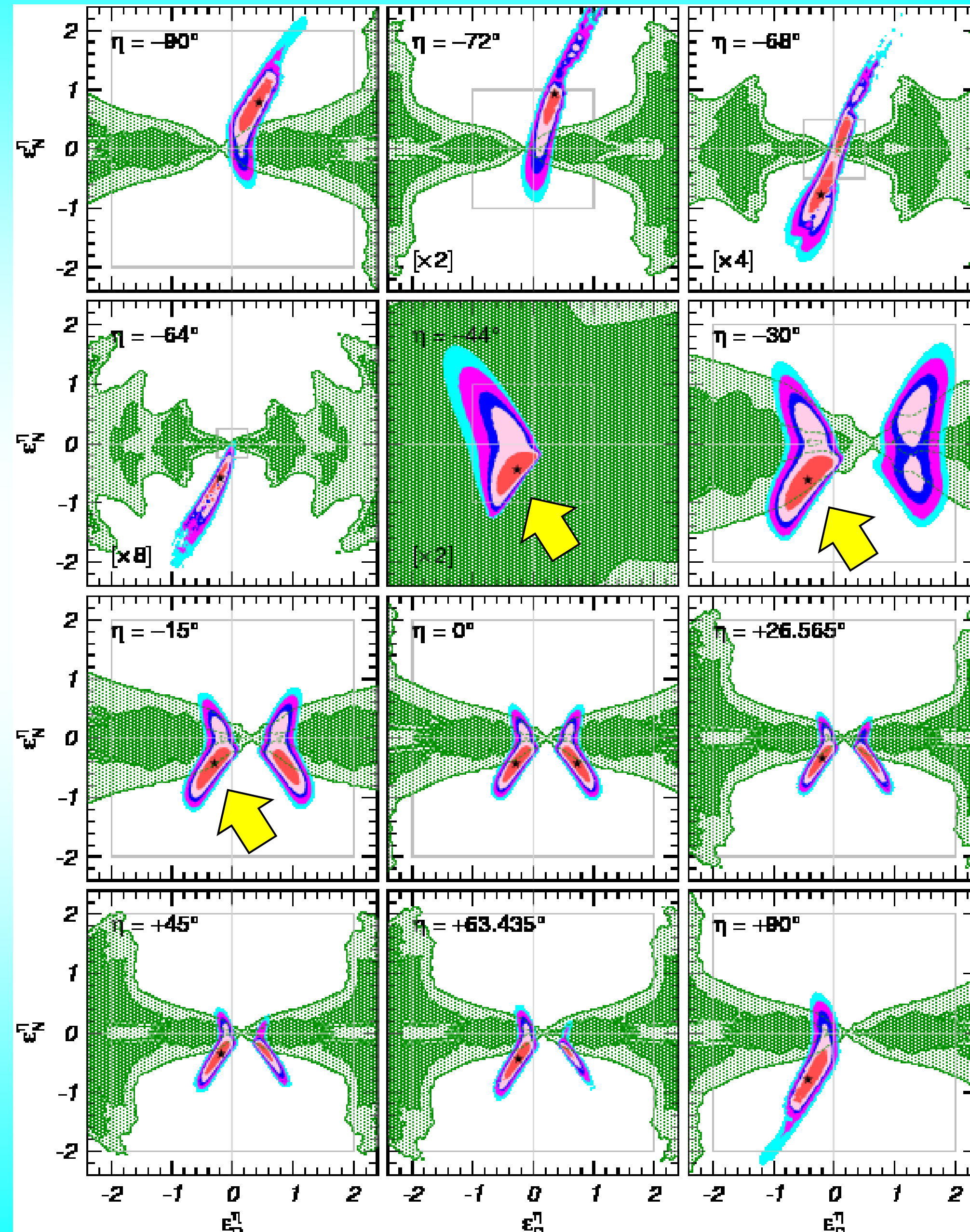

SK-analysis of NSI

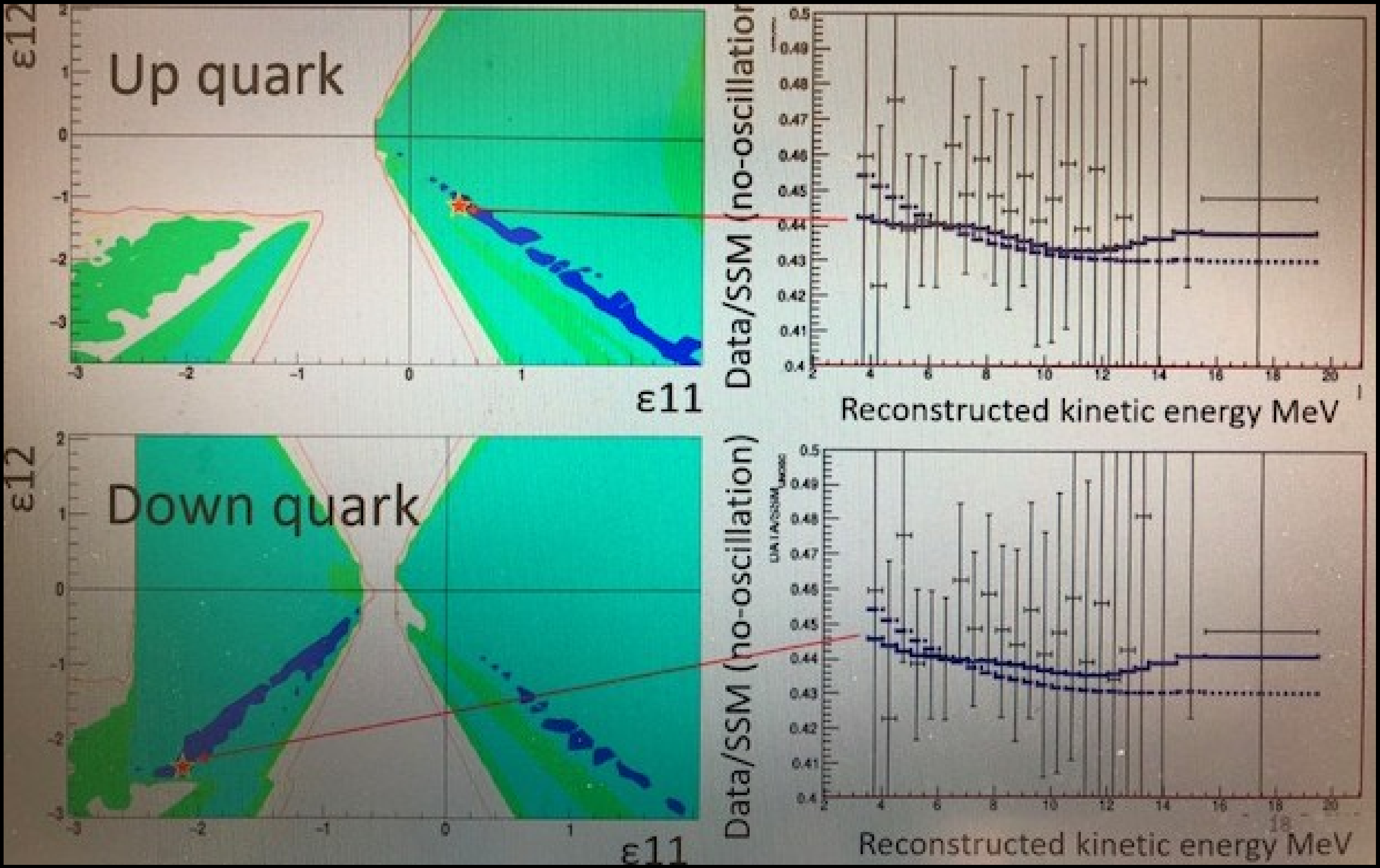

LMA-Dark solution

O.G. Miranda, M.A. Tortola, J. W. F. Valle, JHEP 19 (2006) 008 hep-ph/0406280

Scaling:

$\Delta m_{21}^2 \rightarrow -\Delta m_{21}^2, \quad V \rightarrow -V$

→ invertion 1-2 ordering

P. B. Denton, et al. arXiv:1804.03660 [hep-ph]

$$V_{\alpha\beta}^f = 2V_e \, \varepsilon_{\alpha\beta} \frac{n_f}{n_e}$$

Equivalently, mixing is not changed if

$\cos 2\theta_{12} \rightarrow -\cos 2\theta_{12}, \quad V \rightarrow -V$

$\sin^2 \theta_{21} \rightarrow 1 - \sin^2 \theta_{21}$ dark side: 0.69

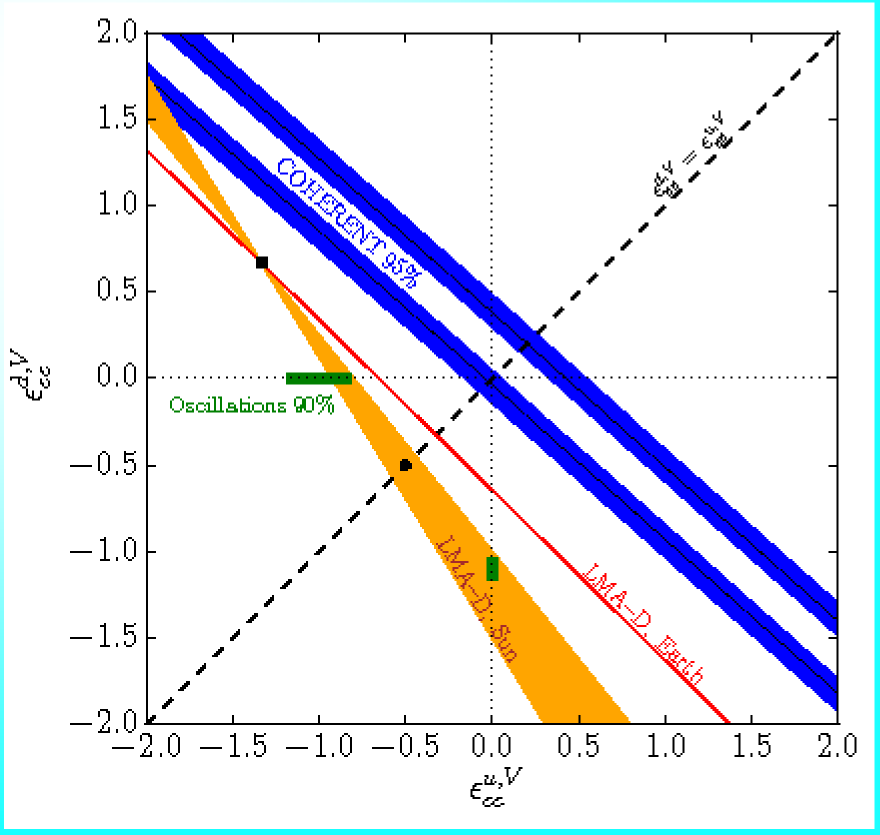

Change of sign of the potential requires NSI

$V = V_e + V_{NSI}$

$V_{NSI} = -2V_e$

Bounds on NSI

P. Coloma, M.C. Gonzalez-Garcia, M. Maltoni, T. Schwetz, 1708.02899 [hep-ph]

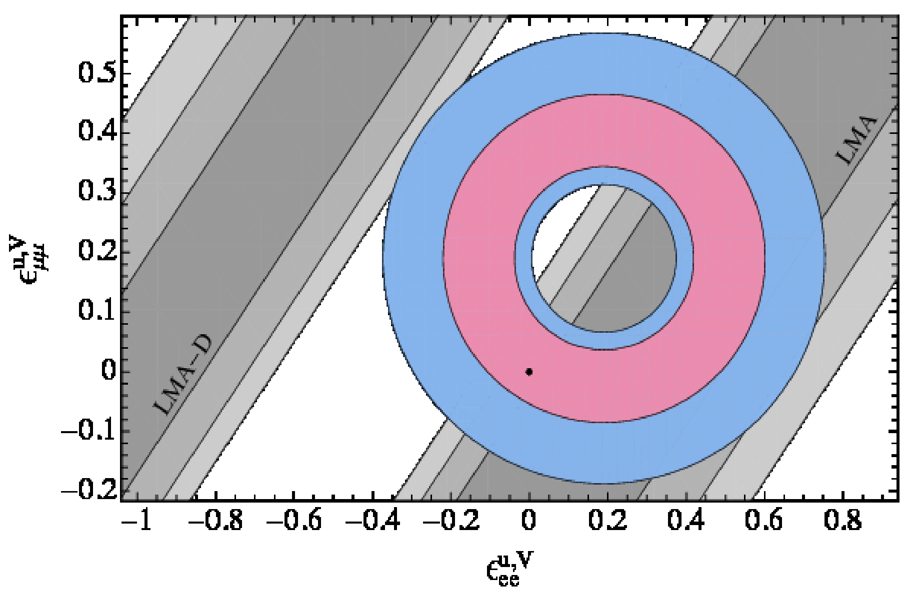

Allowed regions from the COHERENT experiment and allowed regions from the global oscillation fit.

Diagonal shaded bands correspond to the LMA and LMA-D regions as indicated, at 1σ, 2σ, 3σ (2~dof).
The COHERENT regions are at 1σ and 2σ only. 3σ region extends beyond the boundaries of the figure

MSW-Dark can agree with data at 3σ - level

BOREXINO: NSI interactions

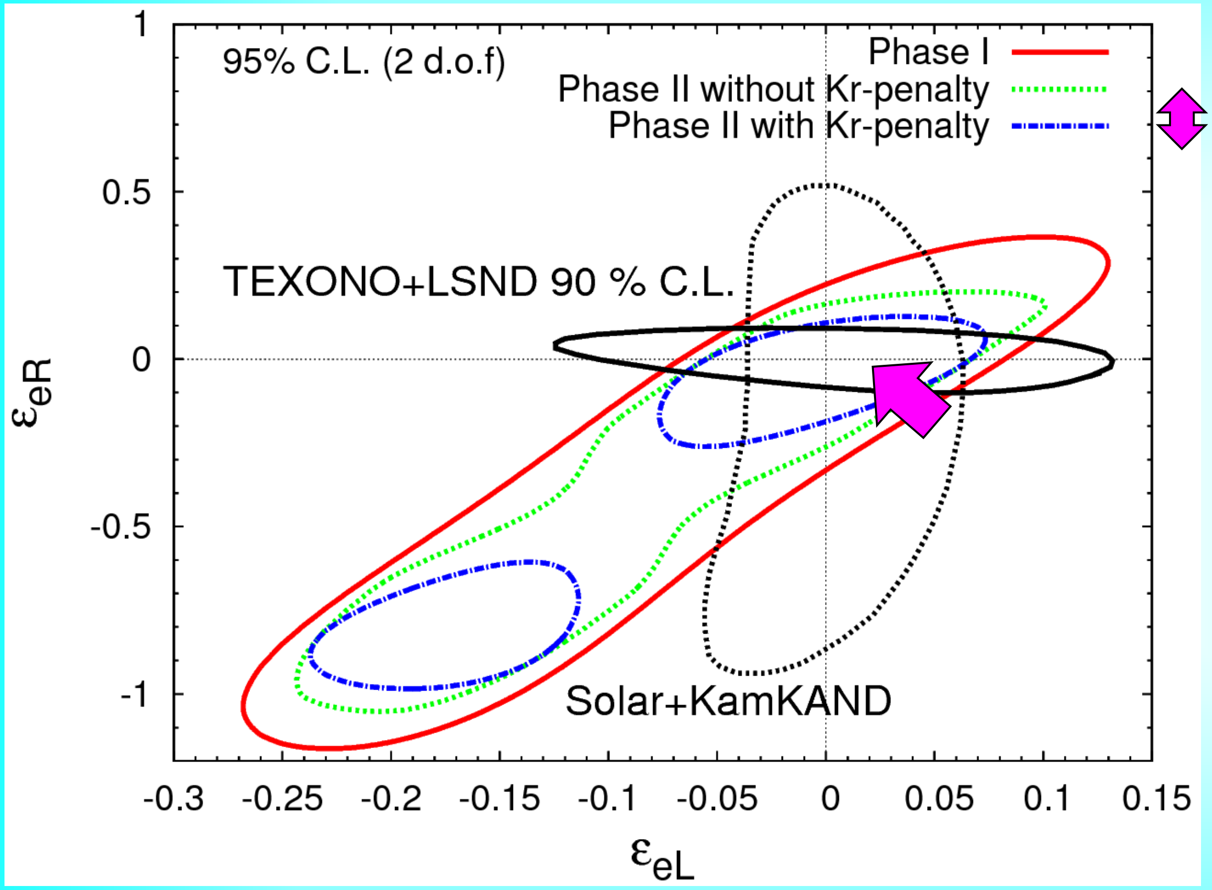

S. Agarwalla

Excludes
1.6 bigger potential,
dark solution on
electrons

ε_e < 0.05 - 0.1

NSI on DM + mixing with sterile

Solar Neutrinos as a Probe of Dark Matter-Neutrino Interactions - F. Capozzi, et al. JCAP 1707 (2017) no.07, 021 arXiv:1702.08464 [hep-ph]

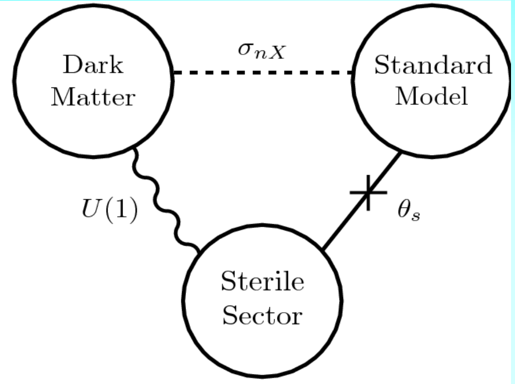

$$\xi = \frac{G_X\, n_X(0)}{V_e(0)}$$ potential on DM

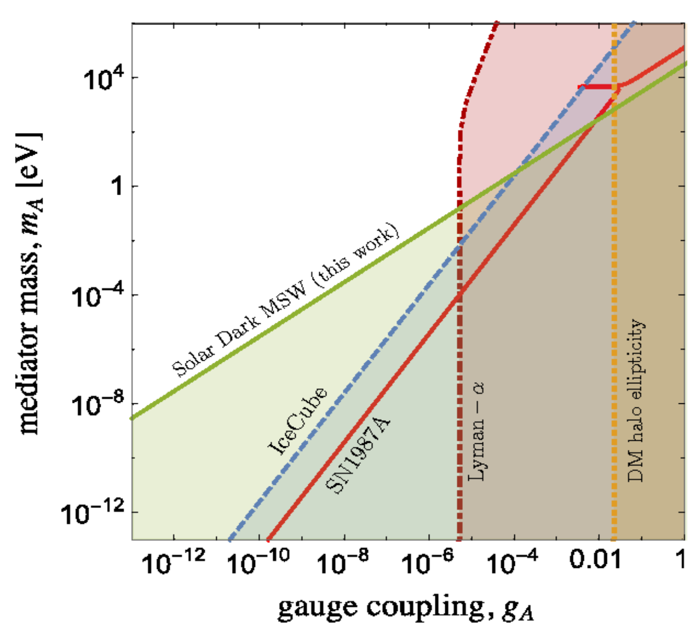

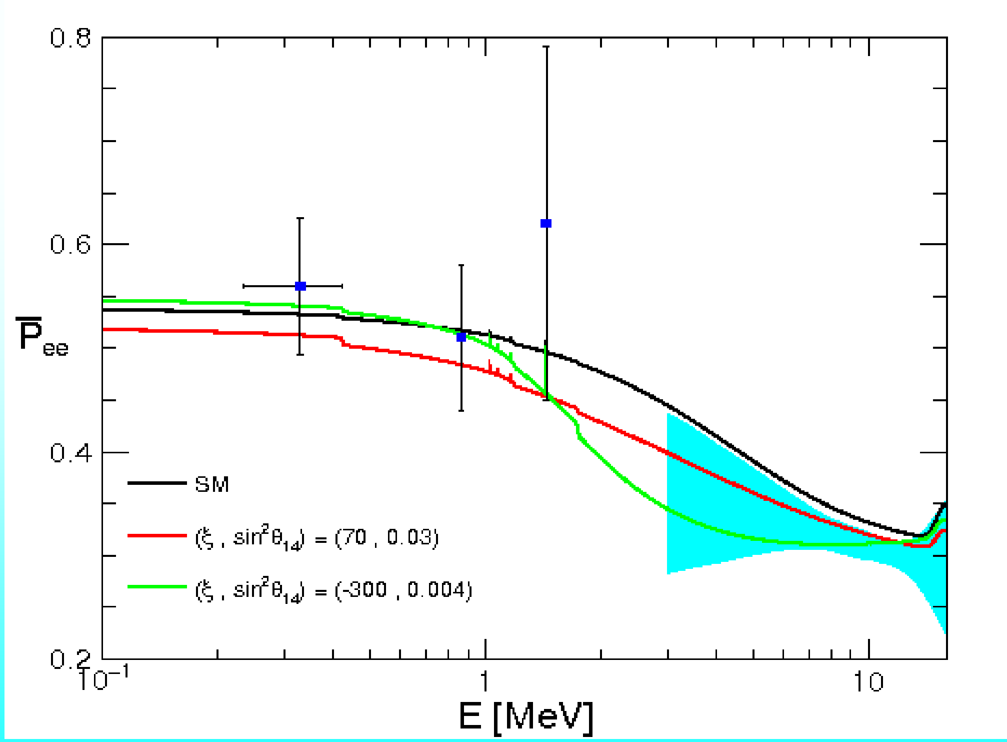

Neutrino decay

Decays of neutrino eigenstates in vacuum and matter

$\nu_i \to \nu_x + \phi$ $x = j, s$ ϕ - light scalar

Neglecting decay in
- the central regions of the Sun and
- the Earth

$$P_{ee} = \Sigma_{i=1,2,3} |U_{ei}^m(n_0)|^2 P_{ie}\, e^{-d_i L/E}$$

$d_i = m_i / \tau_i$ life time at rest $P_{ie} = |U_{ie}|^2$

L – distance from the central parts of the Sun to a detector

$E/L = 10^{-12}\ eV^2 (E/1\ MeV)$ determines sensitivity to d_i :

for $d_i = E/L$ the ν_i flux is suppressed by 2.7

$d_1 < 1.3\ 10^{-13}\ eV^2$

$d_2 < 1.2\ 10^{-12}\ eV^2$ $\tau > 10^{-5}$ sec

d_3 is essentially unsuppressed due to small 1-3 mixing

Conclusion

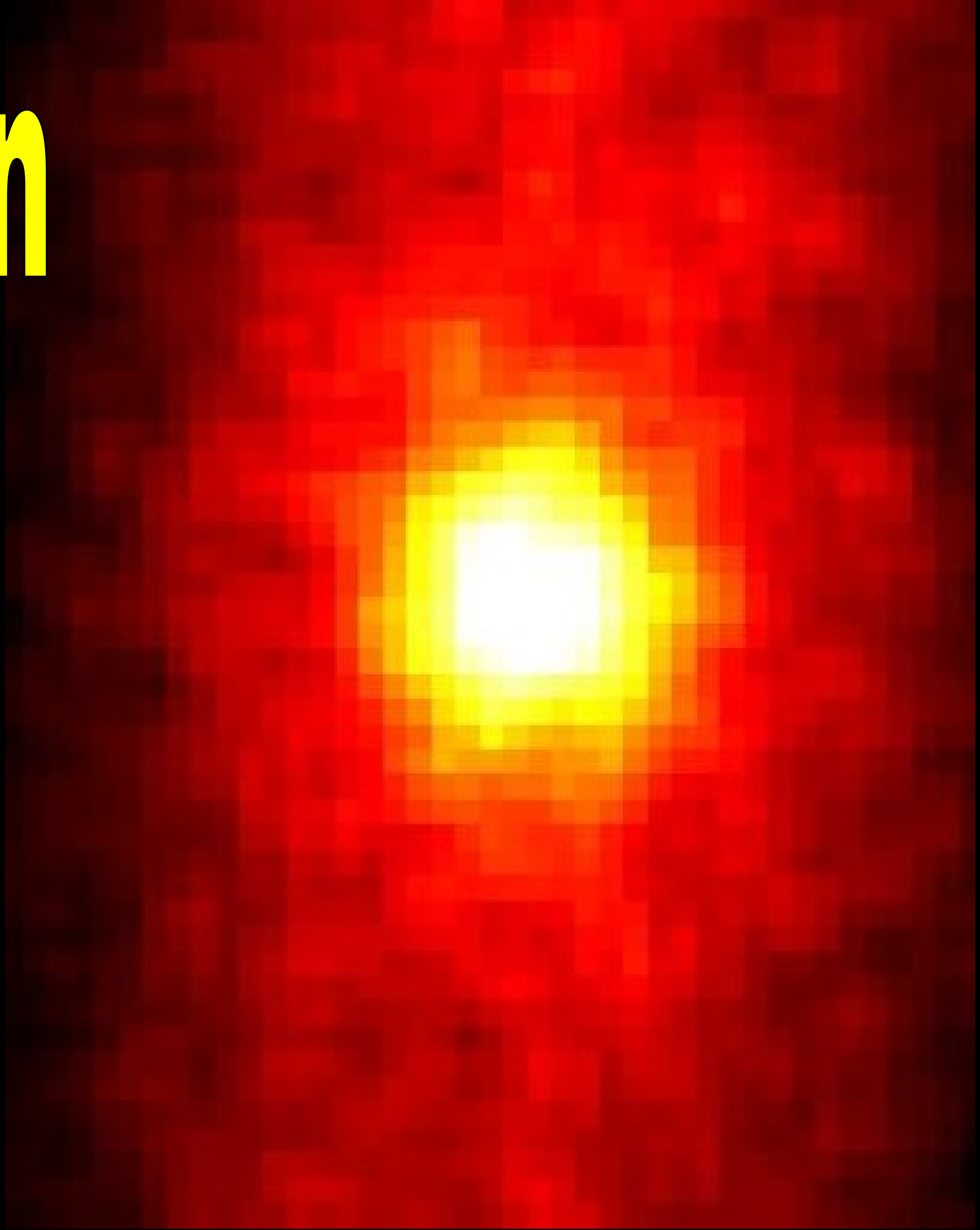

LMA MSW is in a good agreement with all available data

Future: detailed study of oscillations in the Earth - intersting physics (multilayer medium, parametric effects, interference of waves "emitted from different borders between layers", attenuation. Potentially: tomography of the Earth

(1.8σ) - tension related to absence of the spectral up-turn and larger DN asymmetry (1.3 σ) can be expressed as difference of Δm^2_{21} or equivalently, 1.6 times larger matter potential

Still sub-leading effects are possible. O(1) can be realized with certain fine tuning.

NSI can remove both tensions light sterile neutrino – correct the upturn only. More precise measurements of the DN asymmetry can distinguish two possibilities

With achieved precisionnew physics effects at the level of 10% or smaller can be studied with the solar neutrinos

Attenuation effect

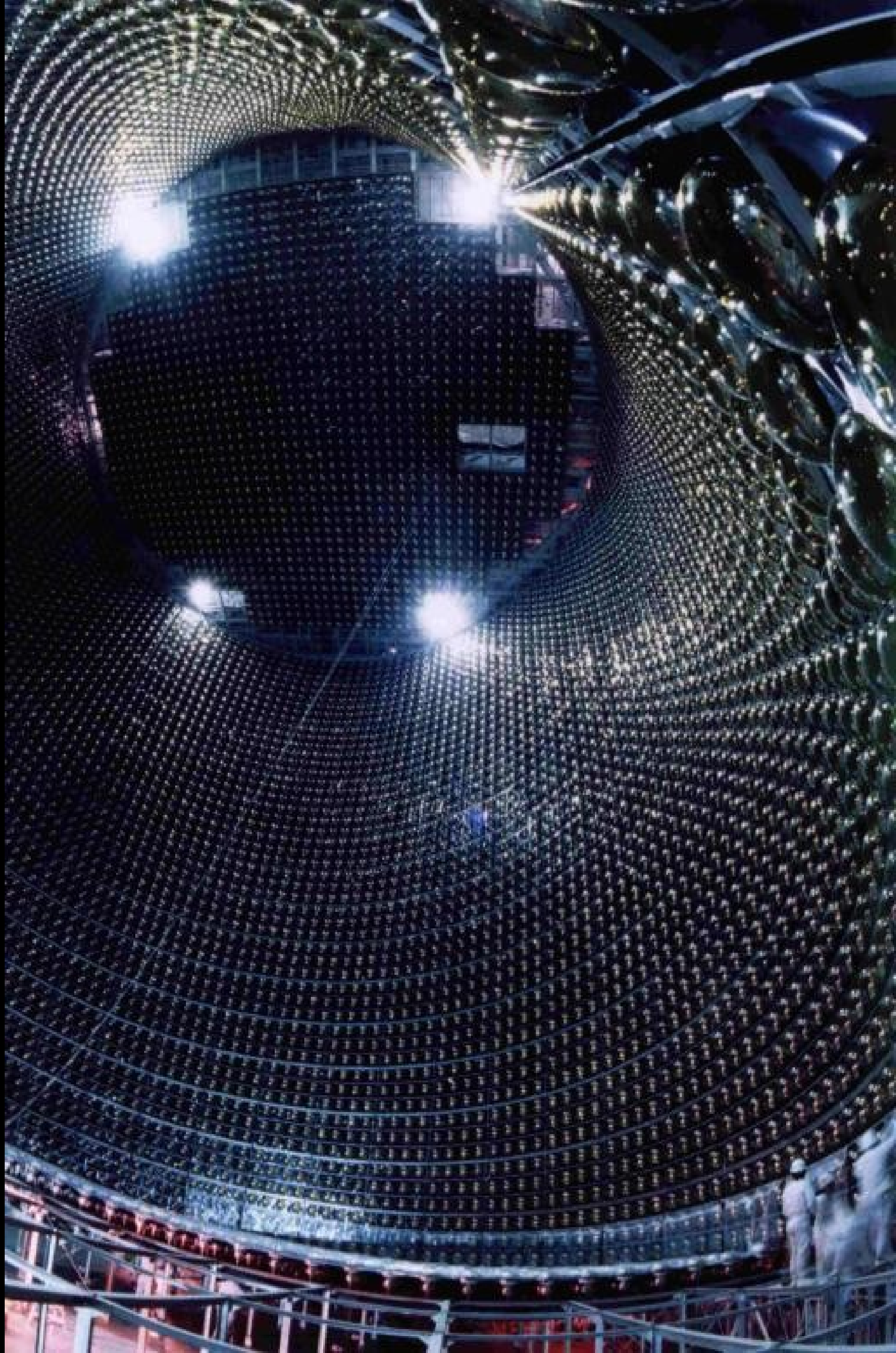

JinPing underground lab

scintillator uploaded
water detectors?

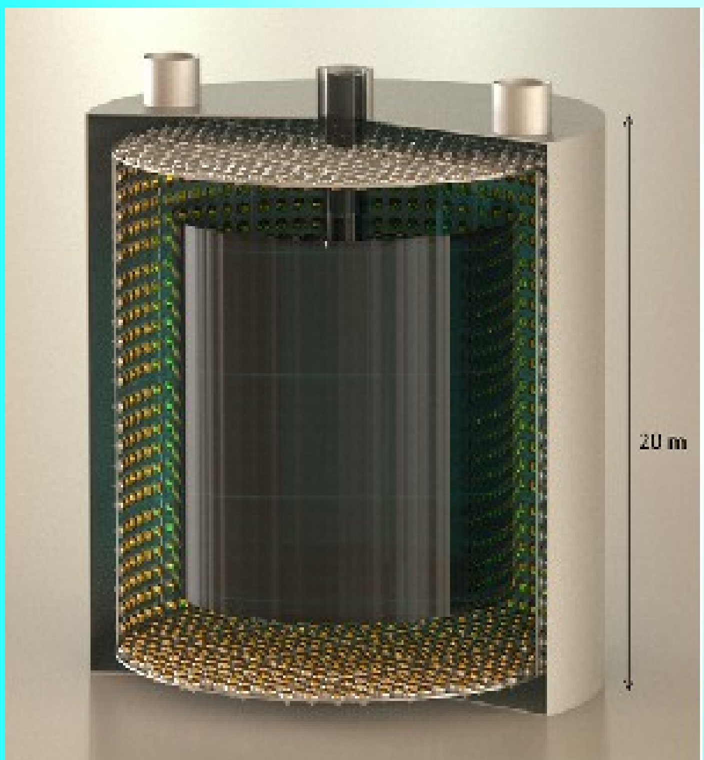

FV: 100 times bigger than BOREXINO

Deeper than SNO

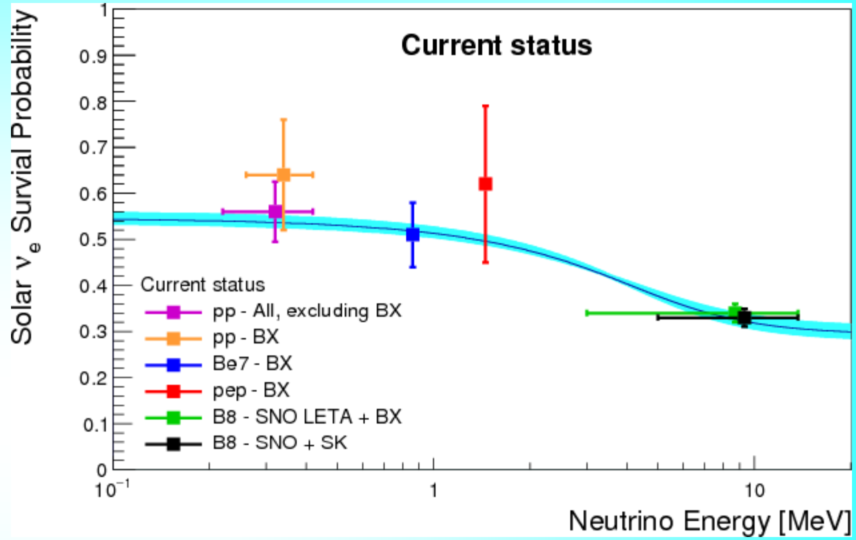

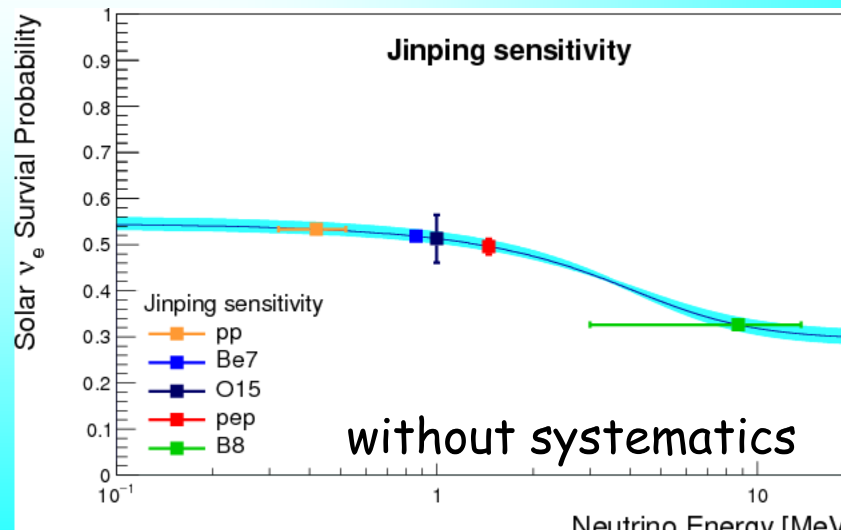

References

A. Ioannisian, A. Smirnov, D. Wyler,
Phys.Rev. D96 (2017) no.3, 036005
arXiv:1702.06097 [hep-ph]

A.N. Ioannisian, A. Yu. Smirnov
Phys.Rev. D96 (2017) no.8, 083009
arXiv:1705.04252 [hep-ph]

DUNE solar neutrino events

A. Ioannisian, A. Smirnov, D. Wyler,
Phys.Rev. D96 (2017) no.3, 036005
arXiv:1702.06097 [hep-ph]

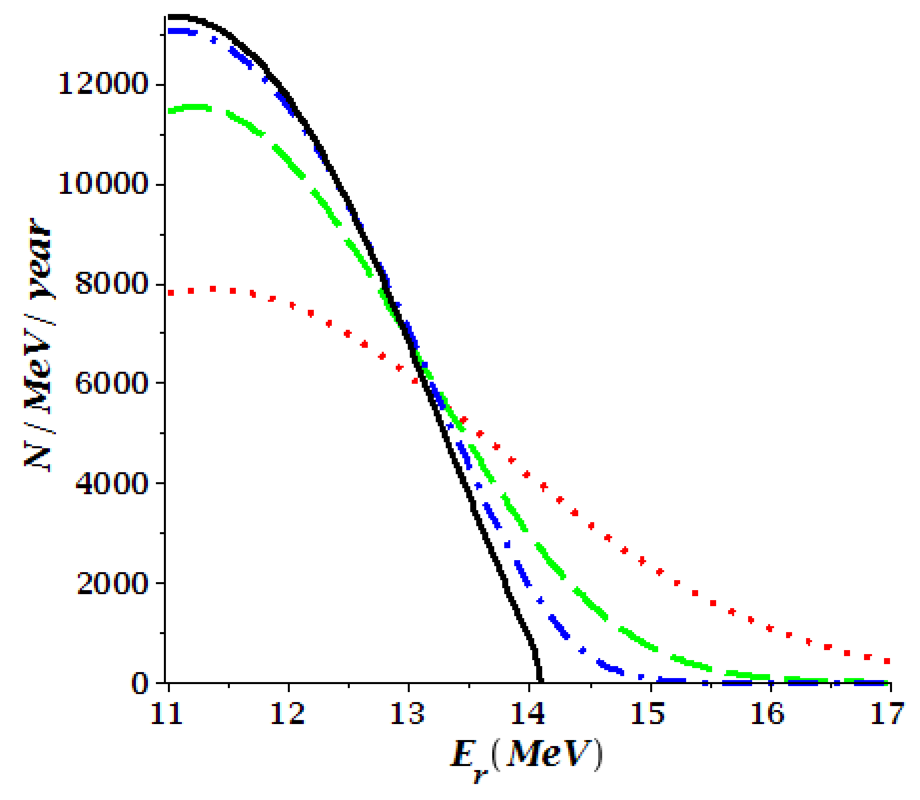

The energy (*ER*) distribution of the annually detected events at DUNE for different energy resolutions *σE*. The solid (black) line represents perfect resolution, *σE*=0, the other lines correspond to *σE*=0.5 MeV - dash-dotted (blue) line, *σE*=1 MeV dashed (green) line, *σE*=2 MeV dotted (red) line. The distributions are normalized to annual number of events 27000 at *Er*> 11 MeV.

Day-Night asymmetry

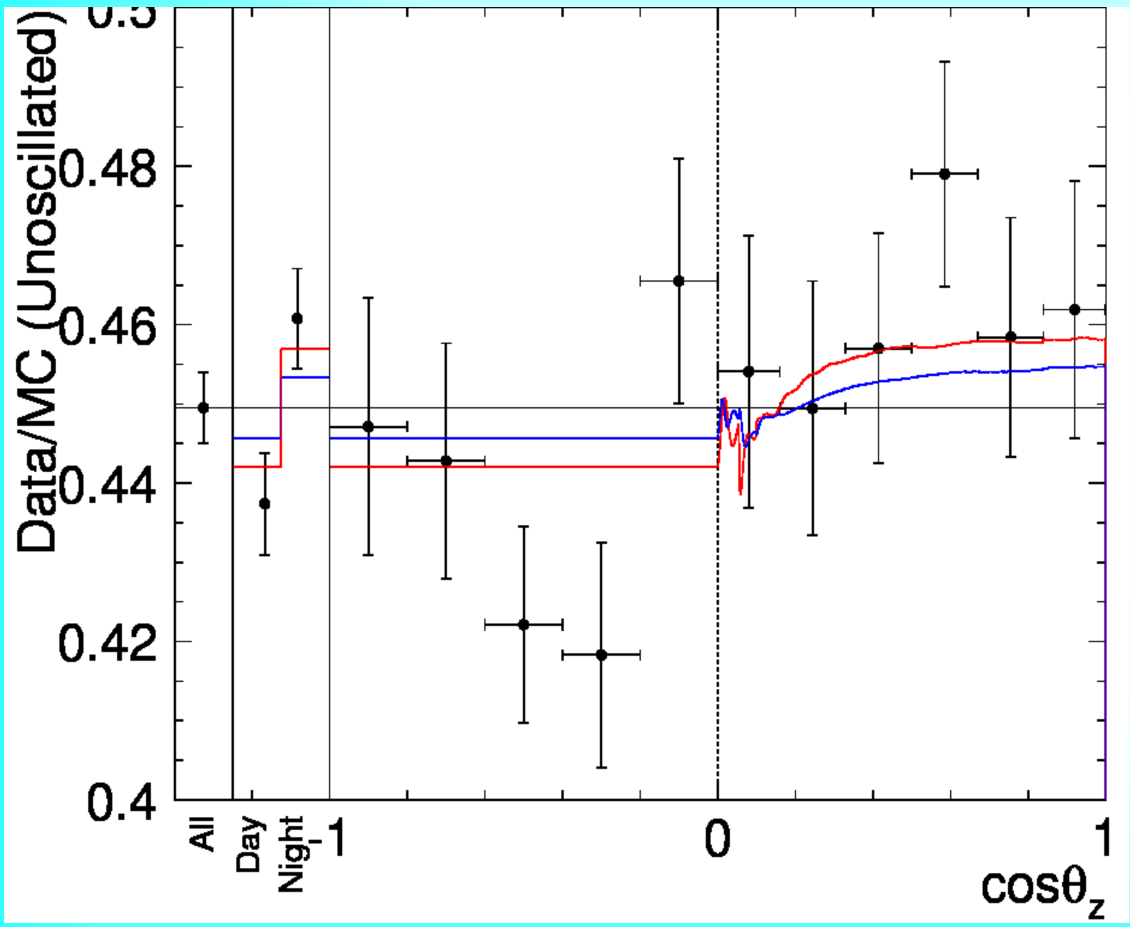

SK-IV solar zenith angle dependence of the solar neutrino data/MC (unoscillated) interaction rate ratio (4.49-19.5 MeV). Red (blue) lines are predictions when using the solar neutrino data (solar neutrino data+KamLAND) best-fit oscillation parameters. The error bars are statistical uncertainties only.

BOREXINO - Solar

Borexino Collaboration (Agostini, M. et al.) arXiv:1707.09279 [hep-ex]

G. Bellini
B. Caccianiga

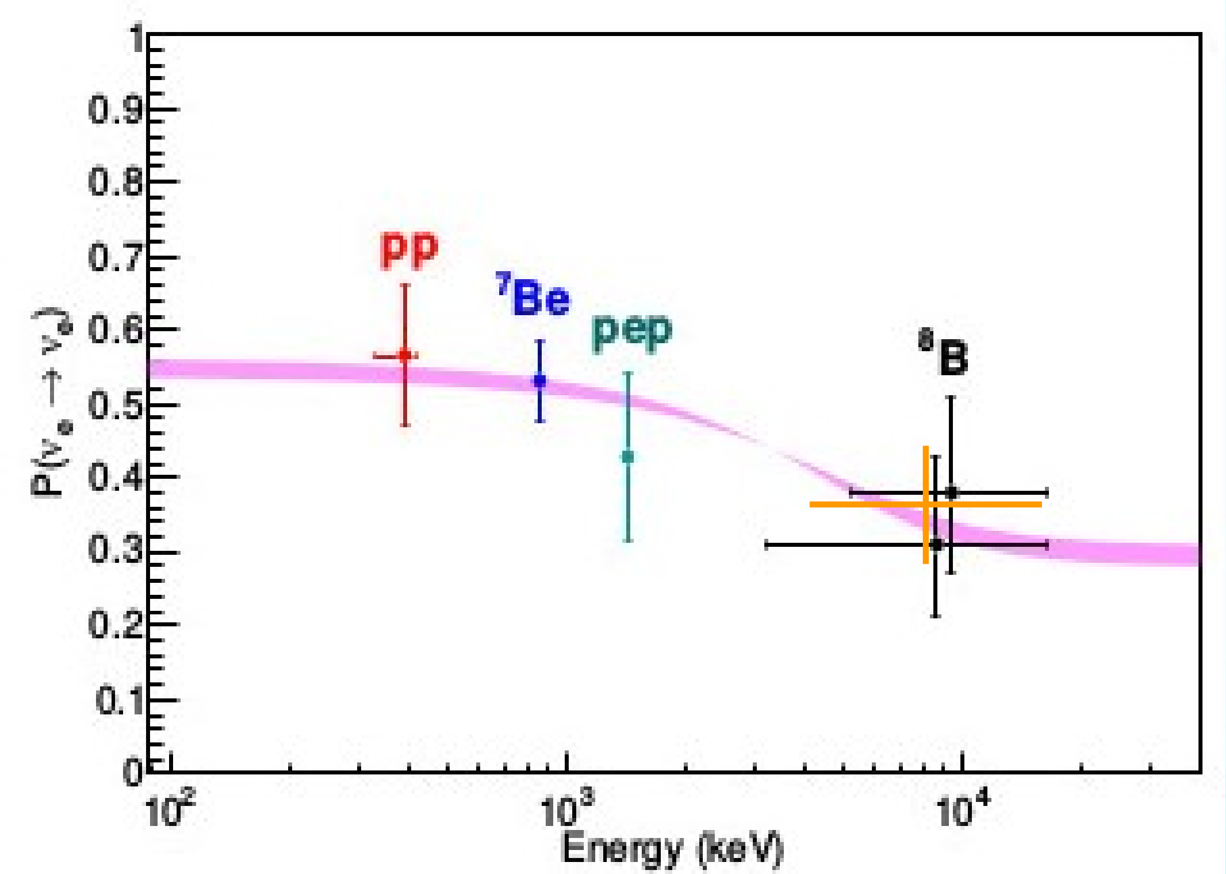

Energy profile of the effect is determined by mixing in matter in production point + oscillations inside the Earth

D. Franco

Scaring agreement

Problems in details
% level precision

Attenuation

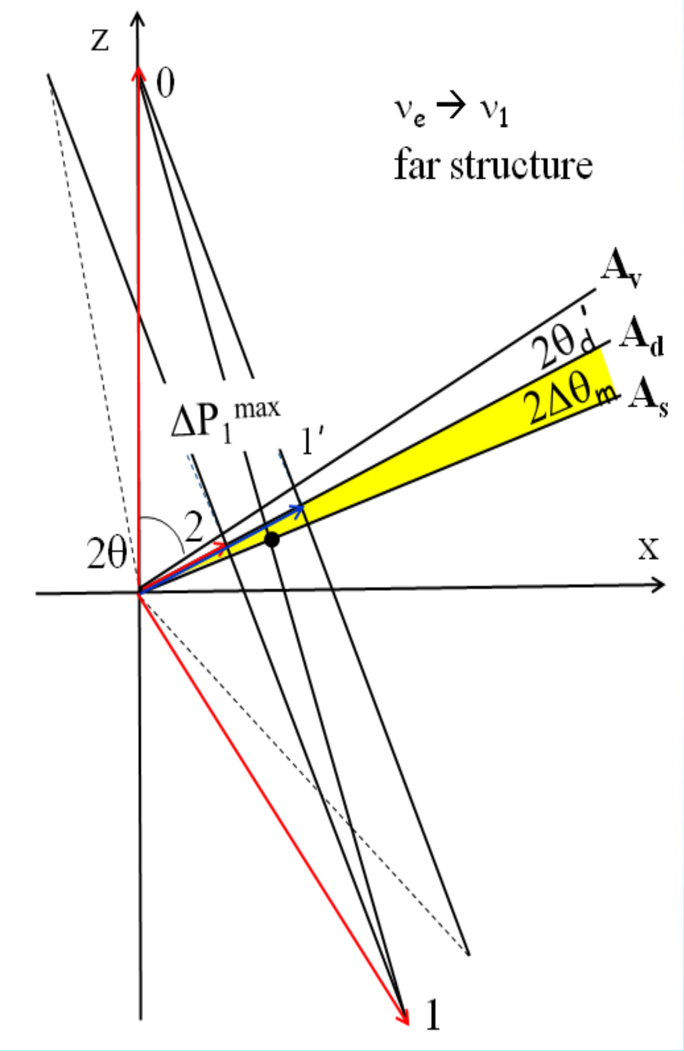

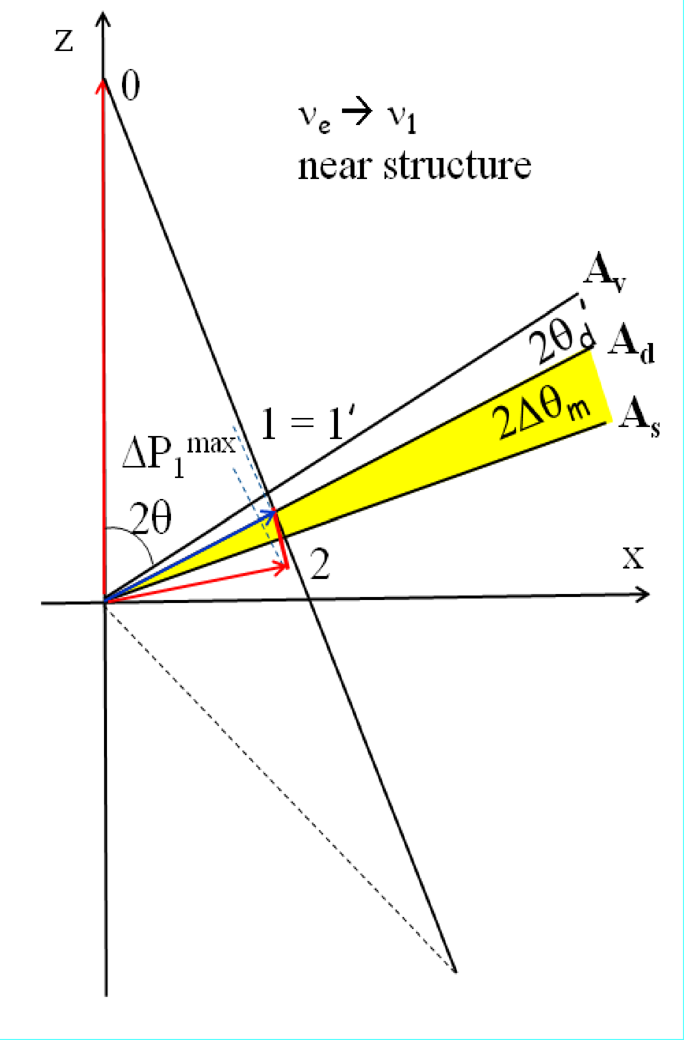

no attenuation

Graphic representation

Spin of electron
in magnetic field

Oscillations

Adiabatic conversion

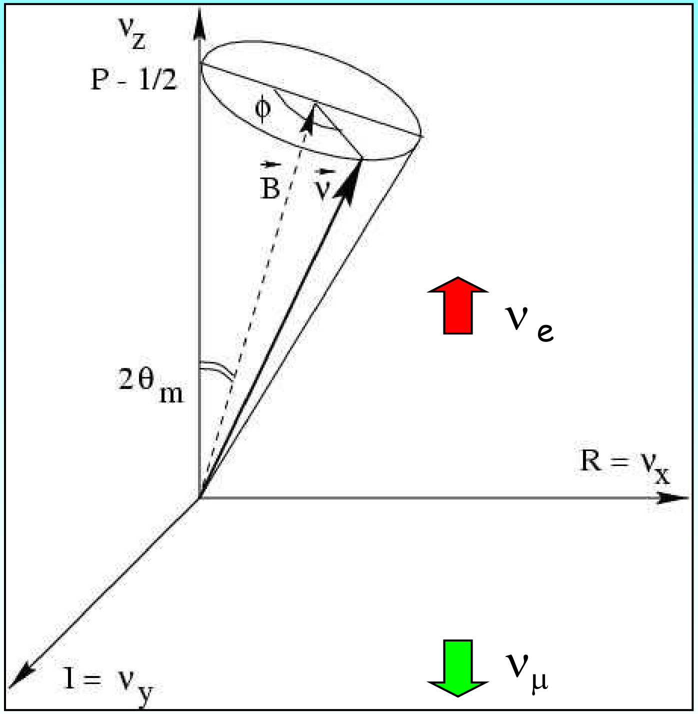

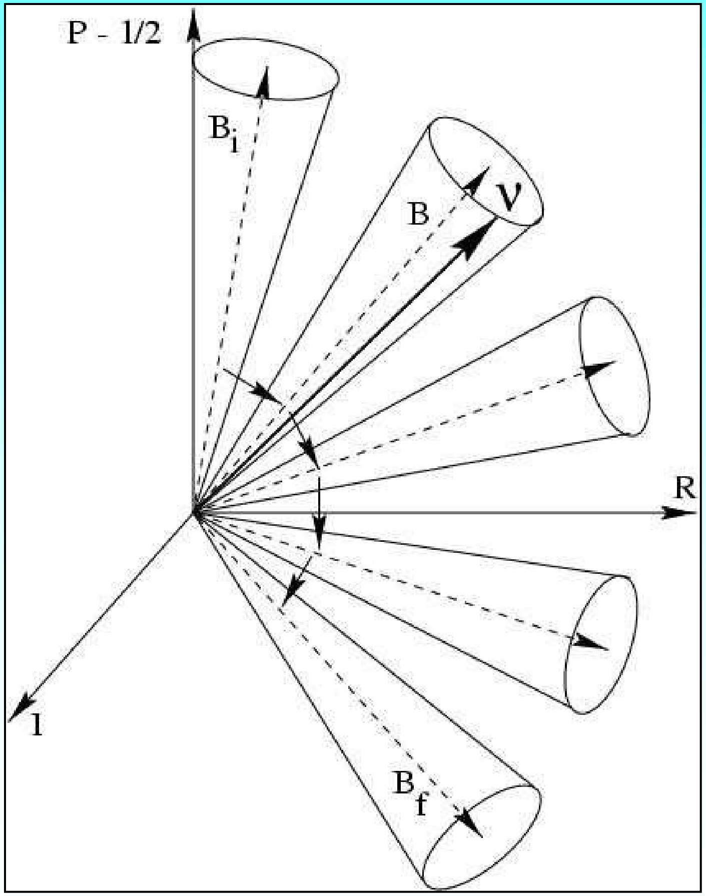

Resonance

Dependence of mixing on density, energy has a resonance character

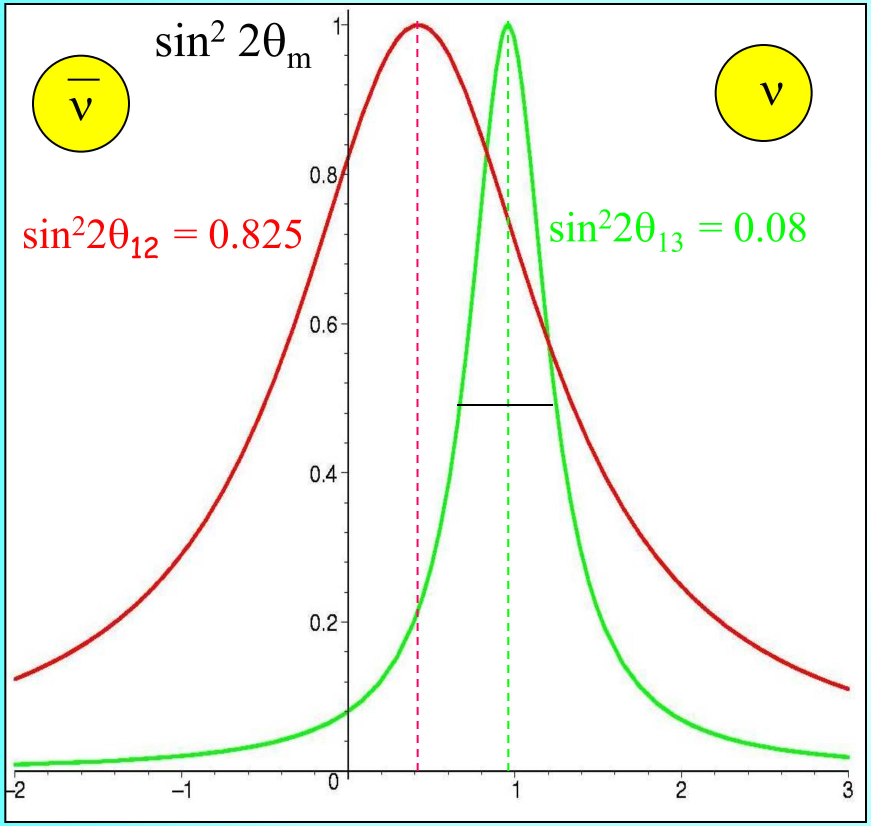

In resonance: $\sin^2 2\theta_m = 1$

Flavor mixing is maximal

$l_\nu = l_0 \cos 2\theta$

Vacuum oscillation length $\approx$ Refraction length

Resonance width: $\Delta n_R = 2 n_R \tan 2\theta$

density $l_\nu / l_0 \sim n E$

$\theta_m \to 0$ $\theta_m = \theta$ $\theta_m = \pi/4$ $\theta_m \to \pi/2$

Mixing is suppressed at high densities $|V| \gg \frac{\Delta m^2}{2E}$ ⇒ Flavor states coincide with eigenstates and vice versa

Oscillations versus MSW

Adiabatic conversion

Different degrees of freedom involved

Oscillations

Vacuum or uniform medium with constant parameters

Phase difference increases between the eigenstates

$\phi(t)$

Mixing does not change

Adiabatic conversion

Non-uniform medium or/and medium with varying in time parameters

Change of mixing in medium → change of flavor of the eigenstates

$\theta_m(t)$

Phase is irrelevant

In non-uniform medium: interplay of both processes

NSI

Two-dimensional projections of
the 1σ, 90\%, 2σ, 99\% and 3σ CL
(2~dof) allowed regions from the analysis
of solar
and KamLAND data in the presence of
non-standard matter potential for
the oscillation parameters (θ12,\Dmq21)
after after marginalizing over the NSI
parameters and for θ13 fixed to
sin2θ13=0.022.
The best-fit point is marked with a star.
The results are shown for fixed values of
the NSI quark coupling
parameter η. For comparison the
corresponding allowed regions for the
analysis in terms of 3ν oscillations without
NSI are shown as black void contours.c

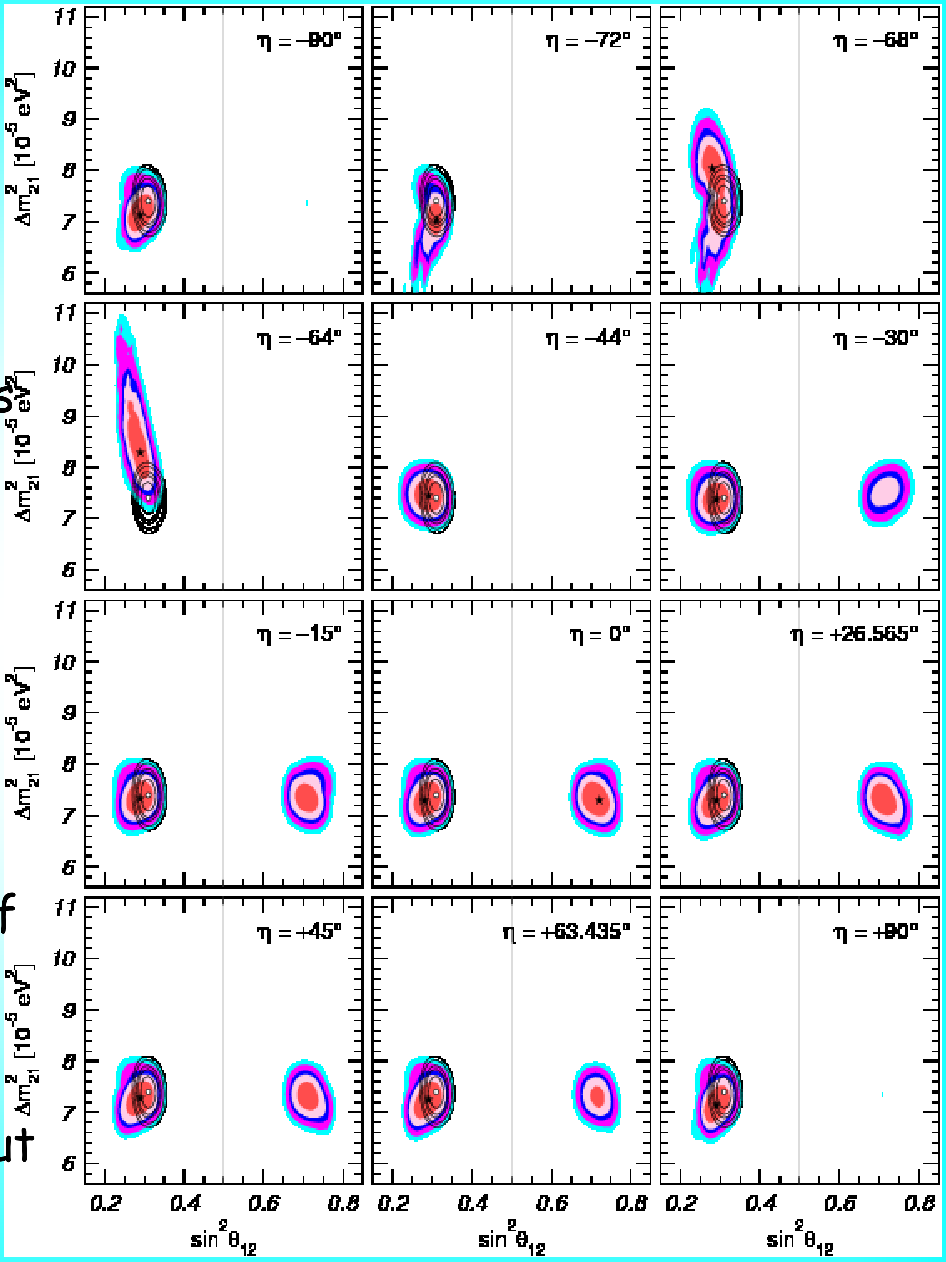

NSI

90\% and 3σ CL (1~dof) allowed ranges from the analysis of solar and KamLAND data in the presence of non-standard neutrino-matter interactions, for the four relevant parameters (the matter potential parameters \EpsηD and \EpsηN as well as the oscillation parameters \Dmq21 and sin2θ12) as a function of the NSI quark coupling parameter η, for sin2θ13=0.022. In each panel the three undisplayed parameters have been marginalized.

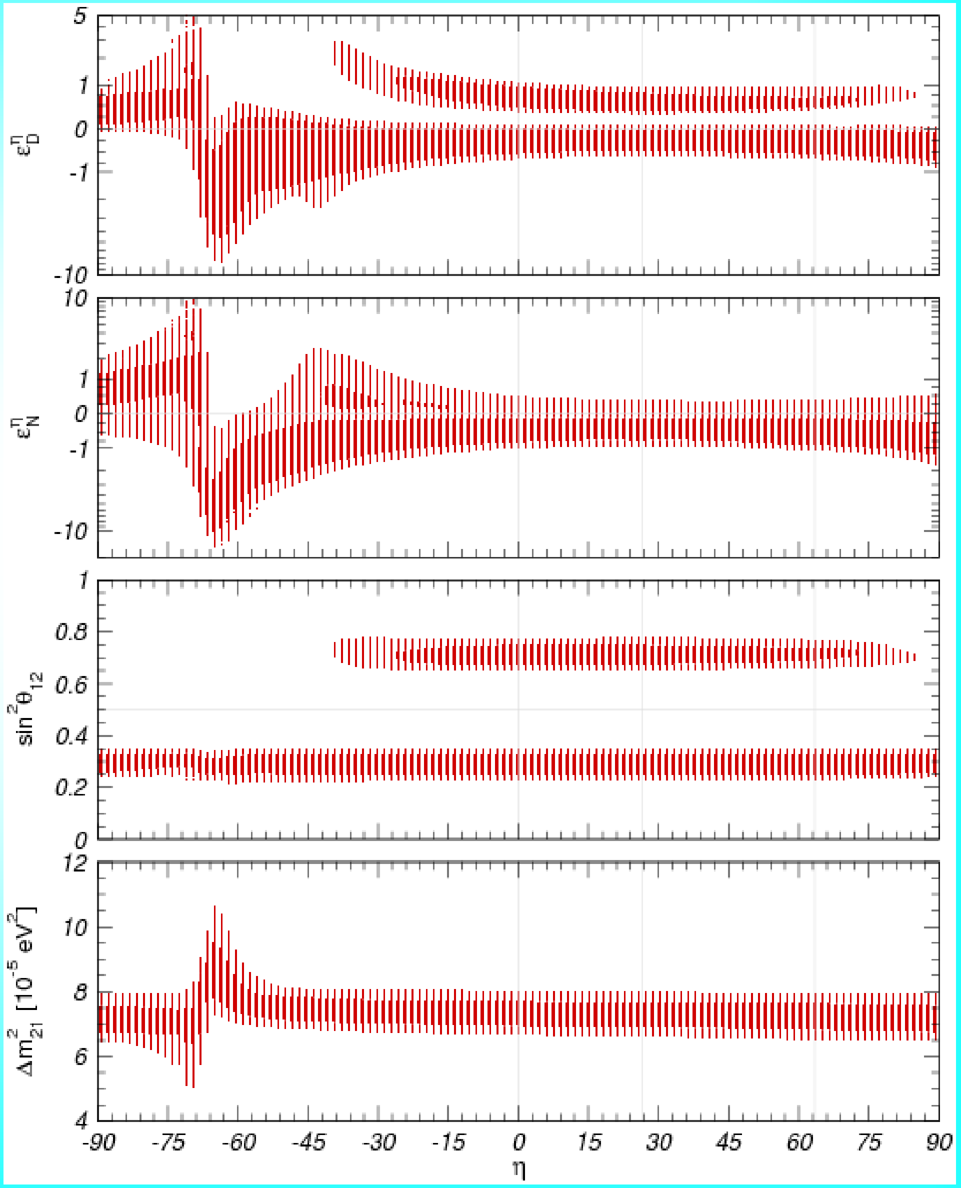

Non-oscillatory transition

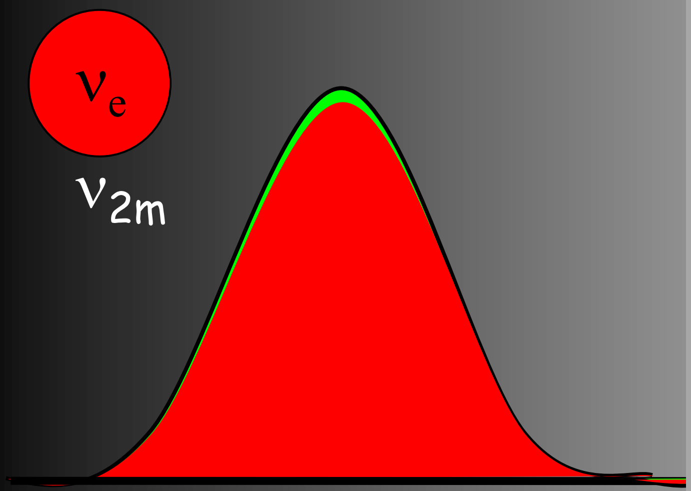

Single eigenstate:
→ no interference
→ no oscillations
→ phase is irrelevant

This happens when mixing is very small in matter with very high density

Adiabaticity

Adiabaticity condition $\left|\frac{d\theta_m}{dt}\right| \ll H_{2m} - H_{1m}$

External conditions (density) change slowly the system has time to adjust them

transitions between the neutrino eigenstates can be neglected

$\nu_{1m} \not\leftrightarrow \nu_{2m}$ ⇒ The eigenstates propagate independently

Shape factors of the eigenstates do not change

Crucial in the resonance layer:

- the mixing changes fast
- level splitting is minimal

Adiabaticity condition $\Delta r_R > l_R$ if vacuum mixing is small

$\Delta r_R = n_R \tan 2\theta \,/\, (dn/dx)_R$ — width of the resonance layer

$l_R = l_\nu \,/\, \sin 2\theta$ — oscillation length in resonance

Attenuation and focusing?

$2\Delta\theta_m = 2\theta_s' - 2\theta_d'$

$J_m = \sin 2\Delta\theta_m \sim \varepsilon$

mass
oscillation: ε
projection: ε

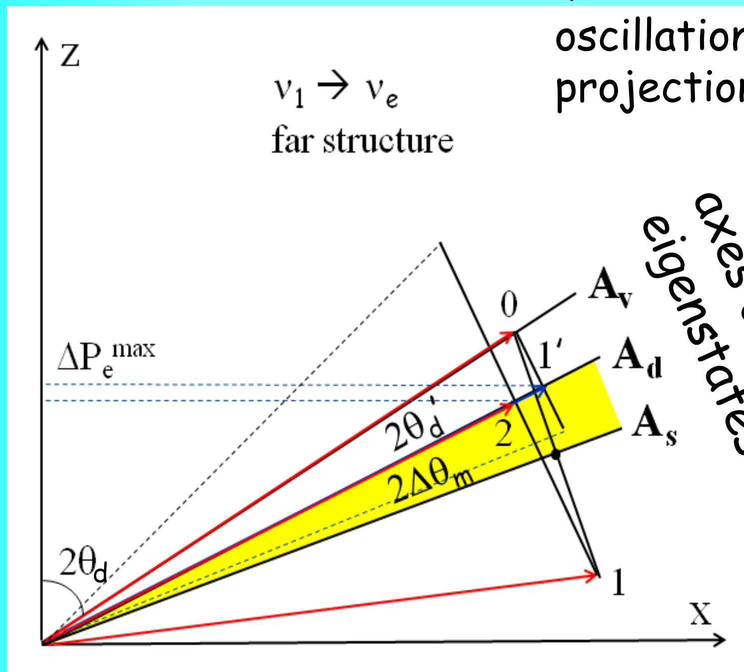

axes of eigenstates

mass
projection: 1
oscillation: ε

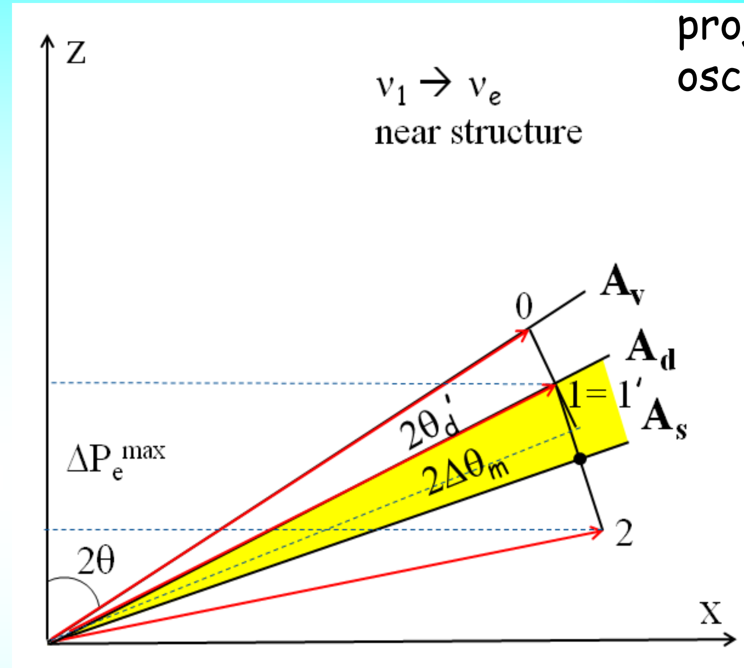

$\Delta P_e^{max} = \cos 2\theta_d \ \sin 2\theta_s' \ J_m \sim \varepsilon^2$

$\Delta P_e^{max} = \cos 2\theta_d' \ \sin 2\theta_s \ J_m \sim \varepsilon$

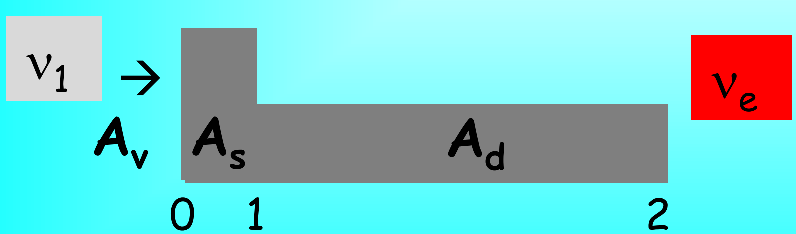

structure attenuation layer detector

LMA-D

Data Denton, Peter B. et al.
arXiv:1804.03660 [hep-ph]

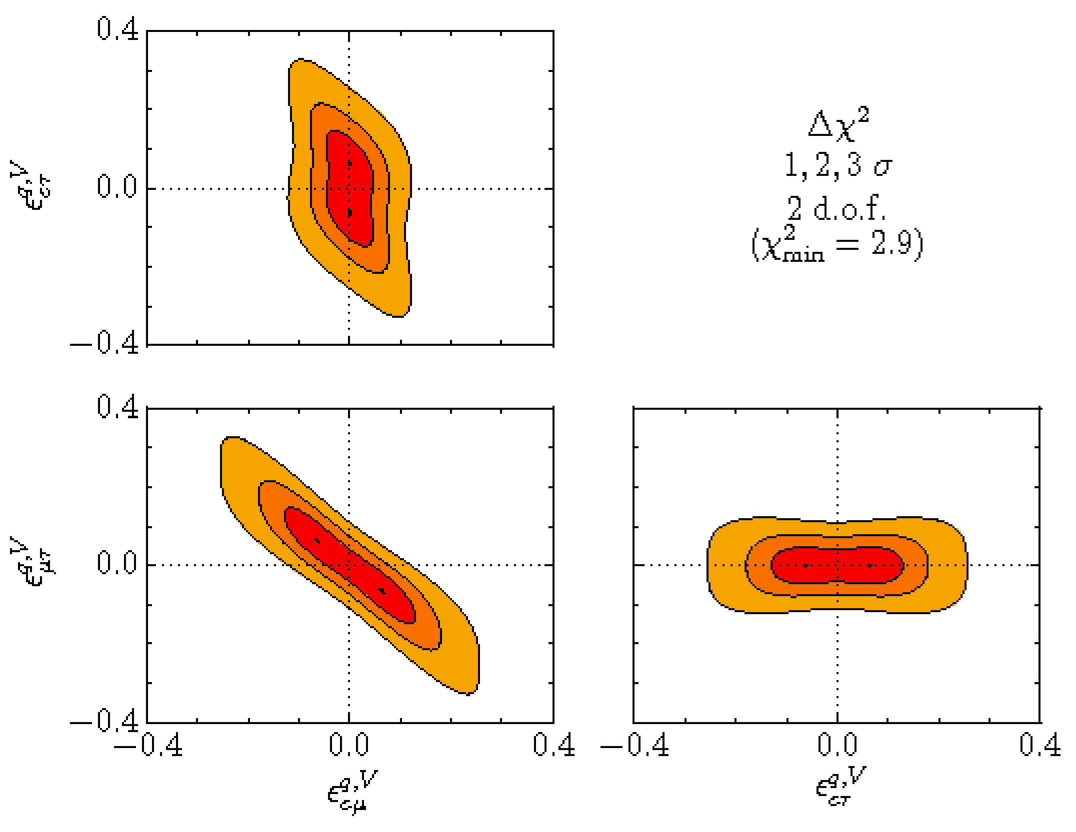

Distinguishing metallicity models with neutrinos

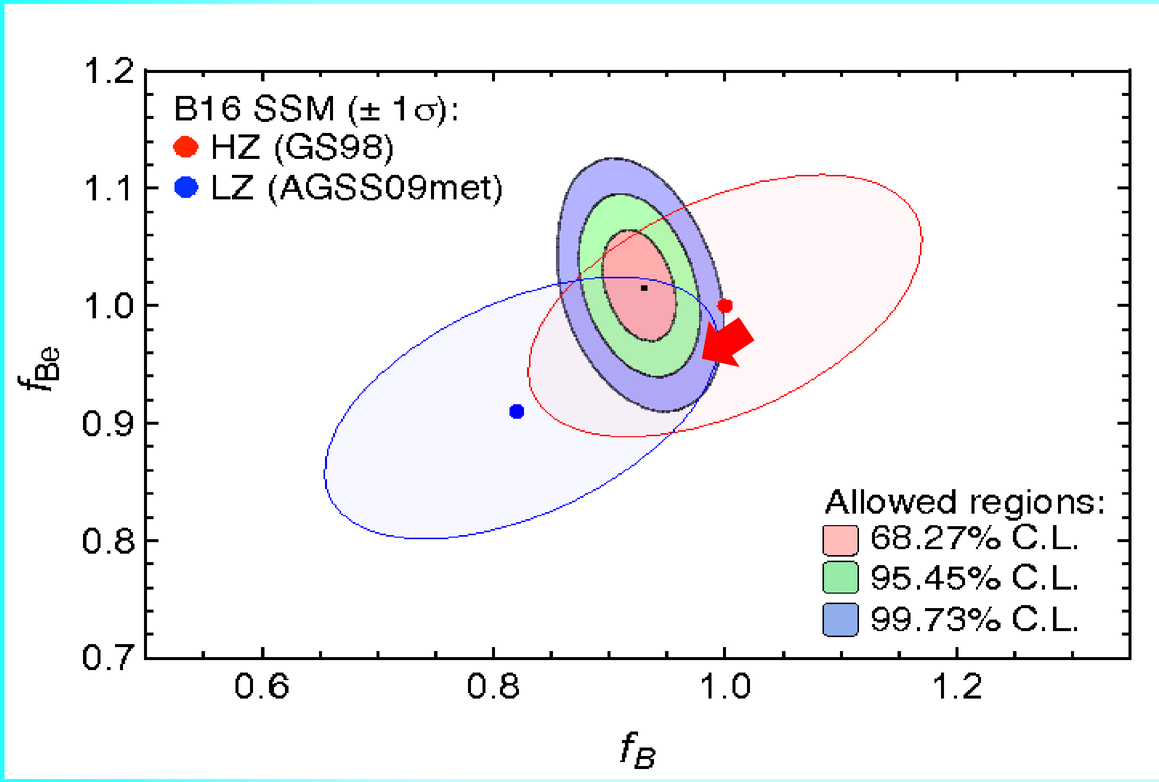

Borexino Collaboration (Agostini, M. et al.) arXiv:1707.09279 [hep-ex]

Theoretical uncertainties should be reduced

LZ is disfavored at 3.1σ level

Allowed contours obtained by combining the new result on 7Be ν's with solar and KamLAND data. $\sin^2\theta_{13} = 0.02$

NSI

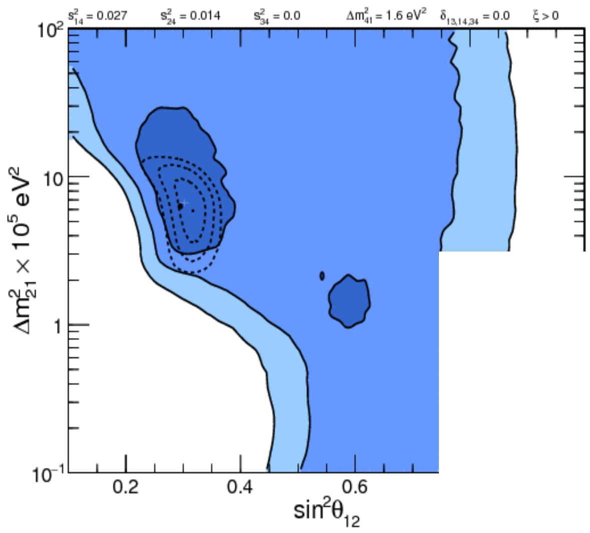

$s^2_{14} = 0.027$
$s^2_{24} = 0.014$
$s^2_{34} = 0.0$
$\Delta m^2_{41} = 1.6$ eV^2
$\delta_{13,14,34} = 0.0$
$\xi > 0$
$\Delta m^2_{21} \times 10^5$ eV^2
$\sin^2\theta_{12}$

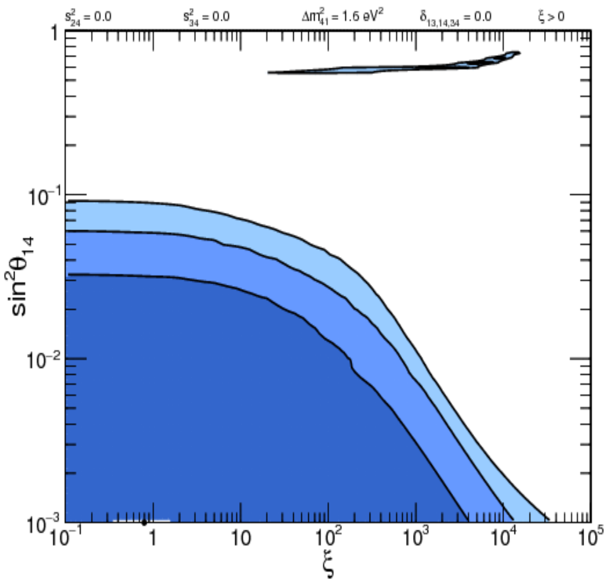

$s^2_{24} = 0.0$
$s^2_{34} = 0.0$
$\Delta m^2_{41} = 1.6$ eV^2
$\delta_{13,14,34} = 0.0$
$\xi > 0$
$\sin^2\theta_{14}$
ξ

Status of
LMA MSW solution

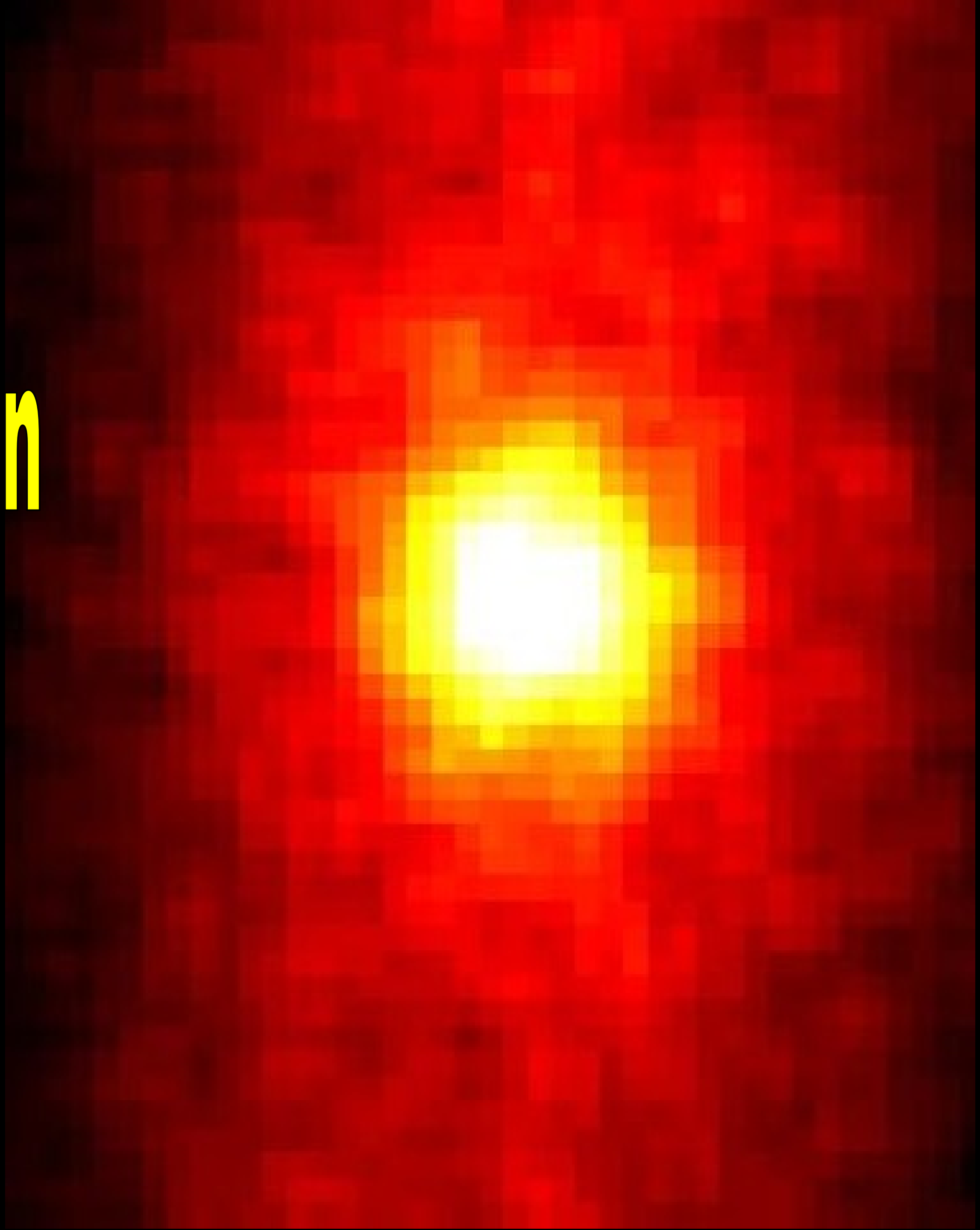

BOREXINO-II

8B spectrum with 1.5 kton y exposure

Borexino Collaboration
(Agostini, M. et al.) 1709.00756 [hep-ex]

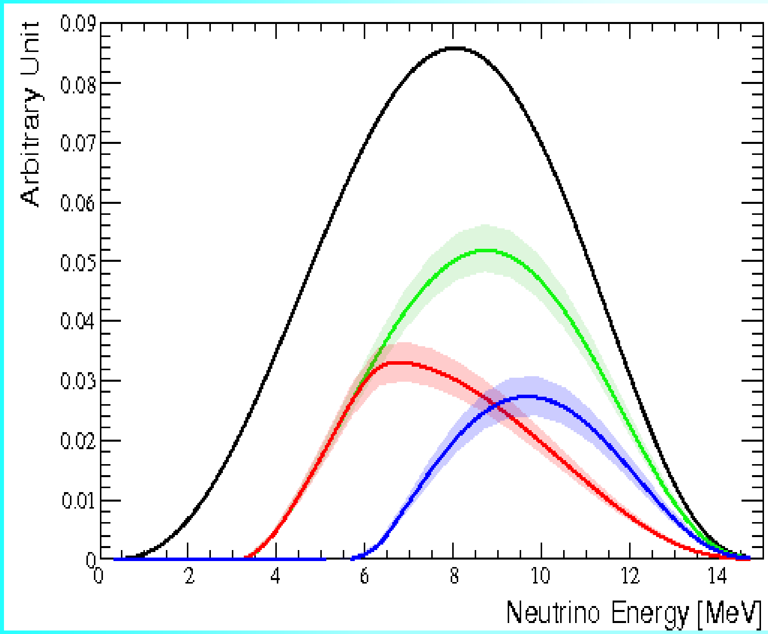

the portions of the nu spectrum contributing to the LE (red), HE (blue), and LE+HE (green) energy windows used in the analysis.

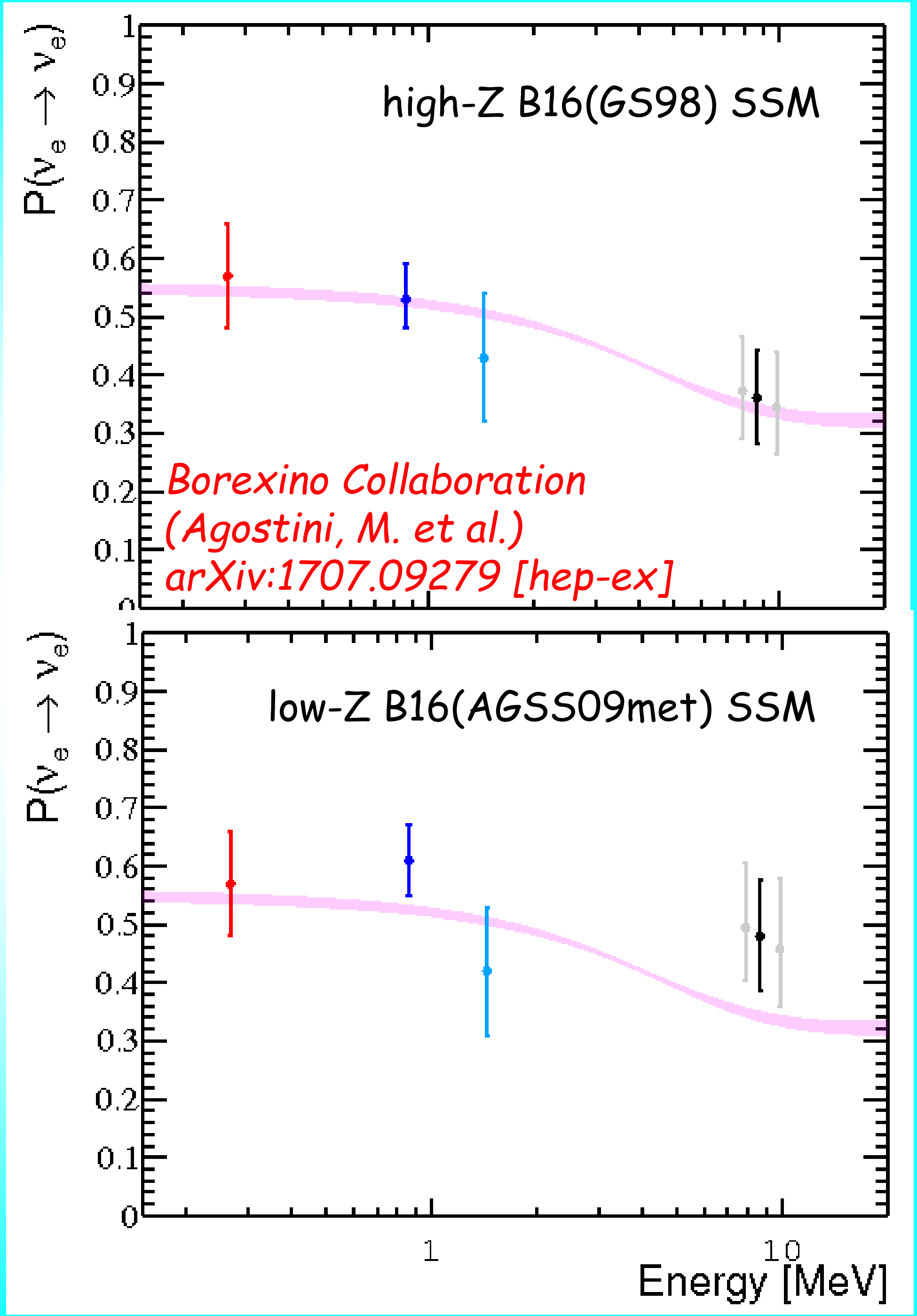

KamLAND and bump

M. Maltoni 2017

Subtracting 5 MeV bump

Different flux assumptions:
- Huber (black),
- Huber reduced by 4% (red),
- Daya-Bay (cyan) measurements of the reactor spectrum (arXiv:1607.05378) (syan).

- The shaded brown areas - the KamLAND 2013 matched well the fit with Huber's fluxes (black).

- Reducing the flux by 4% (red) induces a shift of the region to lower theta12: the lower flux is compensated larger probability .

- Inclusion of the Daya-Bay spectrum (cyan) with the 5-MeV bump leads to extension of the KamLAND region to lower dmqSL. The tension with solar slightly reduced

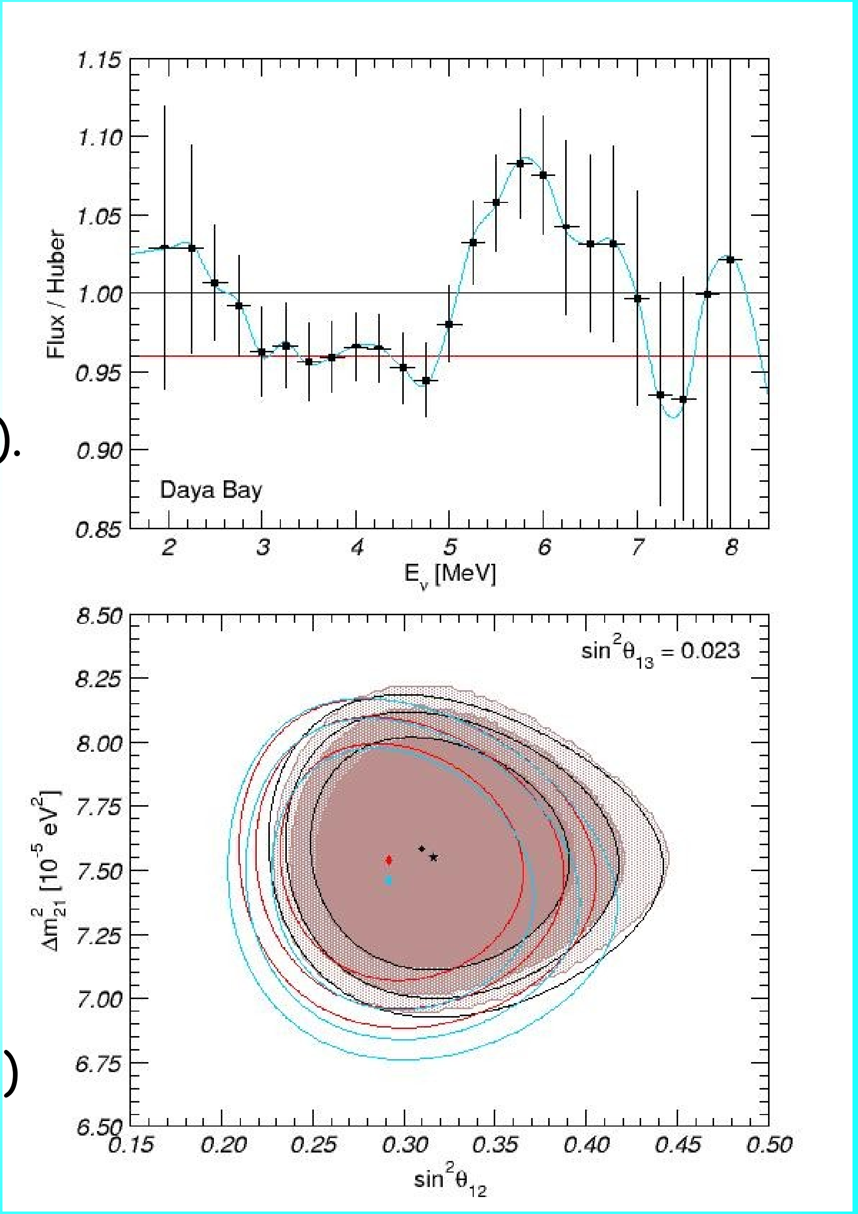

Properties of LMA: scaling

Inside the Sun highly adiabatic conversion →

the averaged survival probability is scale invariant =
no dependence on distance, scales of the density profile, etc.

Function of the combinations

$$\varepsilon_{12} = \frac{2VE}{\Delta m_{21}^2} \qquad \varepsilon_{13} = \frac{2VE}{\Delta m_{31}^2}$$

Very weak dependence

With oscillations in the Earth

$$P_{ee} = P_{ee}(\varepsilon_{12}, \varepsilon_{13}, \phi_E)$$

$$\phi_E = \Delta m_{21}^2 L / 2E$$

L – the length of the trajectory in the Earth

If oscillations in the Earth are averaged

$$P_{ee} = P_{ee}(\varepsilon_{12}, \varepsilon_{13}) = P_{ee}(\varepsilon_{12})$$

Invariance:

$$\Delta m_{ij}^2 \rightarrow a\, \Delta m_{ij}^2, \; V \rightarrow a\, V$$

$$\Delta m_{ij}^2 \rightarrow b\, \Delta m_{ij}^2, \; E \rightarrow b\, E$$

a = -1 flip of the mass hierarchy

Upturn?

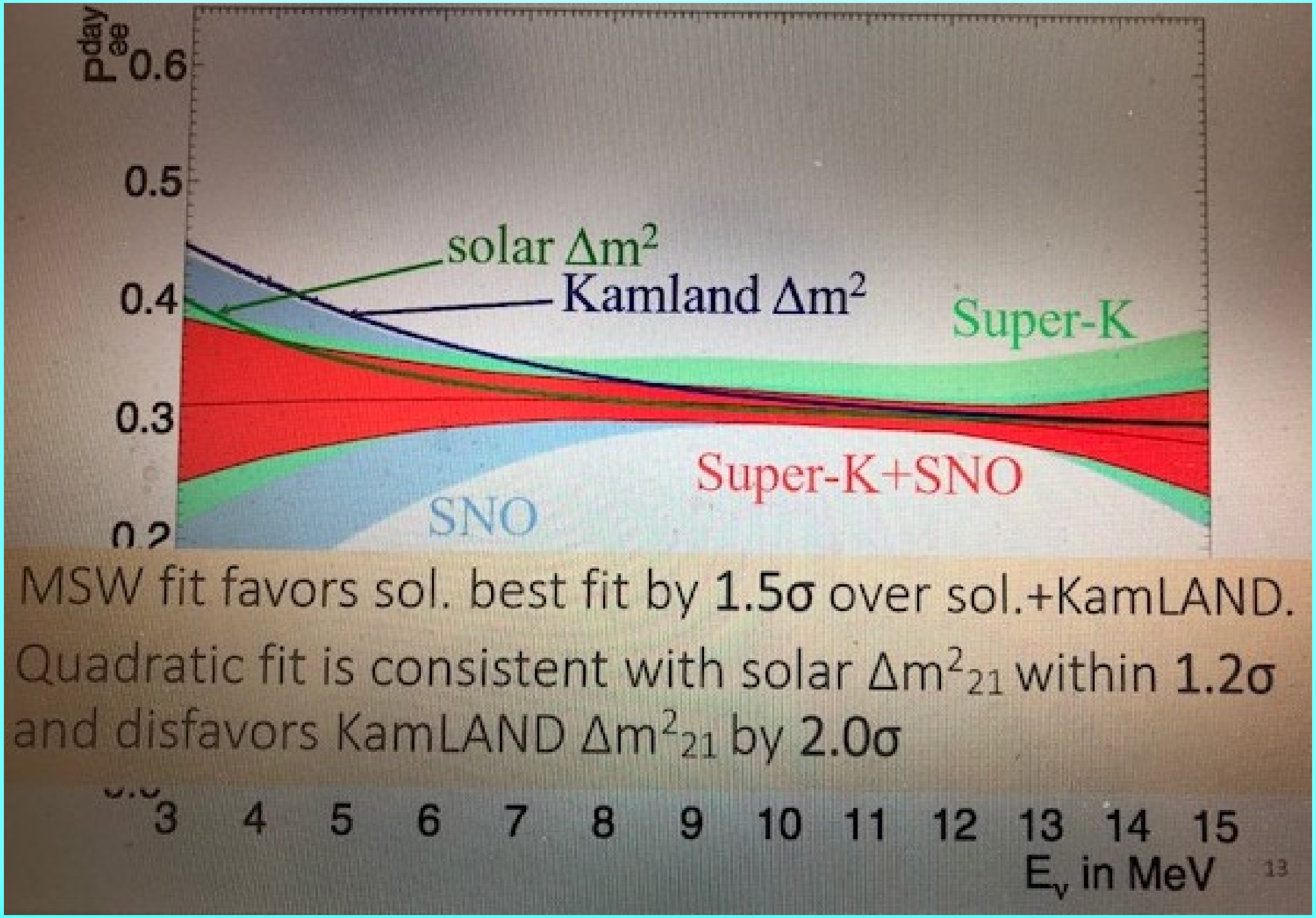

P_{ee}^{day}
0.6
0.5
0.4
0.3
0.2
solar Δm²
Kamland Δm²
Super-K
Super-K+SNO
SNO
MSW fit favors sol. best fit by 1.5σ over sol.+KamLAND.
Quadratic fit is consistent with solar Δm²₂₁ within 1.2σ
and disfavors KamLAND Δm²₂₁ by 2.0σ
3 4 5 6 7 8 9 10 11 12 13 14 15
E_ν in MeV
13

CPT, Lorentz violation

Long range forces

Magnetic moment

Time variations
Appearance of antineutrinos, KamLAND
Effect at the detection BOREXINO

Super-Kamiokande

Y. Koshio

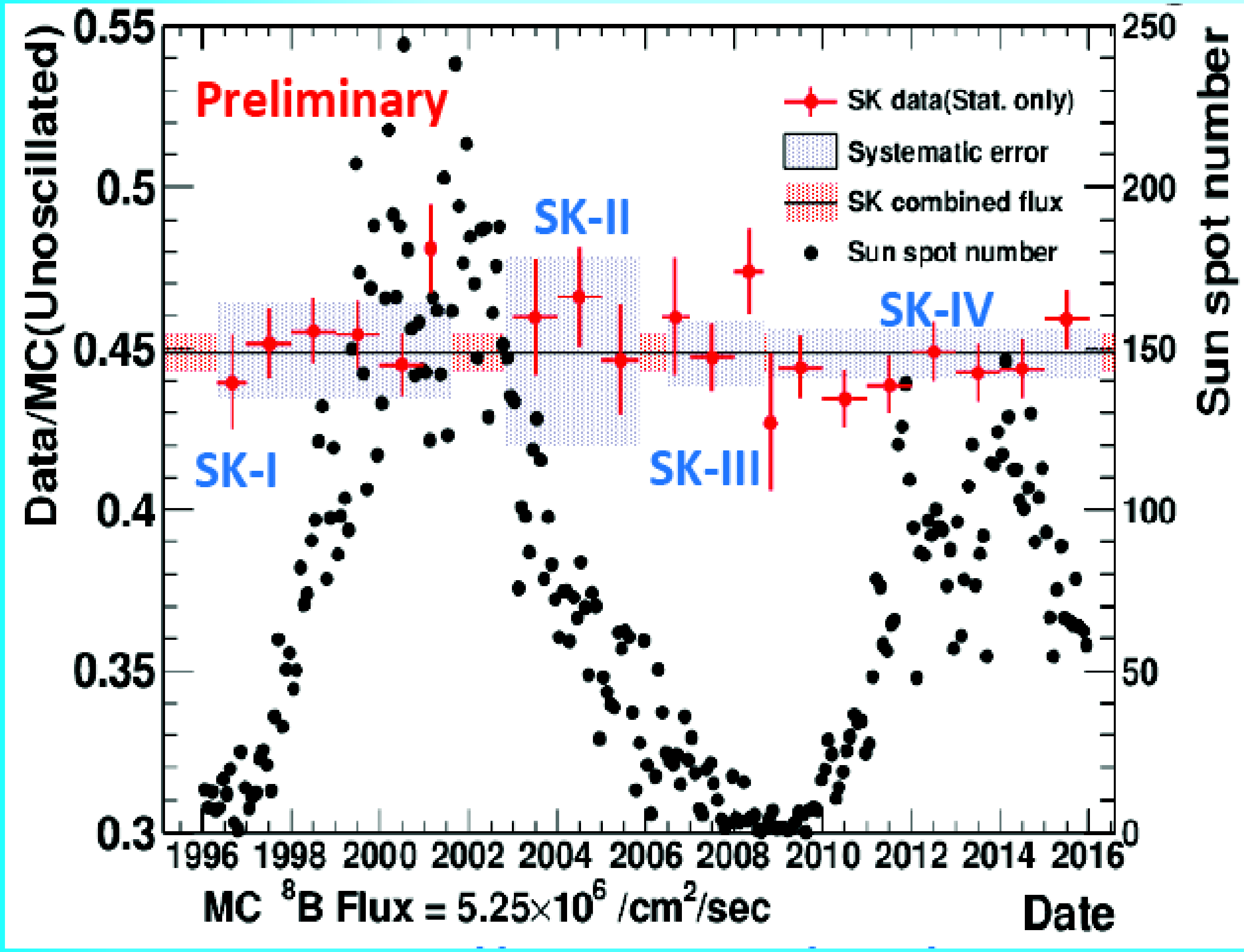

Compare with Homestake signal anti-correlations with solar activity

Related to lower Ar production rate?

Q_{Ar}^{LMA}= 3.1 SNU

Q_{Ar}^{Hom} = 2.56 +/- 0.25 SNU

Neutrino magnetic moment

Borexino Collaboration, M. Agostini et al., arXiv:1707.09355

O. Smirnov

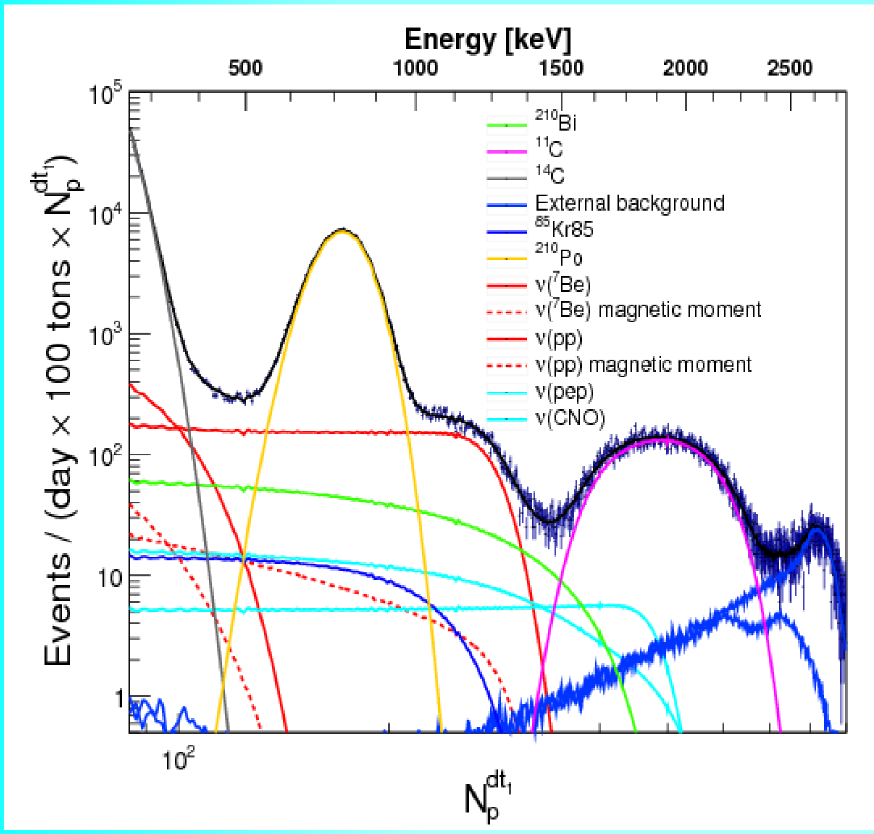

data from 1291.5 days exposure during phase II of the Borexino. No significant deviations from the expected shape of the electron recoil spectrum have been found .

upper limit on the effective neutrino magnetic moment:

$\mu_{eff} < 2.8 \cdot 10^{-11}\ \mu B$, 90\% C.L.

Spectral fit with the neutrino effective moment fixed at the upper limit

(constraints on the sum of the solar neutrino fluxes implied by gallium experiments has been used)

Oscillation waves

~

$$P_{1e} = c_{13}^2 |S_{e1}|^2$$

due to transition to 3ν basis

Approximate (lowest order in ε) result

$$U_{k,k-1} \approx I - i\sigma_2 \sin \Delta\theta_{k-1}$$

Inserting this expression into formula for S and taking the lowest order terms in $\sin\Delta\theta_{k-1} \sim \varepsilon$

$$P_{1e} \sim c_{13}^2 \cos^2\theta_n^f + c_{13}^2 \sin 2\theta_n^f \, \Sigma_{j = 0 \ldots n-1} \sin\Delta\theta_j \cos \phi_j^{after}$$

the 1-2 angle in matter near detector

sum over jumps

total phase acquired after jump j

$$\sin \Delta\theta_j \simeq c_{13}^2 \sin 2\theta_{12} \Delta V_j \frac{E}{\Delta m_{21}^2}$$

ΔV_j - j density jump

Integral formula

Regeneration factor

$$f_{reg} = P_{1e} - P_{1e}^{0} = P_{1e} - c_{13}^{2}\cos^{2}\theta_{12}$$

determines the day-night asymmetry

In the integral form:

A. Ioannisian and A Y S, PRL 93, 241801 (2004), hep-ph/0404060

$$f_{reg} = -\tfrac{1}{2}\, c_{13}^{4}\sin^{2}2\theta_{12}\int_{x_0}^{x_f} dx\, V(x)\, \sin\phi^{m}(x \rightarrow x_f)$$

The phase acquired from the point x to the final point of trajectory

$$\phi^{m}(x \rightarrow x_f)\,(E) = \int_{x}^{x_f} dx\, \Delta_{12}^{m}(x)$$

For potential with jumps explicit integration in f_{reg} reproduces the result of sum of waves emitted from the jumps

Relative D-N asymmetry

A. Ioannisian,
B. A.Y.S., D. Wyler
1702.06097 [hep-ph]

$$A_{DN} = \frac{N - D}{D}$$

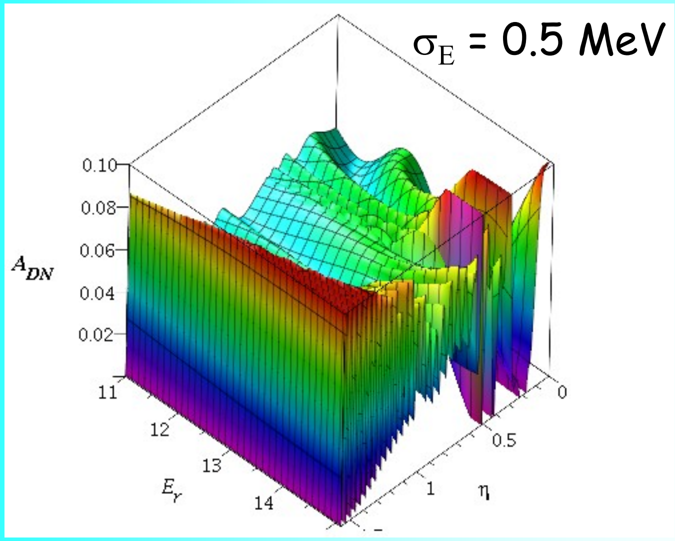

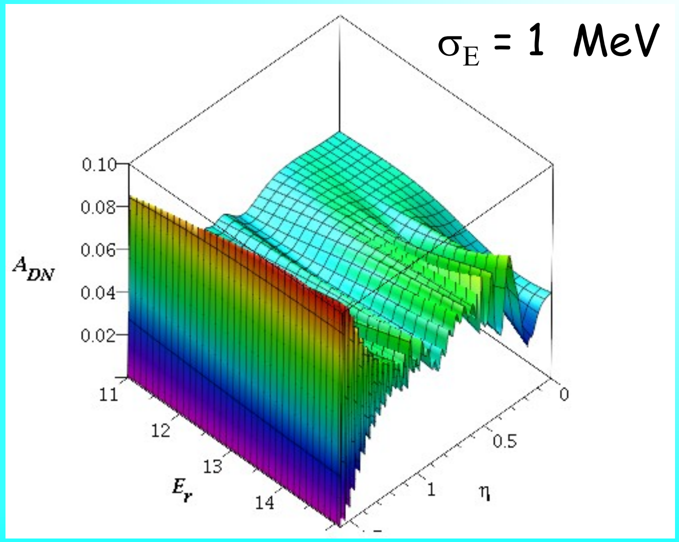

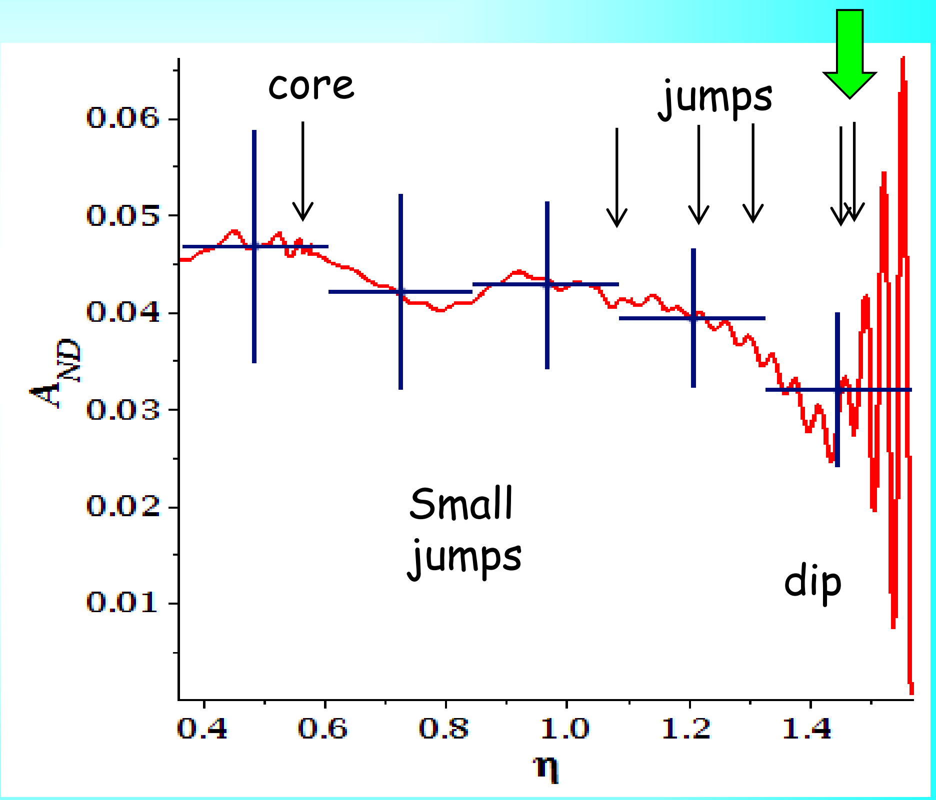

Relative excess of the night events integrated over E > 11 MeV
Sensitivity of DUNE experiment
40 kt, 5 years

Tomography

A. Ioannisian, A. Smirnov, D. Wyler,
Phys.Rev. D96 (2017) no.3, 036005
arXiv:1702.06097 [hep-ph]

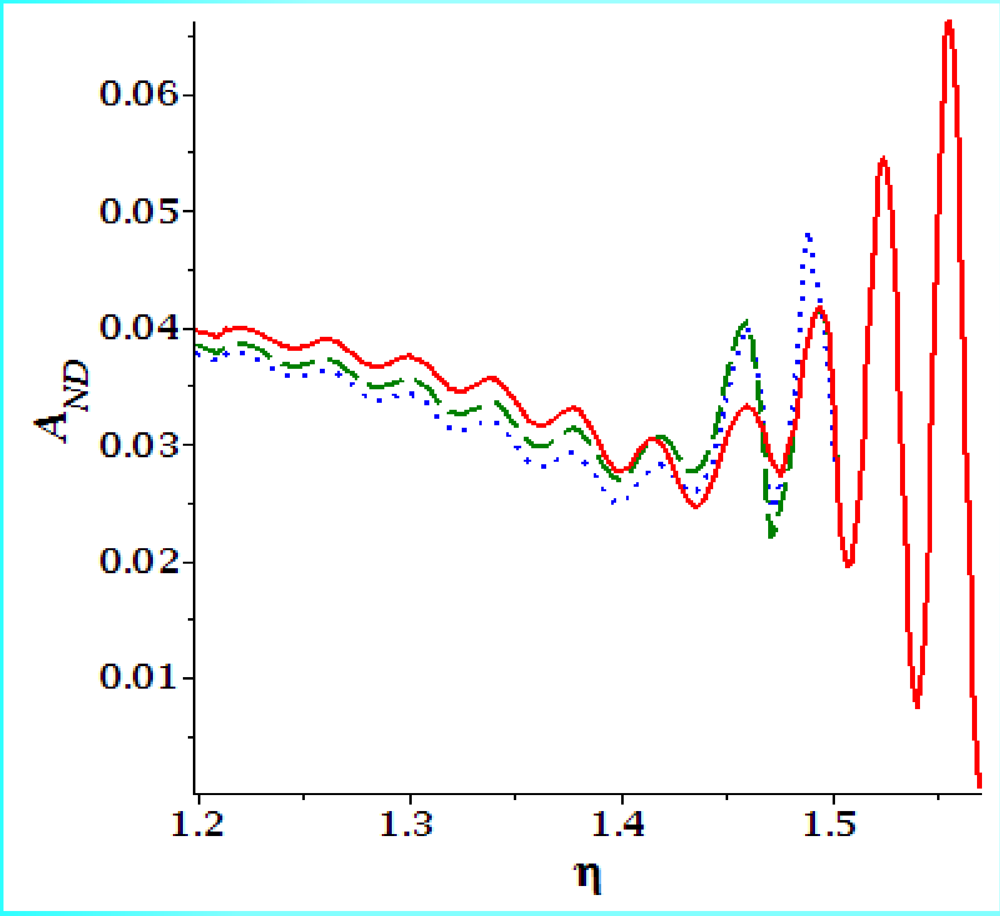

The relative excess of night events integrated over E > 11 MeV as function of the nadir angle for different positions of the density jumps. Jumps at

15 km and 25 km (red)
20.5 km and 30 km (blue dotted)
15 km and 30 km (green-dashed).

Parametric enhancement of oscillations is seen in the 3rd and 4th periods.

Variations of the ν_{Be}- flux

A. Ioannisian, AYS

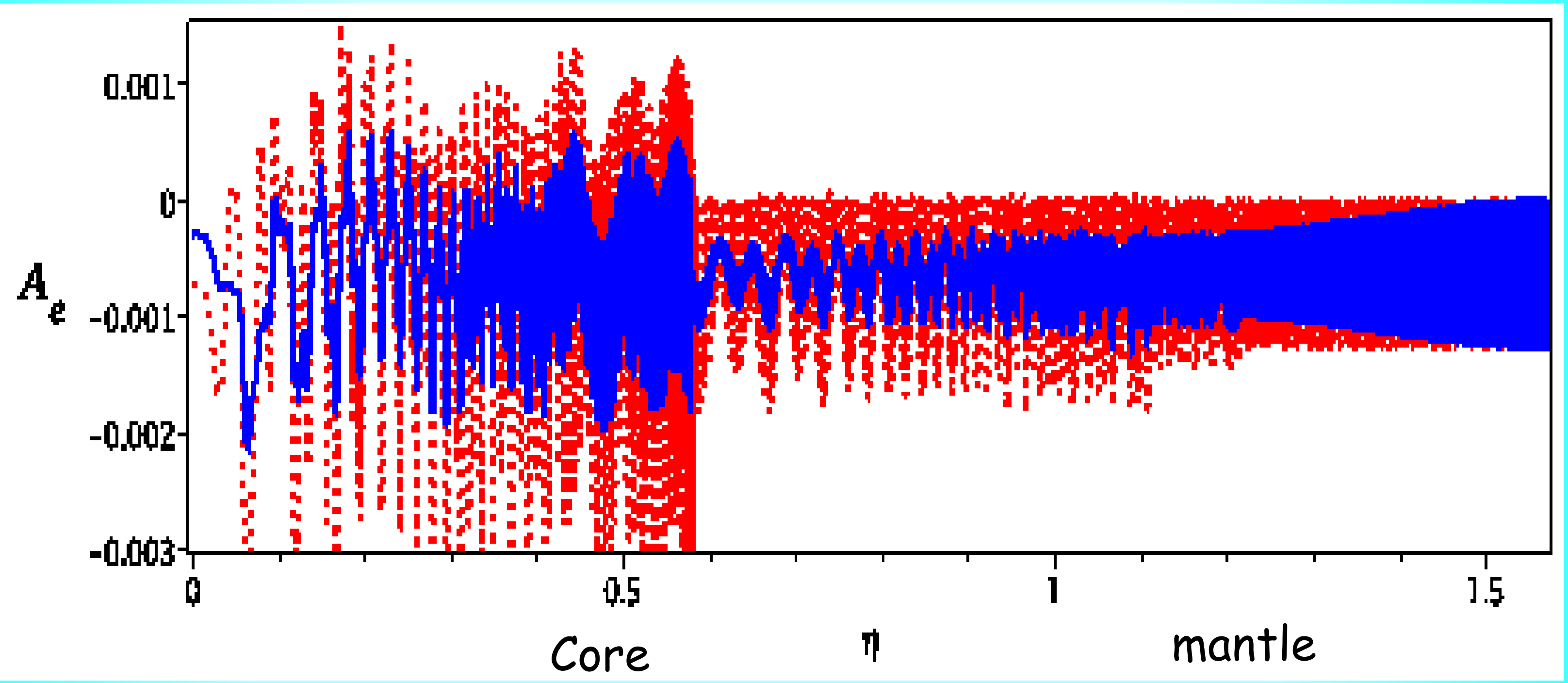

Again 0.1% effect

LMA-D

A Plan to Rule out Large Non-Standard Neutrino Interactions After COHERENT Data Denton, Peter B. et al. arXiv:1804.03660 [hep-ph]

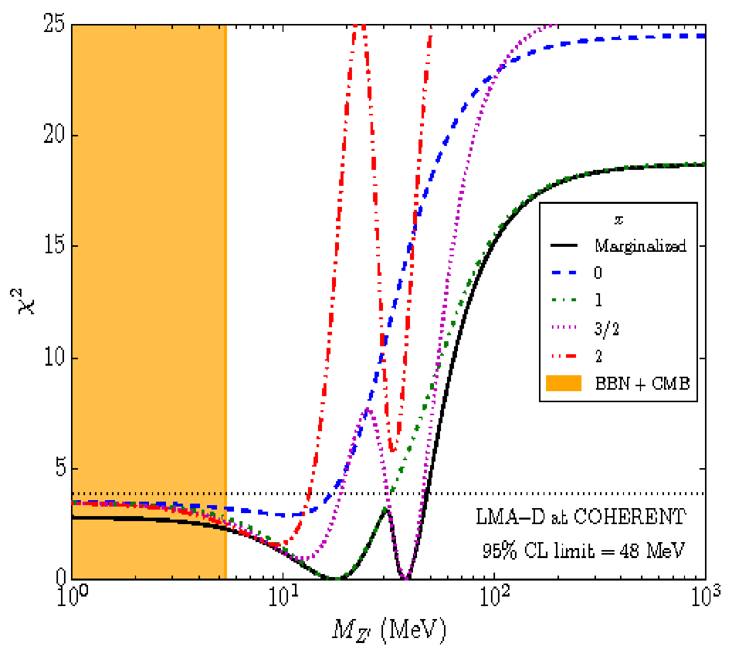

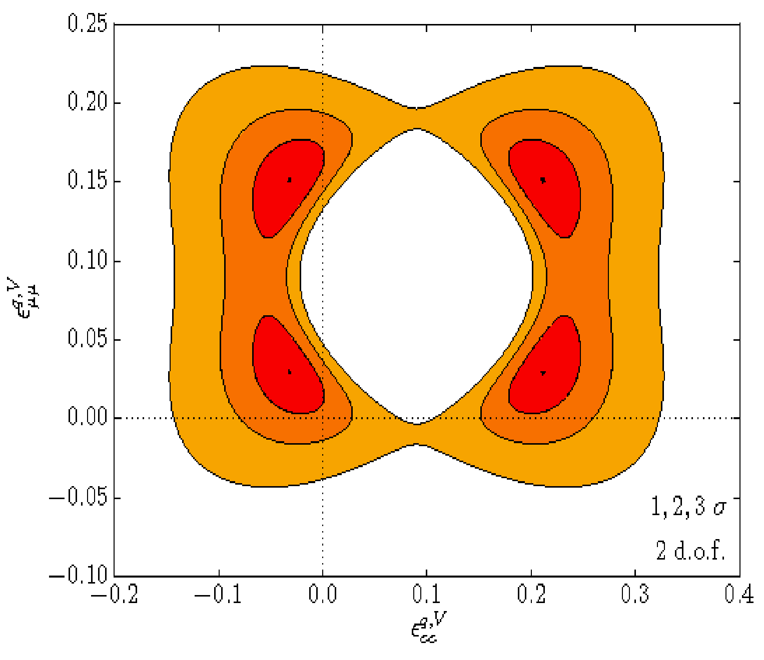

Bounds on NSI

P. Coloma, M.C. Gonzalez-Garcia, M. Maltoni, T. Schwetz, 1708.02899 [hep-ph]

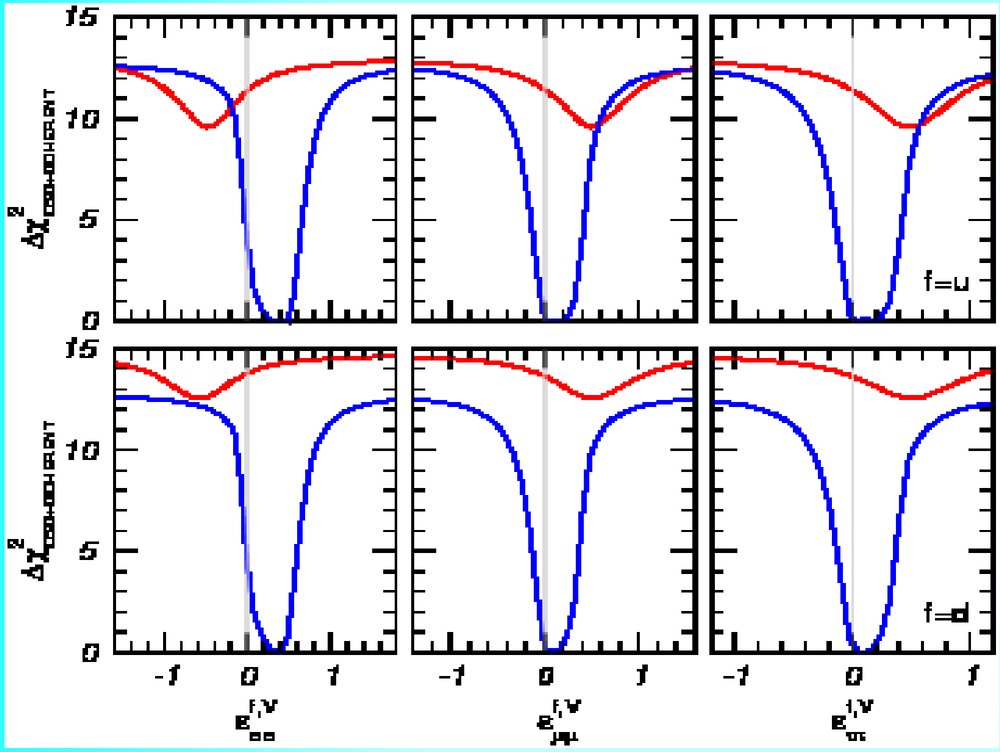

Bounds on the flavour diagonal NSI parameters from the global fit to oscillation plus COHERENT data.

Blue lines - the LMA solution

red lines LMA-D solution

COHERENT experiment, in combination with global oscillation data, excludes the NSI degeneracy at the 3.1σ (3.6σ) CL for NSI with up (down) quarks.

LMA-Dark

Esteban, Ivan et al.
arXiv:1805.04530

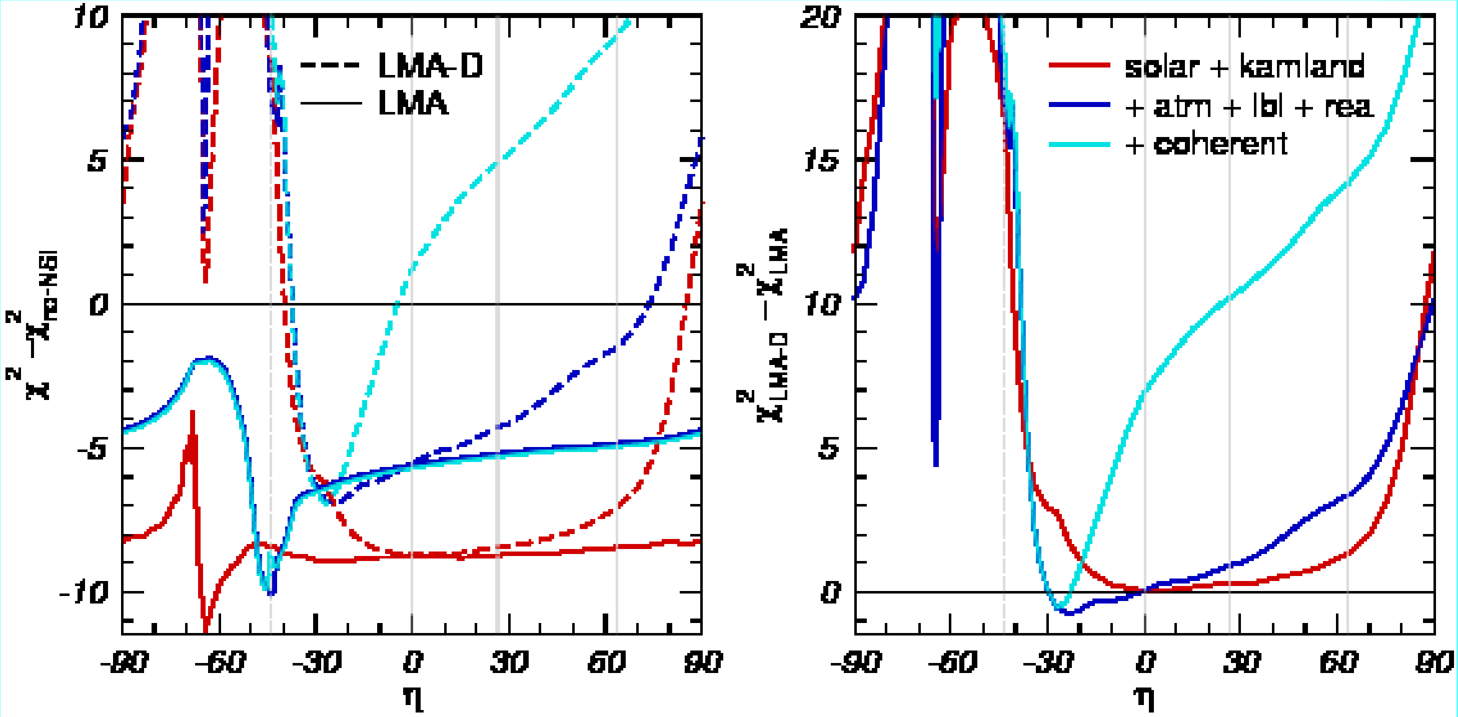

Left: $\chi2LMA(\eta)-\chi2no\text{-}NSI$ (full lines) and $\chi2LMA\text{-}D(\eta)-\chi2no\text{-}NSI$ (dashed lines) for the analysis of different data combinations as a function of the NSI quark coupling parameter η.

Right: $\chi2LMA\text{-}D(\eta)-\chi2LMA(\eta)$ as a function of η.

Day-Night effect

First Indication of Terrestrial Matter Effects on Solar Neutrino Oscillation

Super-Kamiokande collaboration (Renshaw, A. et al.) Phys.Rev.Lett. 112 (2014) 091805 arXiv:1312.5176

$> 3\ \sigma$

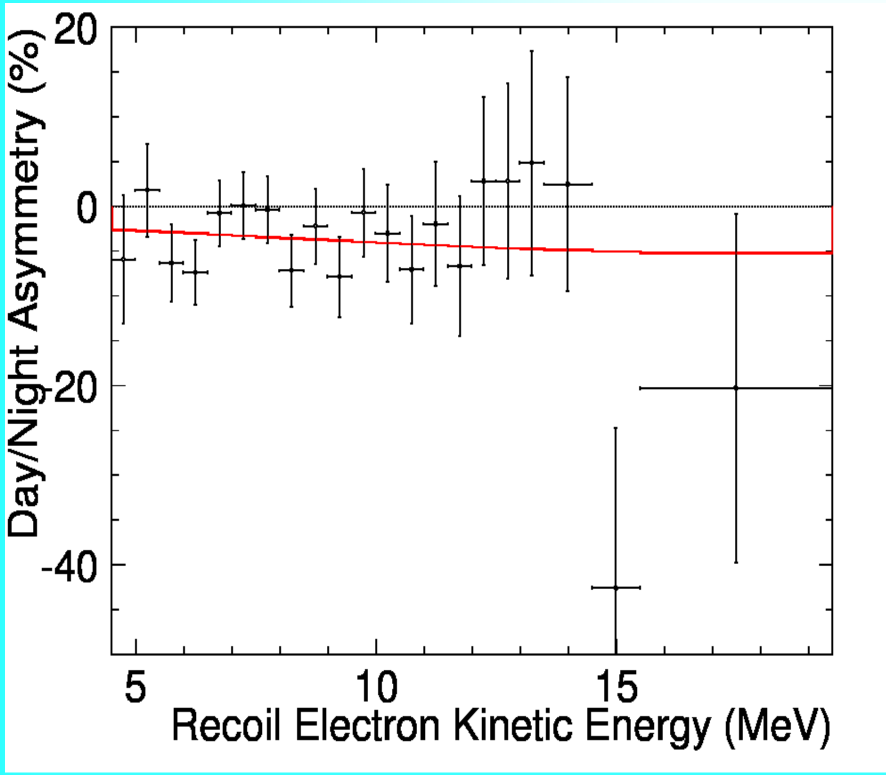

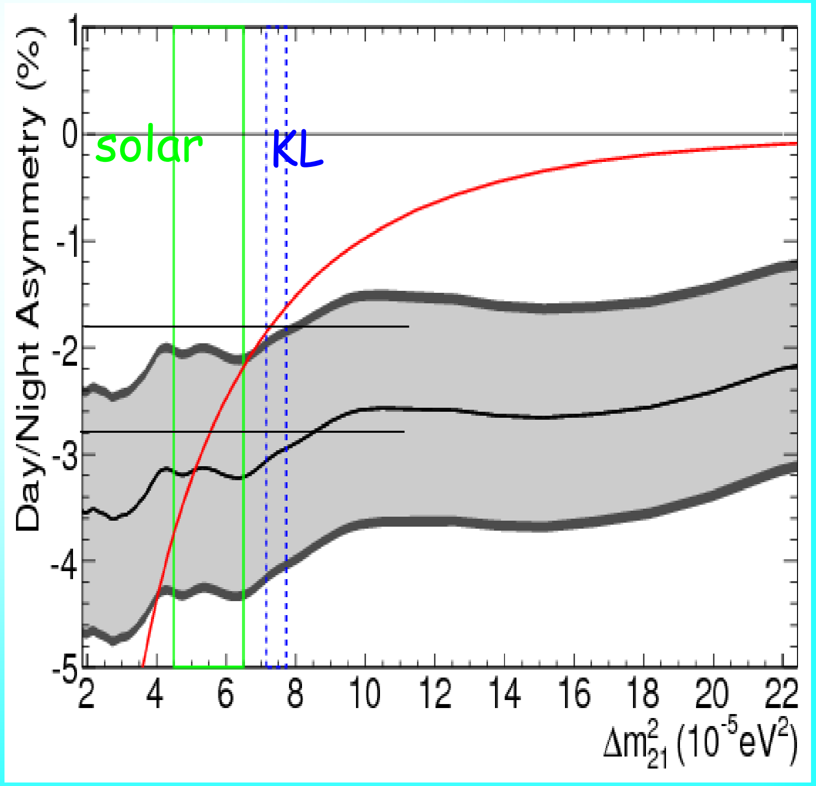

Resonance enhancement

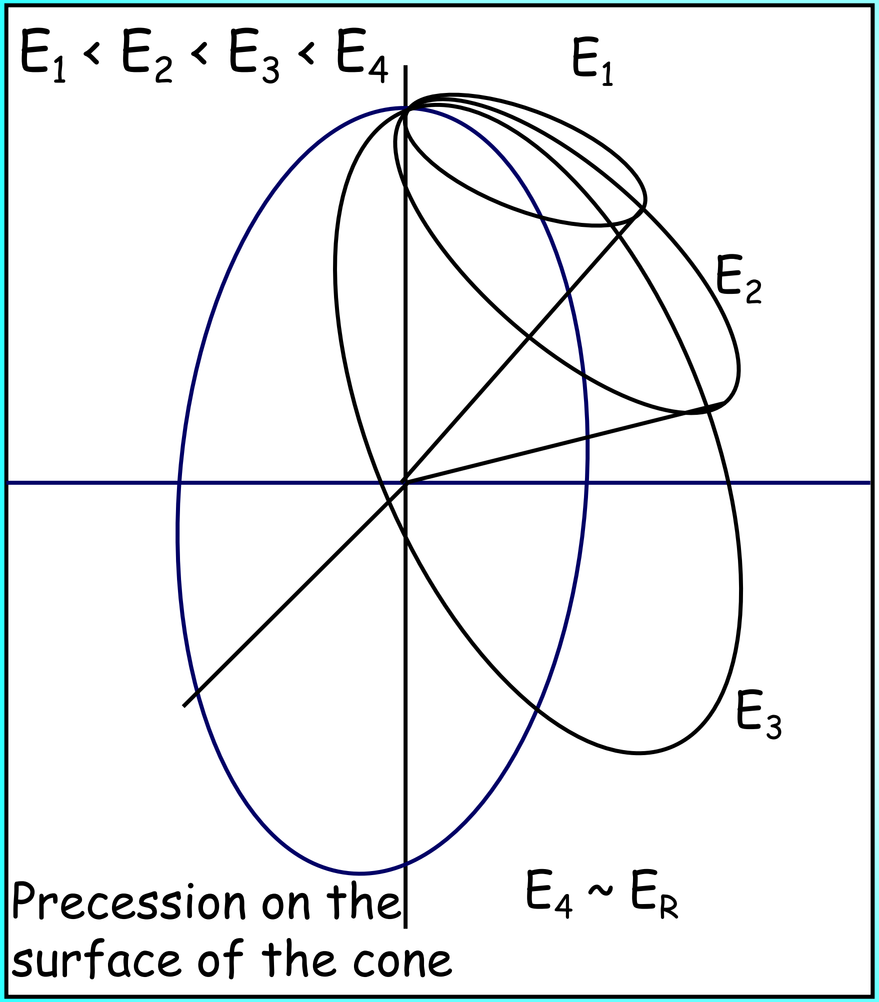

Adiabatic conversion

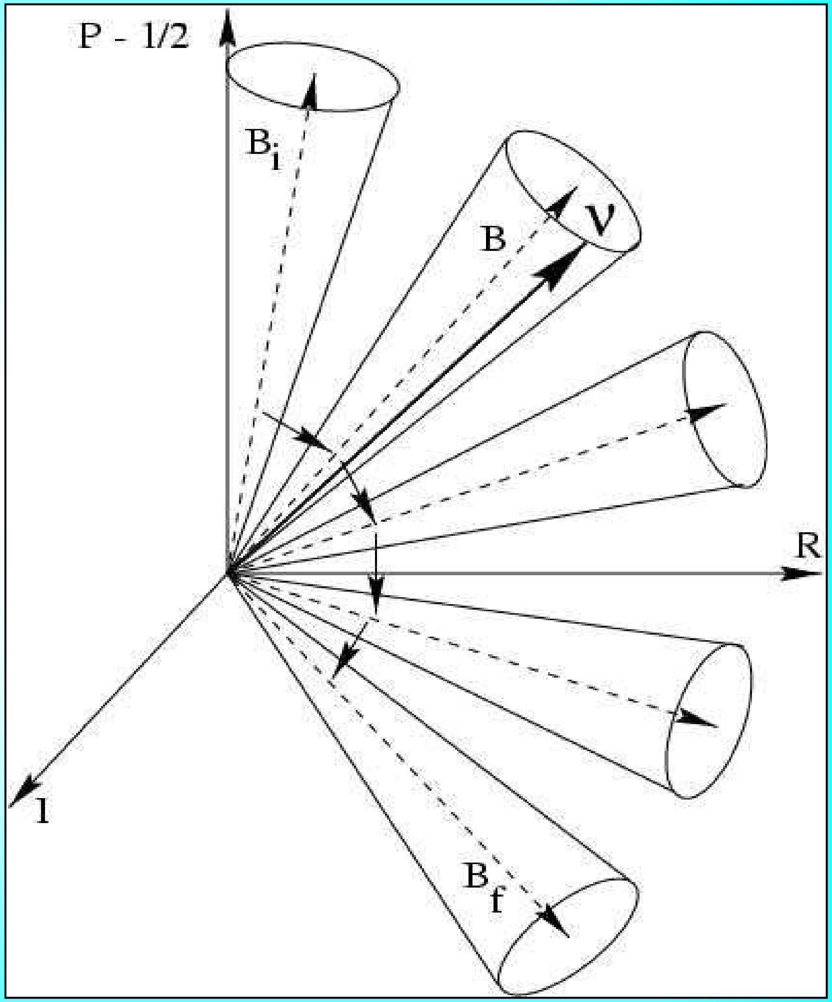

Matter potential

G. L Fogli et al hep-ph/0309100
C. Pena-Garay, H. Minakata, hep-ph 1009.4869 [hep-ph]
M. Maltoni, A.Y.S. 1507.05287 [hep-ph]

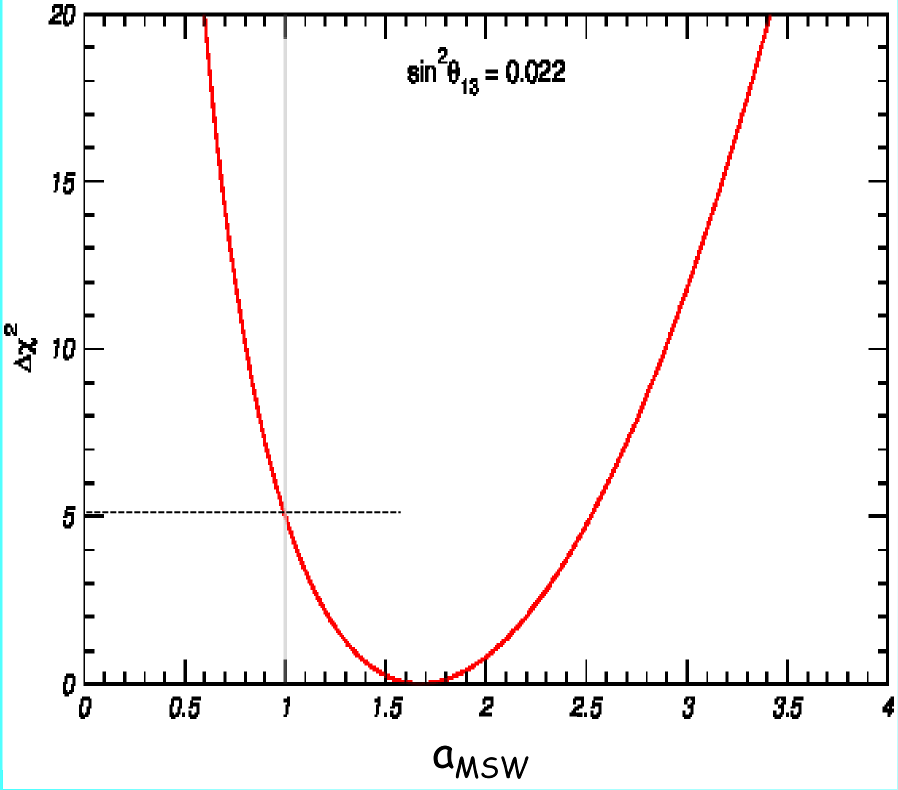

$V = a_{MSW} V_{stand}$

$a_{MSW} = 0$ is disfavoured by > 15 σ

the best fit value $a_{MSW} = 1.66$

$a_{MSW} = 1.0$ is disfavoured by > 2 σ

related to discrepancy of Δm^2_{21} from solar and KamLAND:

$$\frac{\Delta m^2_{21}\,(KL)}{\Delta m^2_{21}\,(Sun)} = 1.6$$

Determination of the matter potential from the solar plus KamLAND data using a_{MSW} as free parameter

Potential enters the probability in combination

$$\frac{V}{\Delta m^2_{21}}$$

Neutrino decay

Signatures

Suppression (energy dependent) of number of the NC events - SNO

Distortion of the energy spectrum:

In the standard case: energy dependent mass composition of the flux:

	Low energies	High energies
	$\cos^2\theta_{12}\,\nu_1,\ \sin^2\theta_{12}\,\nu_2$	ν_2
P_{ee} =	$\cos^4\theta_{12} + \sin^4\theta_{12}$	$\sin^2\theta_{12}$
ν_2 - decay	$\cos^4\theta_{12}$	0
ν_1 - decay	$\sin^4\theta_{12}$	$\sin^2\theta_{12}$